Louisiana State University
LSU Scholarly Repository

LSU Master's Theses | Graduate School

2010

Assessing the suitability of coagulation pretreatment on poultry processing wastewater for optimized dissolved air flotation

Adam James Dassey
Louisiana State University and Agricultural and Mechanical College

Follow this and additional works at: https://repository.lsu.edu/gradschool_theses

 Part of the Engineering Commons

Recommended Citation

Dassey, Adam James, "Assessing the suitability of coagulation pretreatment on poultry processing wastewater for optimized dissolved air flotation" (2010). *LSU Master's Theses*. 2498.
https://repository.lsu.edu/gradschool_theses/2498

This Thesis is brought to you for free and open access by the Graduate School at LSU Scholarly Repository. It has been accepted for inclusion in LSU Master's Theses by an authorized graduate school editor of LSU Scholarly Repository. For more information, please contact gradetd@lsu.edu.

ASSESSING THE SUITABILITY OF COAGULATION PRETREATMENT ON POULTRY PROCESSING WASTEWATER FOR OPTIMIZED DISSOLVED AIR FLOTATION

A Thesis Submitted to the Graduate Faculty of the
Louisiana State University and
Agricultural and Mechanical College
in partial fulfillment of the
requirements for the degree of

Master of Science in Biological and Agricultural Engineering

in

The Department of Biological and Agricultural Engineering

by
Adam James Dassey
B.S., Louisiana State University, 2007
August 2010

Table of Contents

List of Tables

List of Figures

Abstract

Eleven metal coagulants and one polyelectrolyte were assessed on their suitability for assisting a dissolved air flotation (DAF) system in treating poultry processing wastewater. The DAF unit was designed to maximize the microbubble production by varying the pressure, temperature, hydraulic retention time, and air flow parameters. The maximum microbubble flow from the designed system produced 30 mL of air per L of water. This value was considered low compared to other systems, but attempts to increase the microbubble volume in the current system beyond this value resulted in the coalescing of microbubbles due to turbulent conditions. Jar tests were used to identify the best coagulant available and were based on the removal efficiency of total suspended solids (TSS) and volatile suspended solids (VSS). These results were compared to increases in water clarity measured by optical density. Preliminary tests determined that a combination of 800 mg/L of ferric chloride and 900 mg/L of Floccin 1115 would provide the best treatment by removing at least 98% of the TSS and 97% of the VSS while providing a 97% increase in water clarity. Final flotation tests displayed that the flocculated particles could be carried to the surface with 40% recycle ratio of the DAF. The resulting supernatant indicated 94.7% increase in clarity (± 1.4%), 97.3% reduction in TSS (± 0.5%), 96.6% reduction in VSS (± 1.1 %), 91% reduction in COD (chemical oxygen demand), and nearly 100% removal of FOGs (fats, oils, and greases). Despite the high removal efficiencies, flotation was found not to be critically necessary for treatment because the high concentration of coagulants caused settling of the flocs to occur just as rapidly. The combination of these two coagulants was also determined impractical, costing nearly twice the current treatment costs of the processing plant. Due to limited alkalinity and excess phosphate in the wastewater, overdosing was a potential issue but could easily be addressed in future work.

Chapter 1: Introduction

Due to technological and regulatory advancements, the historical slaughterhouses have transitioned to "meat processing plants" and "rendering plants" which have been more efficient and hygienic. However, due to the sheer nature of the operations, large quantities of organic wastes have been generated at these facilities, including shredded flesh pieces, blood, fats, oils, grease, feathers, skin fragments, and other organic matter, all of which pose serious wastewater treatment challenges. Offal recovery systems, typically consisting of primary and secondary mechanical rotary screens, can be expected to remove solids greater than 500 um in size from the processed flow, but significant portions of fats, oils and greases (FOG) will remain present in the processing plant wastewater (Kiepper et al. 2008). The effective removal of fat from poultry processed wastewater is the critical factor in the development of effective advanced physical separation systems for the poultry processing industry (Kiepper et al. 2008).

Currently, Sanderson's Farm in Hammond, LA, processes an average of 125,000 chickens per day which requires a wastewater flow rate of approximately 800 gallons per minute. After preliminary screening, the wastewater is pumped into a covered anaerobic treatment lagoon for the primary settling of heavy solids and decomposition of FOGs. Typically the grease that rises to the top of the supernatant is kept submerged by the cover to assist in breakdown by bacterial action (Reynolds and Richards, 1996). The primary lagoon is connected in series to a secondary facultative lagoon that is capped with various materials, including hay and chicken feathers, where further settling and degradation of organic sludge is accomplished. Once the wastewater exits the settling lagoons it is pumped to an activated sludge system comprised of an aeration basin and a clarifier. After the activated sludge treatment is completed, the water flows through a UV disinfection process that kills any pathogenic microbes before it is released to surrounding drainage systems.

This process of preliminary screening, followed by primary settling and secondary biological aeration is a conventional wastewater treatment practice (Viessman and Hammer, 1985). This wastewater treatment process is commonly employed because of the relatively cheap operation expenses (approximately $150,000 per month at this Sanderson Farms location). The treatment process at Sanderson Farms, however, is limited by the two sedimentation lagoons, which have a combined hydraulic retention time of 7-8 days. Shorter retention times which can result from increased seasonal processing would result in poorer treatment of the wastewater. The low hydraulic loading rates and poor removal efficiencies of small suspended solids (<100 um) are disadvantages of sedimentation lagoons (Timmons et al., 2002).

Instead of using long retention times for the treatment of light weight particles and oils, methods of flotation have been developed to bring the same particles to the surface for speedy removal. Flotation techniques, in which finely suspended particles are separated by adhering to the surface of rising bubbles, have proven efficient, practical and reliable separation methods for the removal of oils, as well as dissolved ions, fats, biomolecules and suspended solids from water (Zouboulis et al., 2000). A popular method of flotation for these water and wastewater treatment challenges has been dissolved air flotation (DAF) (Al-Mutairi et al., 2008; Lundh et al., 2000).

Dissolved air flotation uses pressure saturation to increase the solubility of air in water to produce fine microbubbles for solids removal. The idea is to develop agglomerates with lower density than water, causing the particulates to rise through the water and accumulate at the surface where they can be removed as sludge (Lundh et al. 2000). Dissolved air flotation is an effective method of particle separation because the high concentration of microbubbles and their slow rise rates allow for more collision opportunities with the particulate matter (Al-Shamrani et al., 2002).

DAF has the advantage over sedimentation of being able to operate at higher overflow rates since the rise speed of bubble/particle agglomerates can be much larger than the settling speed of individual particles (Leppinen et al. 2001). By using a DAF unit to treat the wastewater before sending it to the lagoon, retention times can be drastically reduced, which would help increase overall treatment. Previous studies have shown removal efficiencies of 20-70% for BOD, 10-60% for COD, 50-85% for TSS, and 70-95% for oil (Telang, 1996). Achieving these numbers could reduce the size and retention time for the large treatment lagoons, which in turn, would reduce overall treatment time, increase production, and increase profits.

The design of a specific DAF system, however, depends upon the factors such as the volume of wastewater to be treated, the degree and nature of contamination, the extent of treatment required, and any subsequent treatment that is required for the recovered product concentration (Telang, 1996). These factors, in turn, indicate the appropriate dissolution pressure, temperature, flow rate, retention time, recycle ratio, coagulant and flocculent pretreatment, flotation tank design, and baffle setup for the desired treatment. Despite being a system that has been in use for sixty years, many questions remain on the functionality of the system due to the various parameters. Many design references commonly used by engineers and designers provide wide ranges in data, or no data at all, for these common design parameters (Ross et al., 2000; Han et al., 2001; Chung and Kim, 1997).

Each of the previously mentioned variables is capable of affecting the particle removal efficiency of the dissolved air flotation unit. By singling out each of these parameters and addressing them independently, their peak values can be determined and utilized to aid in the design of an effective wastewater treatment system.

1.1 Research Objectives

The wastewater from a poultry processing plant poses many challenges in the treatment arena, especially due to large flows with high solids and oil content. Incorporating a coagulation pretreatment in conjunction with a dissolved air flotation unit for the poultry wastewater was proposed as a means to improve the treatment efficiency of the current process. However, little documented information existed on the performance and optimization of a DAF for chicken processing wastewater application. This study was initiated to asses the overall viability of using a DAF at a chicken processing plant. The specific objectives of the study were to:

1. Design and construct a bench-scale DAF system, with features to vary air flow rate, water flow rate, system pressure, recycle ratio, and hydraulic retention times. Experimentally assess the effects of air flow, HRT, pressure and temperature on bubble production and DAF efficiency (Chapter 2).
2. Evaluate the effectiveness of using several inorganic coagulants and flocculants that can be utilized as a pretreatment in a DAF system for removing organic contaminants and oils in the wastewater (Chapter 3).
3. Determine the overall efficiency of the flotation process and assess the suitability of such a system for treating wastewater from a poultry processing plant (Chapter 4).

Chapter 2: Dissolved Air Flotation Operation

2.1 Introduction

A dissolved air flotation (DAF) unit operates by compressing air and water in a saturation (dissolution) chamber to produce tiny microbubbles used for particulate removal. Typical pressures used to ensure small bubble production range from 50-90 psi (Edzwald, 1995). At these pressures, the air solubility in water increases drastically, causing the water to become supersaturated with air. When the water is released from the dissolution tank and is exposed to atmospheric pressure, the dissolved air is released from saturation and forms tiny microbubbles with diameters ranging from 10 to 100 um with typical diameters of 40 um (Edzwald, 1995). A common occurrence of this process can be seen when the cap of a soda bottle is unscrewed for the first time and the carbonation in the bottle is released. The microbubbles that are released carry to the surface and remove any undesired particulate matter in the waste flow. The incorporation of these micro bubbles into a wastewater flow is achieved by three distinct pressurization methods (Table 2.1).

Table 2.1: Methods of dissolved air flotation pressurization

Name	Description	Positives	Negatives
Full-flow	Pressurizes full raw waste flow in dissolution tank	• Immediate contact between bubbles and particulates • High solid loading	• Ineffective with fragile flocs • High shear on pump head because of solids • Low flows
Partial-flow	Half of the raw waste flow is pressurized and is mixed in with the raw unpressurized flow	• More economical since less flow is pressurized • Less wear on pump	• Low solid loads • Less air available for flotation • Minor pump wear
Recycled-flow	Clean, treated flow is pressurized and mixed with raw untreated waste flow	• No stress on pump because of solids • High solid loading • Low shear	• Large hydraulic load with recycle flow • Requires additional water source

The first method, known as full-flow flotation, pressurizes the waste flow in the dissolution chamber before sending the flow to the flotation tank (Al-Shamrani et al., 2002).

This method eliminates the need for additional water use by dissolving air into the wastewater and allowing the bubbles to make contact with any particulates as the flow is released to atmospheric pressure. Full-flow flotation exposes the floc (accumulated particles) to high shear forces and turbulence from the pump, dissolution tank, and pressure control valve which tend to destroy fragile flocs formed prior to pressurization, thereby limiting the effectiveness in some applications (Ross et al., 2000). Therefore, high floc shear strength is required in this application as well as a pump capable of handling the additional stress of particles in solution. The full-flow flotation method is commonly used for particles which do not need flocculation but require large volumes of air bubbles (Al-Shamrani et al., 2002).

The second method, split-flow flotation, uses a partial aeration system where only about 50% of the wastewater is pressurized. The other half of waste flow is sent directly to the flotation tank where it is mixed back into the pressurized flow. Waters with lower suspended solid concentrations are used with this process since only half of the water is actually aerated when sent into the flotation tank (Al-Shamrani et al., 2002). Compared to the full-flow method, this process is more economical because less water is being pressurized for the separation process (Schwoyer, 1981). However, pump wear still is anticipated due to increased friction resulting from the solids contained in the portion of the water that is pressurized.

The third method, recycle-flow flotation, pressurizes a clean (particulate free) recycle flow drawn from the treated wastewater to dispense the microbubbles back to the sludge flow. The bubble saturated flow is mixed with the treated water in the contact zone of the flotation tank, where the microbubbles produce a dense cloud that collides with the effluent and carries the light weight particles to the surface where they can be skimmed for disposal. The clean water below is then circulated back to the dissolution tank for additional pressurization. This method eliminates the shear of dirty wastewater flow through the pump and allows for higher

flow rates, but requires larger hydraulic loads from the dissolution tank (Schwoyer, 1981). Generally, the benefits of higher air saturation and undisturbed floc formation outweigh the increased total hydraulic loading that a recycle pressurization system imparts on the flotation system (Ross et al., 2000).

2.1.1 Recycle-flow Pressurization

Of the three methods, the recycle-flow pressurization system is the most commonly used process today (Al-Shamrani et al., 2002; Ross et al., 2000, and Schwoyer, 1981). By keeping the waste flow and air saturated flow separate, the operator is capable of controlling the volume of air required to treat a specific wastewater system. The recycle ratio (R_r), defined as:

$$R_r = Q_r/Q_w \qquad \text{Eq. 2-1}$$

Where (Q_r) is the air saturated recycle flow and (Q_w) is the waste flow, is used as a standard measure of the air supplied by a dissolved air flotation unit (Edzwald, 1995). Figure 2.1 displays the interaction between recycle flow and waste flow.

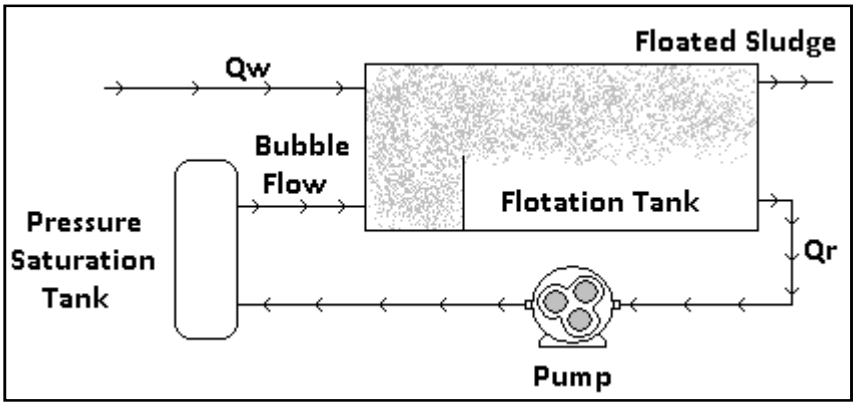

Figure 2.1: Recycle-flow pressurization

Depending on air solubility and the concentration of solids in the waste flow, recycle ratios vary anywhere from 10 to 100% (Metcalf and Eddy, 2003). Lower recycle ratios indicate a more efficient system since less recycle flow is required to treat the waste flow (Ross et al., 2000).

Minimizing the amount of recycle flow in a system is achieved by maximizing bubble production so as to increase the capture efficiency.

Capture efficiency is defined as the ratio of the number of bubble-captured particles over the number of particles initially located in the volume that the bubbles swept (Sarrot et al., 2007). As the bubble concentration increases, so the collision opportunity between bubble and particle also increases, and as the collision between particle and bubble increases, so does the attachment efficiency (Han et al., 2007). Maximizing the air solubility will increase bubble production and provide maximum removal of the targeted pollutant.

2.2 Factors Influencing Air Solubility

Air is a gas composed mainly of nitrogen (78.084%) and oxygen (20.946%) with trace amounts of carbon dioxide (0.032%) and argon (0.934%) (Timmons et al., 2002). These gases transfer to and from water in attempts to reach a state of equilibrium. The equilibrium concentration of a dissolved gas depends mainly upon the temperature of the water and partial pressure of the gas in the atmosphere in contact with the water (Faust and Ally, 1995). In a pressure saturator, however, the hydraulic retention time and air input volumes are also important factors. These four factors and their influence on the solubility of nitrogen and oxygen, and therefore, the overall air solubility, are provided in Table 2.2.

Table 2.2: Factors influencing the solubility of air in a pressure saturator

Variables influencing air solubility	Proportionality to air solubility	Ranges of interest
Pressure	Directly	50-90 psi
Temperature	Inversely	7-28 ^{o}C
Hydraulic Retention Time	Directly	7-25 minutes
Air Input Rate	Directly	0-1 cfh

2.2.1 Pressure

The relationship of air solubility with pressure is defined in Henry's Law, which states that the amount of gas that can be dissolved in a given volume of liquid at a constant temperature is directly proportional to the partial pressure of the gas (P), which is given by:

$$P = K_c M \qquad \text{Eq. 2-2}$$

Where (K_c) is a variation of Henry's constant as defined by Haarhoff and Steinback (1996) for a specified gas and (M) is the molar concentration of the gas in solution. Since air is mostly composed of nitrogen and oxygen, the molar concentration of air (M_a) with respect to pressure is provided by:

$$M_a = M_n + M_o = P_n/K_{c,n} + P_o/K_{c,o} \qquad \text{Eq. 2-3}$$

Where M_n = molar concentration of nitrogen
M_o = molar concentration of oxygen
$K_{c,n}$ = Henry's constant for nitrogen at a given temperature
$K_{c,o}$ = Henry's constant for oxygen at a given temperature

Therefore, as the pressure of the system increases, the amount of air (mostly N_2 and O_2) dissolved into water will also increase. The theoretical effects of pressure on the solubility of nitrogen and oxygen can be found in Appendix A.

Henry's law, however, is found to be an accurate description of the behavior of gases dissolved in liquids only when concentrations and partial pressures are reasonable low (0-45 psi) (Russell, 2006). Instead of increasing linearly forever, Henry's law loses it accuracy and the pressure/solubility curve begins to plateau. Higher pressures will provide greater solubility, but there is a diminishing return in pressures over 500 KPa (73 psi) (De Rijk et al., 1994). Determining when an increase in pressure no longer provides a suitable increase in air solubility due to higher energy consumption would be beneficial in maximizing overall DAF efficiency.

2.2.2 Temperature

Temperature, conversely, has an inverse relationship with air solubility, with cooler water temperatures increasing air solubility and warmer temperatures decreasing air solubility. Henry's law accommodates temperature with its gas constant, K_c, which increases in magnitude with increasing temperature. The relationship of Henry's constant and temperature is expressed in the following van's Hoff-type relationship (Faust and Aly, 1995).

$$\log K_c = \frac{-H^o}{2.3RT} + K \qquad \text{Eq. 2-4}$$

Where K_c = Henry constant
H^o = heat absorbed in the evaporation of 1 mol of gas from solution, kcal/kmol
R = universal gas constant, 1.987 kcal/kmol
T = absolute temperature, ^oK
K = individual gas constant

Cooler water temperatures are more suitable for the DAF application, because the gases are more easily dissolved and the final volume of air dissolved is greater. The increased air solubility at cool water temperatures, however, is offset by reduced saturation efficiency (actual air mass dissolved/theoretical air mass dissolved) at lower temperatures (Haarhoff and Rykaart, 1995). As long as the temperature falls in the range of 5 to 30 ^oC, the dissolution of air into water should have minimal variability for the DAF system.

2.2.3 Hydraulic Retention Time

The hydraulic retention time (Figure 2.2) of the dissolution tank (HRT_d) also has a direct correlation with the solubility of air in water. The hydraulic retention time of a dissolution tank is the quotient of the water volume (V) in the tank and the recycle flow rate (Q_r) of the effluent.

$$HRT_d = V/Q_r \qquad \text{Eq. 2-5}$$

When the recycle flow rates are increased, the HRT_d is decreased, thereby reducing the amount of time for full saturation to be achieved. Longer retention times allow the system to reach equilibrium, which would ensure greater air solubility. The hydraulic retention time of the dissolution tank, however, is often superseded by the hydraulic retention time of the flotation tank (HRT_f).

The HRT_f is characterized as the quotient of the volume (V) of the flotation tank and the combination of the waste flow (Q_w) and recycle flow (Q_r).

$$HRT_f = V/(Q_w + Q_r) \qquad \text{Eq. 2-6}$$

Assuming the waste flow to be defined for a particular system, the recycle flow exiting the dissolution tank is the major operational factor controlling the HRT_f.

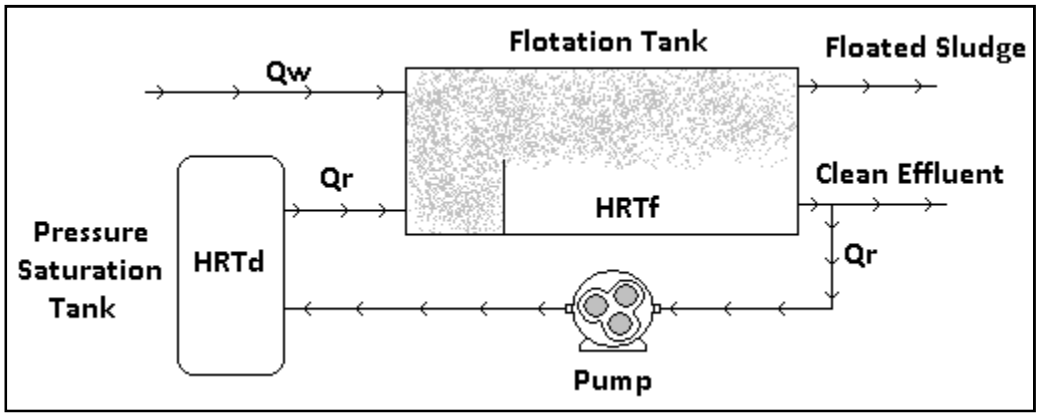

Figure 2.2: Hydraulic retention time of dissolution and flotation tanks

Variations in the HRT_f are designed to provide suitable bubble concentrations and turbulence so that the maximum bubble/floc agglomerates are formed. Kitchener and Gochin (1981) mention that enough recycle flow must exist in order to provide adequate collision opportunities between bubbles and flocs, but that too much flow could break the flocs and detach the bubbles because of turbulent conditions. Good bubble attachment has been seen between

hydraulic surface loadings of 40 and 98 m/h (Lundh et al., 2002), but Chung and coworkers (2000) recommend a surface loading of only 7.5 m/h for their flotation tank.

This wide range of HRT_f, however, does not indicate an effect on the air solubility of the dissolution tank as a result of variations on HRT_d. Haarhoff and Rykaart (1995) agree that the shortcoming of using HRT_f as a guideline for DAF modeling is that the air solubility of the pressure saturator is not taken into account.

2.2.4 Air Flow

Saturation in an air saturator can not be achieved unless the minimum amount of air expected to dissolve in solution is supplied to the system. The amount of air flow needed can be determined from theoretical calculations of air solubility and flow rates.

$$Q_a = Q_r C \qquad \text{Eq. 2-7}$$

Henry's law (Eq. 2-2) is used to determine a theoretical molar concentration of air that will dissolve in water based on temperature and pressure. This value defines the theoretical dissolved volume of air (C). The recycle flow rate (Q_r) is determined by the hydraulic retention times of the system. The product of these two variables provides the minimum air flow rate (Q_a) needed to reach maximum air solubility.

Air is incorporated into the dissolution tank through two typical practices. One method is by having a line open to the atmosphere join the water intake line before reaching the pump. This allows the pump to draw air into the water line before being compressed in the saturation tank. This method provides little control over the air that is brought into the system, but the pump's shear assures air dissolution. The second method is by using a compressor to directly inject the air into the tank. Air flow is easily controlled in this process, but the benefit of extra mixing of the pump is lost.

2.3 Experimental Design

2.3.1 DAF Design

The recycle-flow pressurization design was used in the construction of this bench scale DAF unit. Clean water was pressurized so that the effects of pressure, temperature, retention time, and air flow on air solubility could be determined. This allowed optimizing the system before incorporating a waste flow.

The DAF system was designed with the capability for hands on control of the pressure, air flow, water temperature, and water flow. Power for the system was supplied through four available GFCI outlets accompanied with an immediate cutoff switch. An air compressor and water pump were powered through these outlets during operation. The air and water lines were kept separate until reaching the dissolution tank as seen in Figure 2.3.

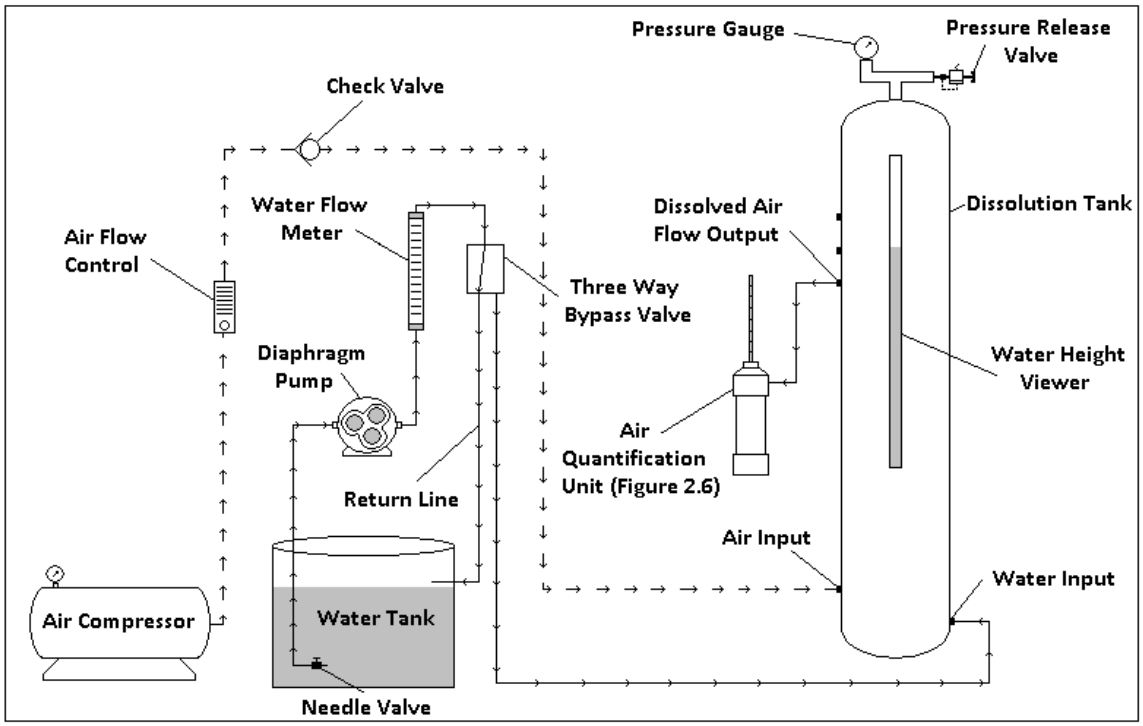

Figure 2.3: DAF Setup

The dissolution tank (Figure 2.4) was made with a 4.5 foot long, 6 inch diameter stainless steel pipe with welded end caps to form a water and airtight tank capable of holding 6.73 gallons

of water. This volume allowed a variation in the retention time from 4 to 50 minutes. Eleven stainless steel threaded female couplings with ½ inch diameter were welded at various locations on the tank for input and output ports. One port at the top of the cap accommodated a pressure gauge and continuous pressure release valve. The pressure gauge could measure up to 160 psi, though the system was not anticipated to exceed 100 psi. The pressure release valve allowed the system to maintain at any pressure ranging from 0 to 100 psi by bleeding off any excess air.

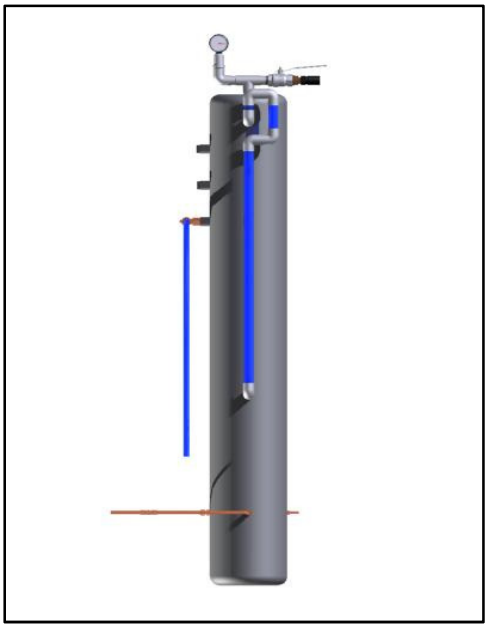

Figure 2.4: Dissolution Tank

Two couplings in the front of the cylinder, separated by about 24 inches, were used to connect a ½ inch clear pvc pipe for observing the water level. Observing the water level was beneficial to the system in two ways. When the water level was too high and posed a dangerous situation, the system was shut down until the water dropped to a satisfactory level. Also, steady state was capable of being maintained between the inflow and outflow by sustaining the water level at a constant height.

Three ports along the upper left side were used as water flow outlets. Only one was used at a time while the other two were plugged. The multiple ports allowed the observation of bubble production from various heights within the column. A 5/32 inch needle valve was used to control the exiting flow of the system.

A diaphragm pump was used to push water into the dissolution tank at high pressures through one port at the bottom of the tank. The pump had an emergency cutoff feature that would shut the pump down when pressures exceeded 100 psi. The pump would not turn back on

until near atmospheric pressures were reached. Instead of draining the system of all pressure and starting over again, a three way valve was placed inline between the pump and tank. This allowed an immediate switch to a return line open to the atmosphere which would turn the pump back on while closing off the dissolution tank with its pressure maintained. The pressure could be adjusted within the tank by loosening the pressure relief valve, and the flow could be redirected to the tank to proceed with the operation. To prevent damage to the diaphragm pump, the water flow was restricted on the suction side of the pump. A needle valve submerged within the clean water tank adjusted the inflow of the pump which was measured with an inline flow meter.

Three additional ports, separated by 120 degrees around the bottom, were used for air injection. Mass transfer is enhanced at the water/air interface by setting up a circulation pattern by air injection below the water surface (Haarhoff and van Vuuren, 1995). Introducing air at the bottom allowed for better mixing throughout the tank as the bubbles displaced the water volume as they carried to the surface (Figure 2.5).

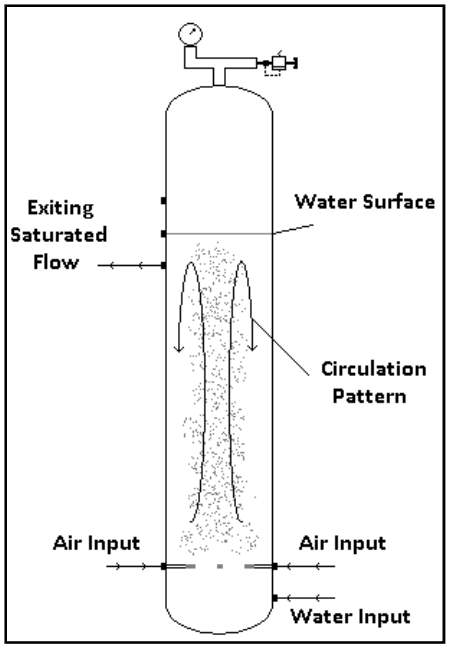

Figure 2.5: Circulation pattern due to air injection

Through each of the ports, a compressor delivered air through 5/8 inch copper tubing which had fine air stones (Aquatic Eco, item #AS1) attached to the ends. Sending air through the stones created small bubbles which provided greater surface area for increased gas transfer into the water. A flow control meter was placed inline between the compressor and tank for air adjustment. A check valve was placed behind the meter to prevent the backflow of water from the tank when the compressor was shut off.

2.3.2 Air Quantification

Increasing the air saturation of the dissolution tank increased the overall efficiency by requiring less recycled flow to remove an equivalent untreated flow. Understanding how the various parameters of the saturator affected air solubility was possible by quantifying the excess air volume that formed microbubbles. The excess dissolved air volume beyond atmospheric saturation is more important than the total air volume leaving the system (Haarhoff and Rykaart, 1995). The quantification of excess air volume was accomplished by measuring the volume of air that was released after depressurization with a simple volume displacement system (Figure 2.6).

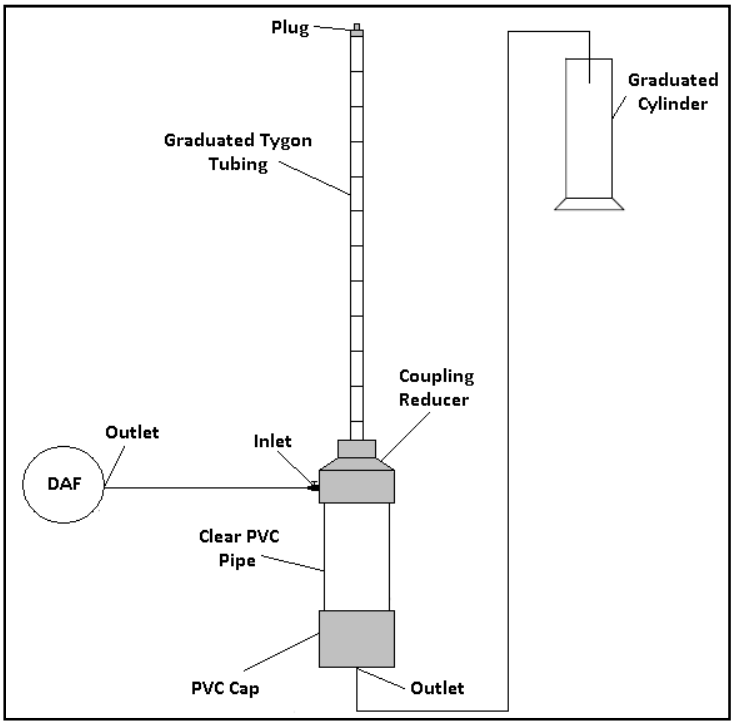

Figure 2.6: Air Quantification Unit

The measuring unit body consisted of a clear 3 inch PVC pipe that was capped on the bottom end and reduced at the top to a ½ inch thread with a coupling/bushing combination. The volume was capable of holding over a liter of water. A ½ inch male thread with 5/8 inch barb was connected to a graduated 5/8 inch ID tygon tubing and was screwed into the top reduced

coupling. The tubing was marked up to100 mL in increments of ten mL. The side of the top cap was threaded for a 3/8 inch needle valve which controls the DAF flow that was entering the system. The bottom cap was threaded with a 3/8 inch barb and 3/8 inch tubing for the outlet flow which was extended to the height of the entire system. Raising the outlet tube to the height of the system prevented the drainage of the system when not in use. Steinbach and Haarhoff (1998) recommend using a similar system for measuring the precipitated air volume with a batch system.

The system quantified the precipitated air volume when the pressure, temperature, retention time, and air flow of the dissolution tank were varied. Each parameter was measured independently from the others. For every measurement taken, the following procedure was followed.

With the inlet closed, the entire system was filled with water so that the water level of the outlet hose was even with the brim of the 5/8 inch graduated tubing. The 3/8 inch outlet tubing remained open to the atmosphere and was dropped into graduated cylinder, while the 5/8 inch tubing was plugged with a rubber stopper to prevent any air release. When ready, the inlet valve was opened to allow the air saturated flow from the DAF system into the measuring unit. The water volume was displaced by the incoming air and water and exited the bottom of the unit where it was measured in a graduated cylinder. When one liter of water was reached, the DAF flow was turned off. During this time, air that was released from solution rose through the 5/8 inch tubing where its total volume was measured. After waiting five minutes to ensure that all the air had released from solution, the plug at the top was removed to equalize the pressure of the system. The mL of air per L of water was measured by reading the volume displaced in the graduated tygon tubing.

2.4 Results and Discussion: System Optimization

The DAF optimization experiments were conducted with an objective to maximize the efficiency of the dissolved air flotation unit by increasing the amount of air dissolved in solution. The effects of the fluctuations in pressure, temperature, hydraulic retention time, and air flow on microbubble production were determined with the air quantification unit.

2.4.1 Pressure

A test was used to measure the microbubble production when varying the pressure of the dissolution tank. The water volume of the dissolution tank was maintained at 20 liters. The flow rate was maintained at 1.8 L/min for a HRT_d of 11 minutes. The temperature was held at 21 ^oC and the air flow was kept steady at 0.3 cfh. The pressure regulator at the top of the saturation tank allowed the pressure to be sustained at 50, 60, 70, 80, and 90 psi. Higher pressures could not be maintained consistently by the regulator and lower pressures would not provide significant results. After one hydraulic retention time (HRT_d), the exiting flow was attached to air quantification unit and the mL of air per L of water was measured in triplicate. When the pressure was changed, three HRT_d were allowed to pass before the measuring process resumed.

The results from this test indicated that the largest average volume of air measured per liter of water was 19.67 mL (± 0.58) and was achieved at 90 psi (Figure 2.7). The best fit curve was linear, which was expected from the pressure/bubble production relationship. The restriction of the pressure regulator prevented any higher pressures from being tested, but it was believed that any increase in pressure would provide little significant advantage in volume of air per liter of water.

Attempting to produce significant quantities of dissolved air bubbles below 50 psi was futile. Without surfactants, the minimum saturation pressure required for DAF to occur was

found to be 3 atm which was explained in terms of the minimum energy needed to be transferred to the liquid phase to form bubbles (Rubio et al. 2002). During this testing, the energy produced below 3 atm (45psi) was not significant enough to create dissolved air bubbles that release from solution and carry to the surface.

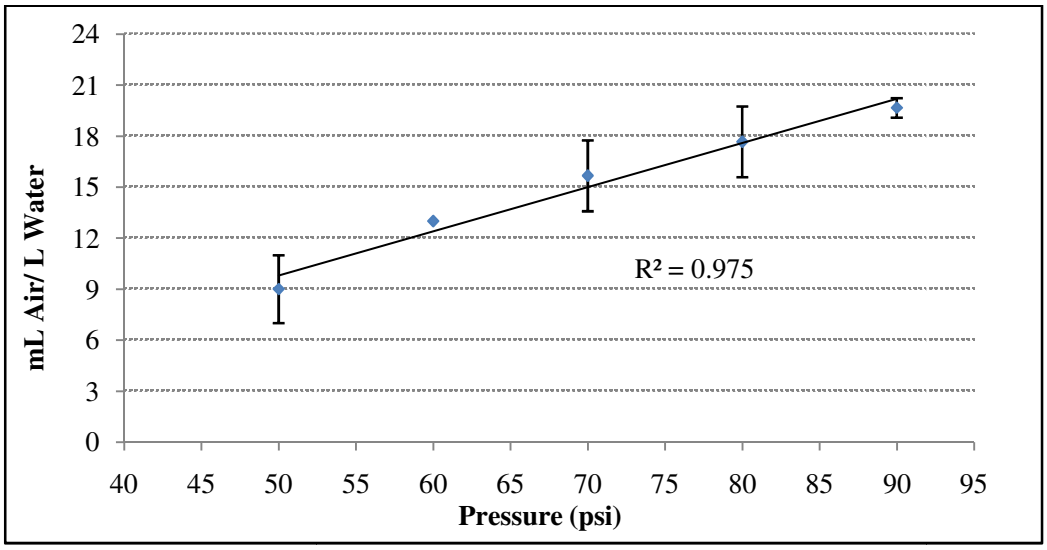

Figure 2.7: The effects of various pressures on the bubble production exiting the dissolution tank. The retention time (11 min), temperature (21 ^{o}C), and air flow (0.3 cfh) were held constant.

It was decided that 90 psi was the best pressure to run the DAF unit despite no statistical difference with 80 psi. At 90 psi, the standard deviation was minimal and provided the highest average microbubble production. There was no benefit seen in running the system at 80 psi, unless it proved to be more energy efficient.

2.4.1.1 Power Consumption

The energy efficiency at various pressures was determined by measuring the power consumption of the pump with a watt meter (P3 Kill A Watt Load Meter) and comparing that value with bubble production previously determined. The air flow rate was maintained at 0.3 cfh. The temperature was held at 21 ^{o}C while the water flow rate was kept at 1.8 L/min for a 20 minute HRT_d. The meter displayed the watts that were consumed by the pump as the pressure in the dissolution tank increased from 0 to 90 psi. Measurements were taken in triplicate during

three different start-up times. This information was important to determine if the increase in air solubility as a result of higher pressure was worth the extra power consumption due to the increased load on the pump.

The results from this test indicated that the power consumption of the pump increased linearly as the pressure of the dissolution tank increased from 0 to 90 psi (Figure 2.8). When the pump ran without pressure on its exiting end, it consumed an average of 24 watts (± 0.0), and when the dissolution tank reached 90 psi the pump doubled it power intake to 50.3 watts (± 2.1). It was anticipated that the increase pressure would put more strain on the pump and require more energy to maintain the flow.

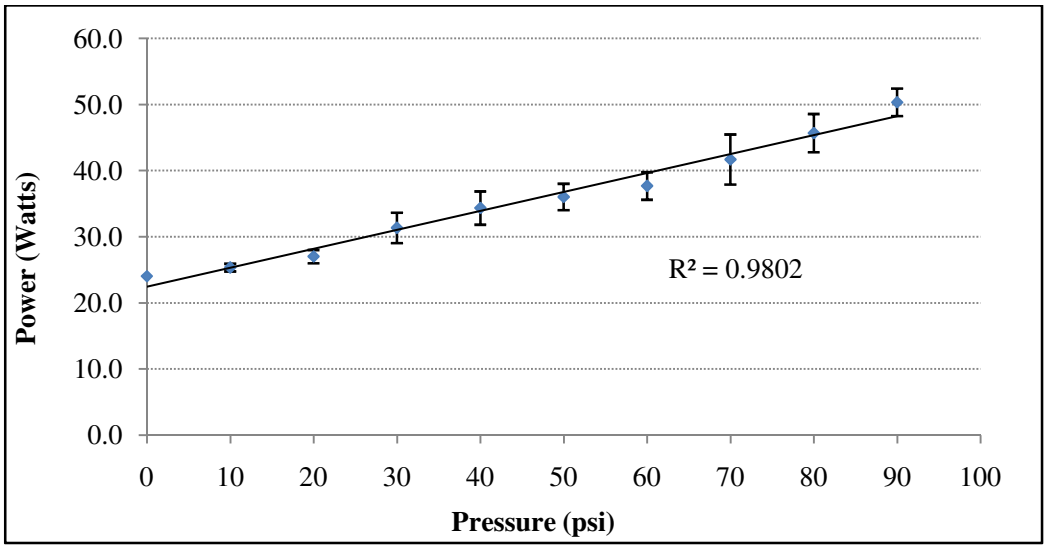

Figure 2.8: The correlation between the increase in pressure in the dissolution tank and the power consumption of the pump.

The values of bubble production and power consumption at various pressures were then compared in Figure 2.9 to determine the efficiency of the system at increasing pressures. The best fit curve was hyperbolic, with an immediate increase from 50 psi to 60 psi, and a peak value achieved at 90 psi. Despite the flattening of the curve at the end, 90 psi was still the most efficient, providing an average of 0.391 mL of air per watt.

The results of the bubble production and power consumption tests indicated that operating a DAF system at 90 psi provided the most air at the lowest energy rate. The flattening of the curve indicated that operating the system above 90 psi would provide no gain in air volume produced per energy usage. Conversely, operating at lower pressures required more energy to achieve the equivalent micro bubble production.

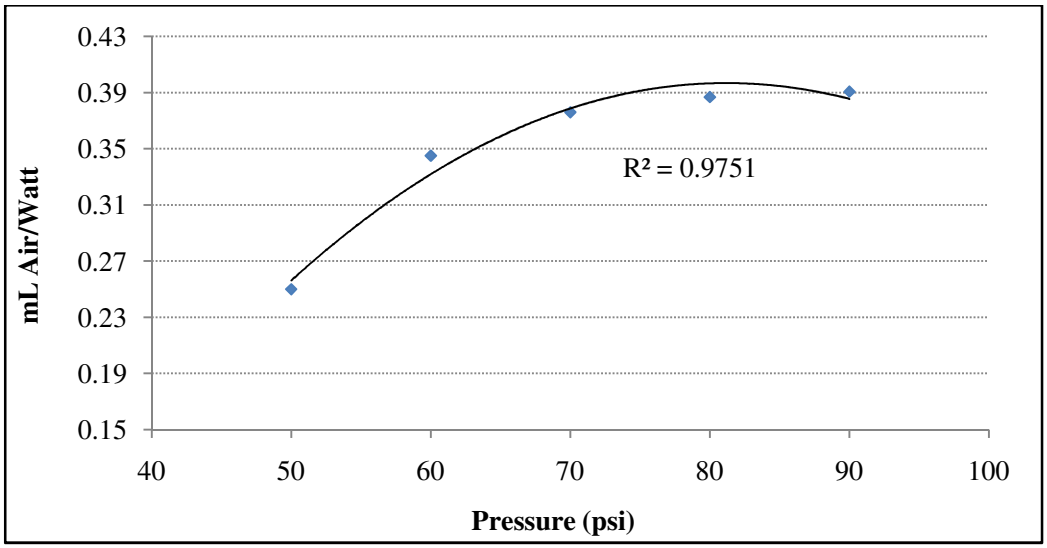

Figure 2.9: The correlation between pressure maintained by the pump and the amount of air released from solution per watt of electricity.

2.4.2 Temperature

A test was used to measure the microbubble production when varying the temperature of the incoming water that would typically be seen in Louisiana throughout the year. The water volume of the dissolution tank was maintained at 20 liters. The flow rate was maintained at 1.8 L/min for a HRT_d of 11 minutes. The pressure remained constant at 80 psi and the air flow was sustained at 0.3 cfh. Ice was used to cool to the water temperature to as low as 7 ^{o}C and water heaters were used to raise the temperature to as high as 35 ^{o}C. After one HRT_d, the exiting flow was attached to air quantification unit and the milliliters of air per liter of water were measured

in triplicate. When the temperature was varied, three HRT_d were allowed to pass before the measuring process resumed.

The results of this test indicated that the bubble production with respect to temperature did not follow as expected (Figure 2.10). The coolest temperature of 7 ^{o}C provided the greatest air solubility, which was expected, and the bubble production had decreased with increasing temperature up until 21 ^{o}C which provided a linear curve. When the temperature continued to increase, however, the bubble production began to increase. This left two data points well outside the anticipated curve.

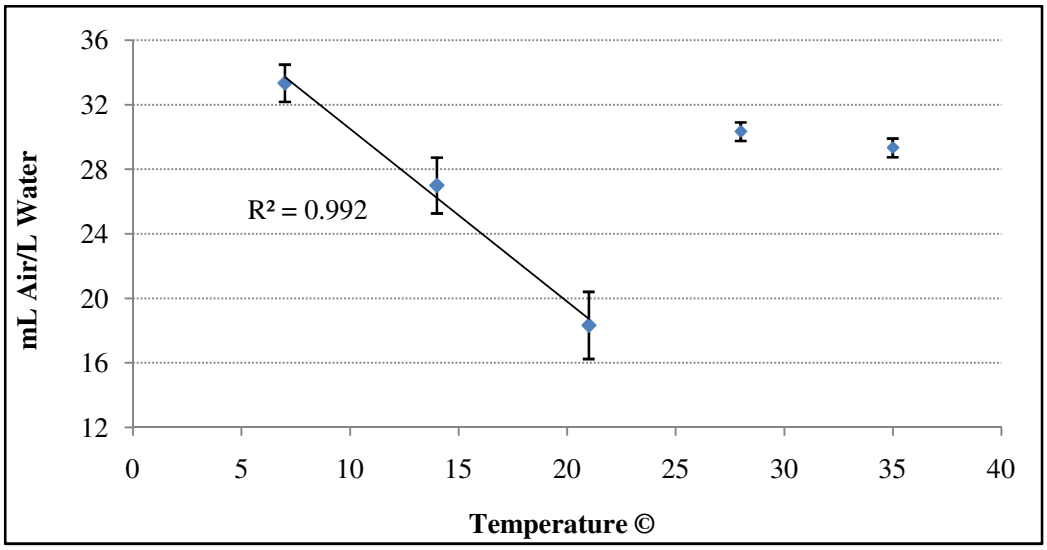

Figure 2.10: The effects of various water temperatures on the bubble production exiting the dissolution tank. The pressure (80 psi), retention time (11 min) and air flow (0.3 cfh) were held constant.

At 28 ^{o}C and 35 ^{o}C larger bubbles were seen in the exiting flow. It was believed that as the water temperature increased, the lower air solubility prevented complete dissolution from all the air that was injected through the system. Since measurements were taken while the system was in continuous operation, larger bubbles from the air input could have been sucked into the exiting flow. Even if the outflow is perturbed by a few big bubbles, they still represent practically all the gas (Ponasse et al., 1998). Even though an appropriate curve was not seen

with this data, it did indicate that microbubble production may be difficult when the temperatures become exceedingly warm, which would be a problem in Louisiana during summer months.

2.4.3 Hydraulic Retention Time

A test was used to measure the microbubble production when varying the retention time of the system. The water volume of the dissolution tank was maintained at 20 liters. The temperature was held at 21 ^{o}C and the air flow was steady at 0.3 cfh. The pressure remained constant at 80 psi. The flow rates were varied at 0.8, 1.3, 1.8, 2.3, and 2.8 L/min. These flows corresponded to 25, 15.4, 11.1, 8.7, and 7.1 minute retention times respectively. Two exiting flows were used to maintain the overall flow rate. One flow remained at 0.8 L/min and was always directed towards the air quantification unit when measurements were taken. The other line increased from 0, 0.5, 1.0, 1.5, to 2.0 L/min to accommodate the larger flows. After one hydraulic retention time (HRT_d), the results were measured in triplicate. When changing to a different flow rate and retention time, three HRT_d were allowed to pass before the measuring process resumed.

The results from this test indicated that an increase in flow rate resulted in a decrease in bubble production (Figure 2.11). Hydraulic loading has the expected effect on saturator efficiency, namely that higher loading leads to lower bubble production (Haarhoff and Rykaart, 1995). The limited amount of time for air to dissolve in solution resulted in poor air solubility and bubble production. The slowest flow used was 0.8 L/min, which provided the greatest amount of dissolved air averaging 25.33 ml air/L water (± 0.58). As the flows increased, the retention times decreased, allowing for a shorter time for air to become fully dissolved.

For this plan of study, a longer HRT_d was desired to allow for greater air solubility within the dissolution tank. A HRT_d greater than 25 minutes may have provided even greater air

solubility, but decreasing the exiting flow also adversely affects the flotation process. If the exiting flow of the dissolution tank is too slow, then the HRT_f is too long, resulting in poor mixing of waste flow and microbubbles for flotation. Since a 1 L beaker was used as the flotation vessel for treating the wastewater, a flow of 1.1 L/min was determined to be adequate to provide an appropriate particulate collisions and HRT_f.

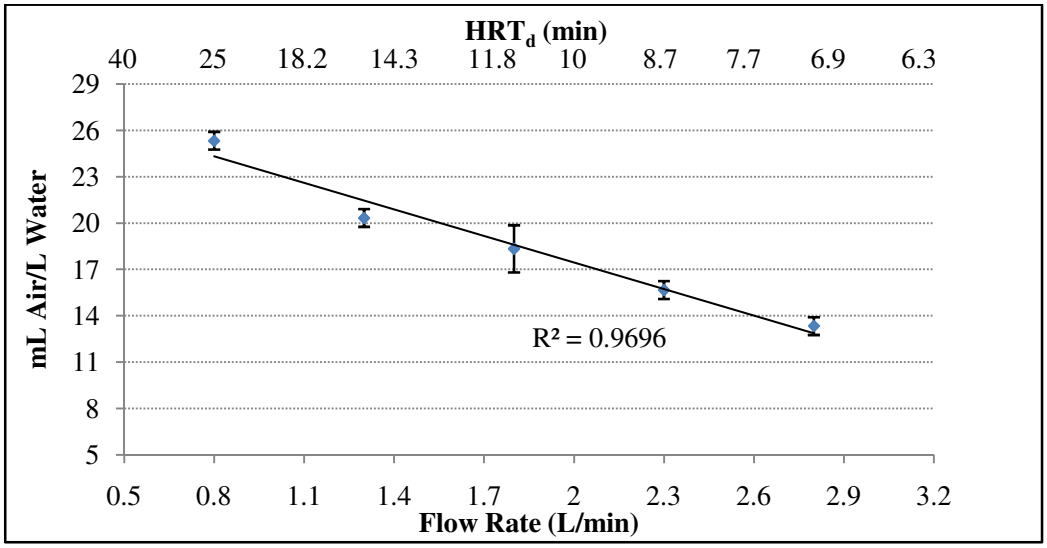

Figure 2.11: The effects of various retention times on the bubble production exiting the dissolution tank. The pressure (80 psi), temperature (21 ^{o}C), and air flow (0.3 cfh) were held constant.

2.4.4 Air Flow

A test was used to determine if increasing the air flow beyond the theoretical required air flow determined by Equation 2-7 would provide any added value in bubble production. The water volume of the dissolution tank was maintained at 20 liters. The flow rate was maintained at 1.8 L/min for a HRT_d of 11 minutes, and the pressure was maintained at 80 psi. The water temperature was noted at 21 ^{o}C and was held constant throughout the test. Under these conditions, it was determined by Equation 2-7 that 0.34 cfh air flow was required to maintain maximum air saturation. An air flow meter varied the incoming air at 0, 0.2, 0.4, 0.6, and 0.8 cfh. After one hydraulic retention time passed, the exiting flow was attached to air quantification

unit and the mL of air per L of water was measured. The measuring process was repeated in triplicate. When switching to a different air flow rate, three HRT_d were allowed to pass before the measurement process resumed.

The results from this test indicated that increasing the air flow beyond the theoretically required air flow (0.34 cfh) provided no statistical value (Figure 2.12). The best fit curve was hyperbolic as it indicated a maximum bubble production around 0.6 cfh and decreased at 0.8 cfh. Even though 0.6 cfh had the highest bubble production, its standard deviation intersected with 0.8 cfh and came close to 0.4 cfh. These values showed no statistical variation.

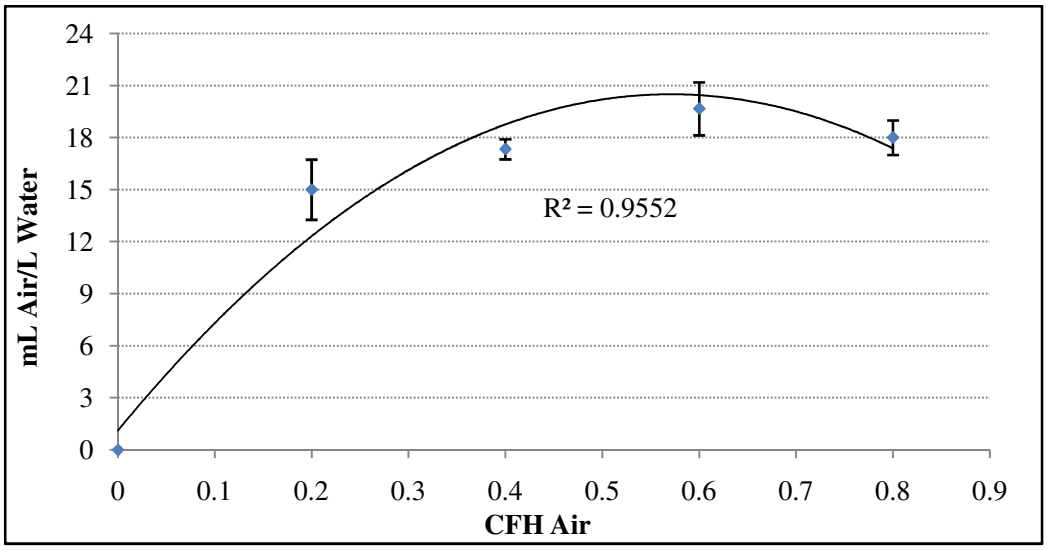

Figure 2.12: The effects of various air flows on the bubble production exiting the dissolution tank. The pressure (80 psi), temperature (21 ^{o}C), and retention time (11 min) were held constant.

It was also noted that when the air flow was increased beyond 0.4 cfh, the microbubble flow was disturbed by additional large bubbles. The increased air input created bubbles with smaller surface areas and poorer gas transfers. Instead of dissolving in solution, these bubbles were drawn out in the exit flow. Since these large bubbles had no added value for the flotation process, the incoming air flow was not increased past 0.4 cfh for further testing. It was determined that the excess air flow negatively impacted the dissolution tank and was not necessary for maximizing microbubble production.

2.4.5 Maximum Production

A test was used to determine the maximum bubble concentration that would exit the dissolution tank when supplying additional aeration. The ideal pressure, temperature, hydraulic retention time, and air flow previously determined were held constant. The water volume of the dissolution tank was maintained at 20 liters. The flow rate was maintained at 1.1 L/min for a HRT_d of 18.2 minutes. The water temperature was 12 ^oC and the pressure of the dissolution tank was maintained at 90 psi. The air flow was held constant at 0.3 cfh. After one HRT_d had passed, the water inflow and outflow were turned off and the system was aerated for an additional 0, 5, 10, 15, 20, 30, 60, 120, and1080 minutes at a rate of 0.3 cfh. The pressure release valve prevented an increase in pressure while the system was being aerated. After the allotted time elapsed, the air was shut off and the system remained undisturbed for five minutes. After this time, the exiting flow line was connected to the air quantification unit and the mL of air per L of water was measured. This process was repeated in triplicate. When the time aerated was varied, the system was allowed to run for three HRT_d to return to start-up conditions.

From this test, an increasing linear trend was observed with the bubble volume as the time of aeration increased to 20 minutes (Figure 2.13). The best fit curve, however, was hyperbolic since the bubble volume plateaued at 30 and 60 minutes, and did not reach a maximum volume (around 107 ml air per L of water) until 120 minutes (2 hours) of aeration. 107 ml air per L of water (± 2.1) was confirmed to be the maximum amount of air that could be released from the saturated water flow since an equal value was recorded after 1080 minutes (18 hours) of aeration. This value was also congruent with the maximum theoretical amount of air that would dissolve at that temperature and pressure (109 ml/L).

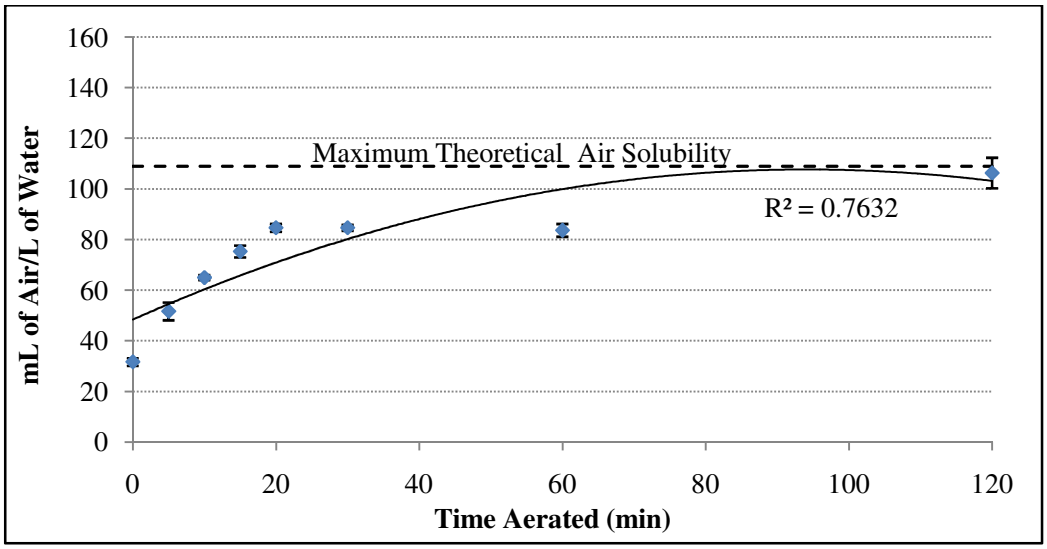

Figure 2.13: The time of aeration required to achieve maximum bubble production released from the exiting flow. The pressure (90 psi), temperature (12 ^{o}C), and air flow (0.3 cfh) were held constant.

It was noted that at immediate startup and no additional aeration, around 30 mL of air (± 1.5) was produced from a liter of water. More importantly was that the air volume that was measured came solely from microbubble production. However, the same microbubble consistency was not seen with the other tests in this set.

As the air solubility increased as a result of longer aeration times, the bubbles exiting the flow were much larger in diameter (approximately 2 mm in diameter as compared to 40 um). Vlyssides and coworkers (2004) indicated a similar problem, stating that during depressurization of water saturated with air, bubbles smaller than 1 um were formed, but through mechanisms not thoroughly understood, they joined and produced a range of bubbles, with sizes between 1 um and a few millimeters.

Wang and Ouyang (1994) indicated that the bubble size distribution was connected with the degree of turbulence caused by the passage of the liquid flow through the nozzle. The supersaturated flow that exited the 5/32 inch nozzle created turbulent flow which caused the microbubbles to coalesce and form larger bubbles.

It was decided that the additional air bubbles were of no use when the dissolution tank reached full saturation because the exiting bubbles were too large. The microbubble production achieved after immediate startup and continuous running was the most suitable for this system.

2.5 Conclusion

Based on the results from the preliminary experiments conducted on the specific setup and within the specified ranges, it appeared that 90 psi, 0.34 cfh air flow, and 1.1 L/min, would provide the greatest concentration of microbubbles in the flotation unit. Temperature would not be controlled for future testing, but warmer waters would result in poorer microbubble production. The raw data that supports these values can be found in Appendix A. However, it should be noted that methods of determining these values did not consider the interaction that these variables would have on one another.

Adjusting, each value of pressure, temperature, retention time, and air flow in conjunction with the others would have required 625 combinations of tests to run. To simplify the measuring process, each variable was studied independently of the others. With each variable optimized under specific conditions, it was believed that the combination of these variables would provide a maximum microbubble production.

From the measurements, it was estimated that these values would provide about 30 ml of microbubbles per liter of water at 12 ^{o}C. Warmer water temperatures would result in slightly lower microbubble production. Increasing the air solubility above 25 or 30 ml/L initiated a new problem due to formation of larger bubbles. By maintaining a lower solubility efficiency with shorter aeration and operation times, the effects of large bubbles were reduced.

Previous authors indicated that these large bubbles disturbing the microbubble flow were a result of the release point and exit nozzle of the air saturated flow. Since these parameters were not taken into consideration during the design of the DAF, they were considered to be

limiting factors in this system's efficiency. Future adjustments to the nozzle and flow release point were recommended to reduce bubble coalescing and large bubble formation.

Chapter 3: Coagulation and Flocculation

3.1 Wastewater Characterization

The wastewater of a poultry processing plant can be described as an oil emulsion with a large suspended solid content. An emulsion is a heterogeneous system, including at least one nomiscible liquid dispersed in another in the form of droplets (Bensadok et al., 2007). This slurry of fats, oils, greases, and fine particles will remain in suspension because of their size, charge, and particle weight. When a liquid contains a suspension of particles that are too small to settle out, even when subjected to the pull of gravity over long periods of time, it is said to be a stabilized colloidal suspension (Schwoyer, 1981).

Colloidal solids and dispersed oils do not respond to flotation, even with the highest values of saturation pressure and recycle ratio invested, unless they are coagulated (Geraldes et al., 2008; Schwoyer, 1981). The purpose of coagulation is to aggregate these particles into larger sizes that will settle quickly or become more accessible for flotation (Faust and Aly, 1997). Han (2001) showed that the removal efficiency increased as the particle size increased above 1 um, and that maximum efficiency was obtained when the particles and bubbles were of similar sizes. Filho and Brandao (2001) have recorded DAF removal efficiencies of 77-90% for turbidity, 70-89% for COD, and 74-95% for TSS with coagulation pretreatment.

3.2 Coagulation Process

Coagulation is the process of chemically changing colloids so that they are able to form bigger particles by coming close to one another (Jarvis et al., 2005). It involves the formation of chemical flocs that absorb, entrap, or otherwise bring together suspended matter that are colloidal (Nemerow, 1978). The aggregation process of these particles to form flocs is described as colloidal destabilization. Four mechanisms of destabilization exist: compression of the

double layer, adsorption for neutralization of charges, entrapment in a precipitate, and adsorption for interparticle bridging (Faust and Aly, 1998).

3.2.1 Destabilization

Colloids are stable in aqueous systems, by virtue of the electrostatic charge on their surfaces (Faust and Aly, 1998). The electrostatic charge is formed across the diffuse double layer due to a potential gradient between the shear surface of the colloid and the bulk solution. The magnitude of this electrostatic potential is measured by zeta potential (ζ), which is indicated by the following equation.

$$\zeta = \frac{4\pi q d}{D} \qquad \text{Eq. 3-1}$$

Where q = charge per unit area
d = thickness of the layer surrounding the shear surface through which the charge is effective
D = dielectric constant of the liquid

When a coagulant is added to the wastewater, its positively charged ions enter the double layer of the colloid and decrease the zeta potential. The double layer is physically reduced in size because of this loss in charge. This first mechanism of destabilization is the double layer compression method.

The second method of charge neutralization is continued with excess absorption of positive ions onto the colloid. This also reduces the zeta potential to an extent where charge reversal is a possibility. These first two methods of destabilization reduce the repulsive charges and make floc formation more likely.

With the zeta potential reduced, the attractive van der Waals forces between particles become dominant and an interaction between colloids occur. This interaction is the entrapment of low zeta potential colloids with precipitates of no net charge (Faust and Aly, 1998). A physical destabilization of the colloid is observed when entrapment occurs.

The final mechanism of destabilization is the interparticle bridging between two destabilized colloids. With the repulsive charges overpowered by the van der Waals forces, the particles come into contact and form bonds. This process of bridging the coagulated colloids to form larger aggregates is known as flocculation (Gregor et al. 1997).

The aggregation process (flocculation) is largely dependent on the duration and amount of agitation applied to the water. The degree of agitation is based on the power imparted on the water, which is measured by the velocity gradient (G) (Reynolds and Richards, 1996).

$$G = \sqrt{\frac{P}{\mu V}} \qquad \text{Eq. 3-2}$$

Where P = power imparted to the water, (N-m/s)
μ = absolute viscosity of the water, (N-s/m^2)
V = basin volume, (m^3)

The rate of particle collisions is proportional to the velocity gradient. However, the rate of shear is also proportional to the velocity gradient, which would destroy flocs if it is too great a value. The power imparted on the water is the controlling factor of the velocity gradient and is measured by turbulent and laminar flow for rapid mixing.

$$\text{Turbulent: } P = K_T n^3 D_i^5 \rho \qquad \text{Eq. 3-3}$$

$$\text{Laminar: } P = K_L n^2 D_i^3 \mu \qquad \text{Eq. 3-4}$$

Where K_T = impeller constant for turbulent flow
K_L = impeller constant for laminar flow
n = rotational speed, (rps)
D_i = impeller diameter, (m)
ρ = density of liquid, (kg/m^3)
μ = absolute viscosity of liquid

The characteristic flow, is subsequently determined by the Reynolds number for impellers, which is given by:

$$N_{Re} = \frac{D_i^2 n \rho}{\mu} \qquad \text{Eq. 3-5}$$

Where $N_{Re} > 10{,}000$ indicates turbulent flow

$N_{Re} < 20$ indicates laminar flow

The second stage of mixing requires a gentler agitation for appropriate flocculation, and its power is measured by:

$$P = C_D A \rho \frac{v^3}{2} \quad \text{Eq. 3.6}$$

Where C_D = coefficient of drag

A = paddle blade area, (m^2)

v = velocity of the paddle blade, (mps)

Metcalf and Eddy (2003) indicate that the typical G values for rapid mixing in wastewater treatment are 500-1500 s^{-1} with a detention time of 5-30 s. The typical G values for flocculation in wastewater treatment are 50-100 s^{-1} with a detention time of 30-60 min.

3.2.2 Metal Salts

A variety of coagulants exist that are used to treat wastewater systems that are classified as colloidal suspensions or oil emulsions. The most widely used coagulants for water and wastewater treatment are aluminum and iron salts (Viessman and Hammer, 1985). When added to the water body, the aluminum and iron cations undergo hydration reactions which produce metal hydroxides, as seen by Equations 3-7 and 3-8 (Faust and Aly, 1998).

$$Al^{3+} + 3H_2O = Al(OH)_3 + 3H^+ \quad \text{Eq. 3-7}$$

$$Fe^{3+} + 3H_2O = Fe(OH)_3 + 3H^+ \quad \text{Eq. 3-8}$$

These metal hydroxides that form are the counterions that begin the destabilization process of the colloids. They are effective in reducing the zeta potential of a colloid because of their high charge densities. In order to complete the coagulation of colloids, it is very important to have most of the added metal coagulant precipitated out as the metal hydroxide floc at the end of the coagulation process (Schwoyer, 1981).

To produce the hydroxide floc, sufficient alkalinity must be present in the water to react with the aluminum and iron cations (Reynolds and Richards, 1996). The alkalinity is a measure of the water's ability to neutralize an acid, and is naturally in the form of bicarbonate. Most variations of iron and aluminum coagulants require approximately 0.5 mg/L of alkalinity in the form of $CaCO_3$ for every 1 mg/L of coagulant used (Cheremisinoff, 2002). If there is insufficient alkalinity in solution, then sodium carbonate or calcium hydroxide is added to supply the $CaCO_3$ needed to complete the hydration reaction (Viessman and Hammer, 1985).

3.2.3 Synthetic Polyelectrolytes

Despite being popular chemical additives for many water treatment applications, the inorganic metal salts often have problems with floc strength. Inorganic coagulants produce lighter, more fragile flocs that are more differentiated in size due to their slow growth and tendency to shear during mechanical and hydraulic stirring (Schwoyer, 1981). Turbulence after chemical treatment is expected in a DAF system, and if the flocs do not maintain their integrity then the operation will not yield anticipated results.

However, results that are observed with synthetic polyelectrolytes are that flocs grow to full uniform sizes more rapidly and are less fragile than flocs of inorganic coagulants (Schwoyer, 1981). Synthetic polyelectrolytes are water soluble, high molecular weight, organic polymers containing chemical groups that undergo electrolytic dissociation in solution, resulting in a long chain of highly charged ions (Viessman and Hammer, 1985). These chemicals can be used as flocculating aids for the primary coagulants (like aluminum and iron salts) if the binding is not satisfactory. Under certain operating conditions, however, polyelectrolytes are capable of neutralizing the surface charges of the colloids as well as forming the interparticle bridges.

3.3 Wastewater Testing

Samples of the wastewater were collected at Sanderson Farms' processing plant after the initial screening process which removed feathers and other large pieces, but before any secondary treatment was initiated. The samples were stored in five gallon carboys and used as needed. If a sample was not being used on collection day, it was refrigerated until testing required it. Samples that were older than three days old were discarded. The raw wastewater was tested for optical density, total suspended solids (TSS), volatile suspended solids (VSS), chemical oxygen demand (COD), fats-oils-greases (FOG), and metals for comparison with testing values. Due to inherent variability associated with poultry processing rates and water usage, a certain degree of inconsistency was expected in the sampled wastewater. Therefore, the properties under investigation were tested on three waste samples collected on different days.

The peak absorbance of the wastewater was determined by using a Genesys 6 UV-Vis Scanning Spectrophotometer on 25, 50, 75, and 100% concentrations of the wastewater. The wavelength of the peak absorbance was then used to determine the optical density of the raw and treated wastewater. The samples measured for optical density were diluted 1:0.75 with distilled water to lower the absorption values within the range of the spectrophotometer. TSS (209 D), VSS (209 E), and COD (508) were determined using Standard Methods (1980). Samples were sent to Callegari Environmental Center for determining FOG (503 A) and metal content within the raw and treated wastewater.

The UV-Vis scanning spectrophotometer indicated that a wavelength of 412 nm would be ideal for quantifying the optical density of samples tested in a visible spectrophotometer (Spectronic Genesys 20). At 412 nm the spectrophotometer measured 3.34 as absorbance of the raw water, which was about as high as the spectrophotometer would read without exceeding the range of the instrument. The absorbance values of sampled supernatant were directly correlated

with TSS during later coagulation testing, providing R^2 values as high as 0.978 (Appendix D). This indicated that the absorbance values were a good indicator of water clarity typically measured by turbidity meters.

The TSS and VSS averaged 3347 mg/L and 2667 mg/L respectively. Although these were extremely high values, such concentrations were expected from a typical wastewater. The original COD value was provided by the treatment plant where they indicated an approximate concentration of 10,000 mg/L from the raw wastewater. The original FOG (fats, oils, and greases) values of the raw samples were 14,297 mg/L which confirmed the presence of a dense oil emulsion. The raw water data is available in Appendix B.

3.4 Chemical Testing

Eleven metal coagulant samples from Southern Water Consultants (Decatur, Alabama) and one polyelectrolyte from Integrated Engineers Inc. (Oakhurst, California) were tested on the poultry wastewater (Table 3.1). Four of the coagulants were aluminum based (EC-309, EC-409, EC-509, EC-609), four of the coagulants were iron based (Ferric Chloride, Ferric Sulfate, Ferrous Chloride, Ferrous Sulfate), and three were specific for oil emulsion breaking (CPF-4168, CPF-4265, CPF-4275). The one polyelectrolyte (Floccin 1115) was an unknown proprietary granular polymer mixed with sodium montmorillonite (clay).

3.4.1 Aluminum Coagulants

A jar test was set up to analyze the effect of the aluminum coagulants (EC-309, EC-409, EC-509, and EC-609) at concentrations of 100, 200, 300, 400, 500, and 600mg/L. A flash mix of 120 rpm (G: 90 s^{-1}) was used for two minutes (GT: 10,800), followed by a 20 minute slow mix of 30 rpm (G: 13.9 s^{-1}, GT: 16,680) and a one hour settling time. The G and GT values were on the low end recommended by Metcalf and Eddy (2003) for all coagulants, so excessive shear was not suspected. However, insufficient particle collision during flocculation may have been

possible. After settling, the height of the settled solids was measured, and pictures were taken to note the compactness of settled solids. The supernatant was collected from the treated samples and tested for TSS and VSS. Optical density of the supernatant was also tested to quantify fine particulates and color (say from blood) since they are not accounted for in TSS and VSS testing.

Table 3.1: Metal coagulants and polyelectrolyte tested for floc formation of the poultry wastewater

Category	Name	Composition	Characteristic
Aluminum Based Coagulants	EC - 309	Polyaluminum Chloride Solution (16% Al_2O_3)	• pH range 5.5-9.0 • Form $Al(OH)_3$ in the presence of sufficient alkalinity for charge neutralization
	EC - 409	Aluminum Chlorohydrate Solution (24% Al_2O_3)	
	EC - 509	90% EC-309, 10% $Fe_2(SO_4)_3$	
	EC - 609	90% EC-409, 10% $Fe_2(SO_4)_3$	
Iron Based Coagulants	Ferric Chloride	$FeCl_3$	• pH range 4.0-12.0 • Form $Fe(OH)_3$ in the presence of sufficient alkalinity for charge neutralization
	Ferric Sulfate	$Fe_2(SO_4)_3$	
	Ferrous Chloride	$FeCl_2$	
	Ferrous Sulfate	$FeSO_4$	
Oil Emulsion Breakers	CPF - 4168	Ferric Chloride Solution (3% Epi-amine)	• Epi-amine and Poly-DADMAC are cationic synthetic polymers • React with solids by charge neutralization and bridging
	CPF - 4265	Ferric Sulfate Solution (5% Epi-amine)	
	CPF - 4275	Ferric Sulfate Solution (5% Poly-DADMAC)	
Synthetic Polyelectrolyte	Floccin 1115	Granular Polymer with Sodium Montmorillonite	• Clay assists in the formation of larger heavier flocs

All four coagulants showed an increase in performance with increasing doses with the best results obtained at concentrations of 600 mg/L. At this concentration, the flocs settled most rapidly and were more compact after settling. The supernatant was relatively clear with a slight red tint. The high organic load constituted by blood and organic materials caused the red color and most of the turbidity (Sena et al., 2009). The worst results were obtained at a concentration of 100 mg/L. At this dosage settling was poor, leaving the supernatant cloudy with particulates.

From the aluminum group, EC-309 showed the best potential at 600 mg/L dosage by reducing the TSS and VSS in the supernatant by 96.6% and 94.5% respectively (Figure 3.1).

The absorbance reading from this supernatant also indicated the best visibility with a 76.4% increase in water clarity (Figure 3.2). The raw data and statistics of the aluminum coagulant testing can be found in Appendix C.

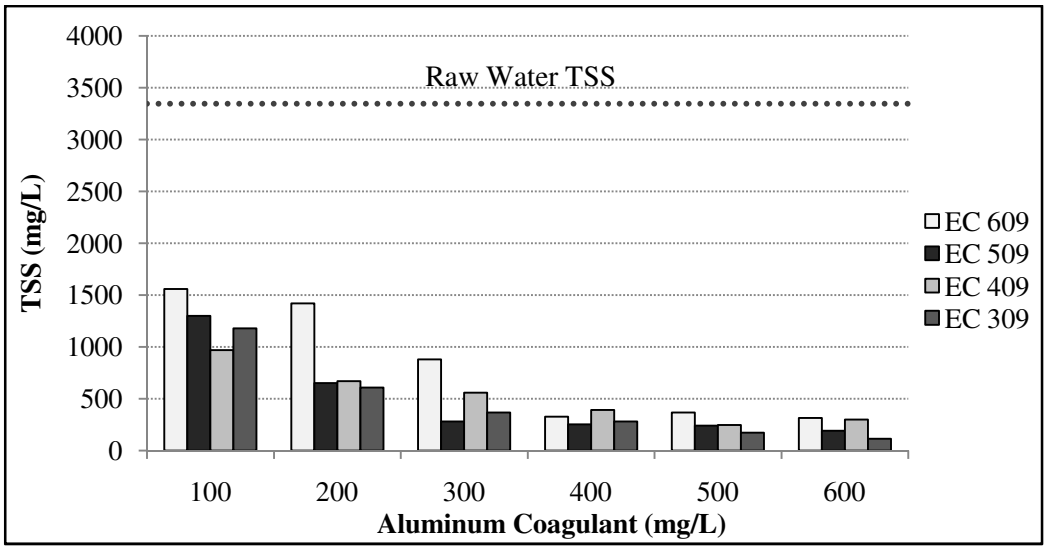

Figure 3.1: The concentration of TSS in the supernatant of poultry processing wastewater after treatment with aluminum coagulants. Samples were mixed at 120 rpm for 2 minutes, followed by 30 rpm for 20 minutes, and one hour of settling.

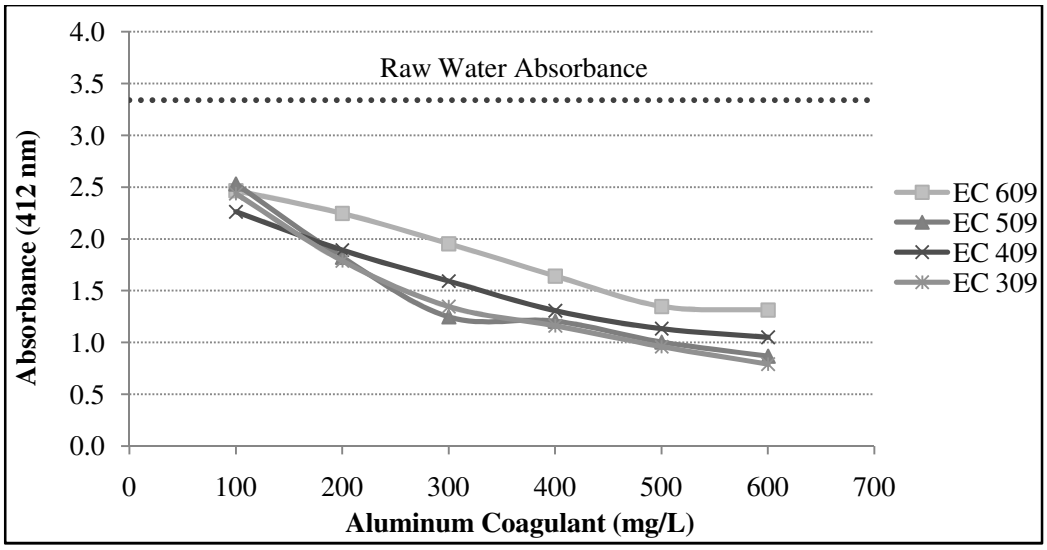

Figure 3.2: The absorbance at 412 nm of the supernatant of poultry processing wastewater after treatment with aluminum coagulants. Samples were mixed at 120 rpm for 2 minutes, followed by 30 rpm for 20 minutes, and one hour of settling.

Even though 600 mg/L of EC 309 was chosen as the best coagulant dose to reduce TSS and increase water clarity, there was only a 6% difference in TSS removal between EC 309 and

the worst aluminum coagulant. At 600 mg/L, all the coagulants had reduced the TSS by at least 90%. Even 300 mg/L of EC 509 was able to reduce the TSS by 91.6%. Despite the similarities, EC 309 was chosen for continued testing because of its overall highest removal values.

3.4.2 Iron Coagulants

A jar test was set up to analyze the effect of the iron coagulants (ferric chloride, ferric sulfate, ferrous chloride, and ferrous sulfate) at concentrations of 100, 200, 300, 400, 500, and 600mg/L. A flash mix of 120 rpm (G: 90 s^{-1}) was used for two minutes (GT: 10,800), followed by a 20 minute slow mix of 30 rpm (G: 13.9 s^{-1}, GT: 16,680) and a one hour settling time. After settling, the height of the settled solids was measured, and pictures were taken to note the compactness of settled solids. The supernatant was collected from the treated samples and tested for TSS, VSS, and optical density.

Best results were achieved at a concentration of 600 mg/L for all of the coagulants, with better clarity and lower suspended solids in the supernatant. The TSS and VSS readings at 600 mg/L were comparable for ferrous sulfate, ferric chloride and ferric sulfate with concentrations differing by a maximum of 60 mg/L (Figure 3.3). Ferric chloride showed strong solids removal by reducing the TSS by 89.4% and VSS by 89.5%. Ferric chloride also exceeded in reducing the red color of the wastewater caused by blood and organics. Its optical density reading at 600 mg/L was 0.817 which indicated a 75.5% increase in water clarity (Figure 3.4). The superior water clarity achieved by ferric chloride determined it to be the best achieving iron coagulant. The raw data and statistics for the iron coagulant testing can be found in Appendix C.

Similarly to the aluminum coagulants, there was only a 1.7% difference in TSS removal between three of the iron coagulants when the concentration was raised to 600 mg/L. The TSS and the optical density tests showed a little disparity between the coagulants, but nothing that

would solidify using one coagulant over another every time. Despite the similarities, ferric chloride was chosen for continued testing because of its overall highest values.

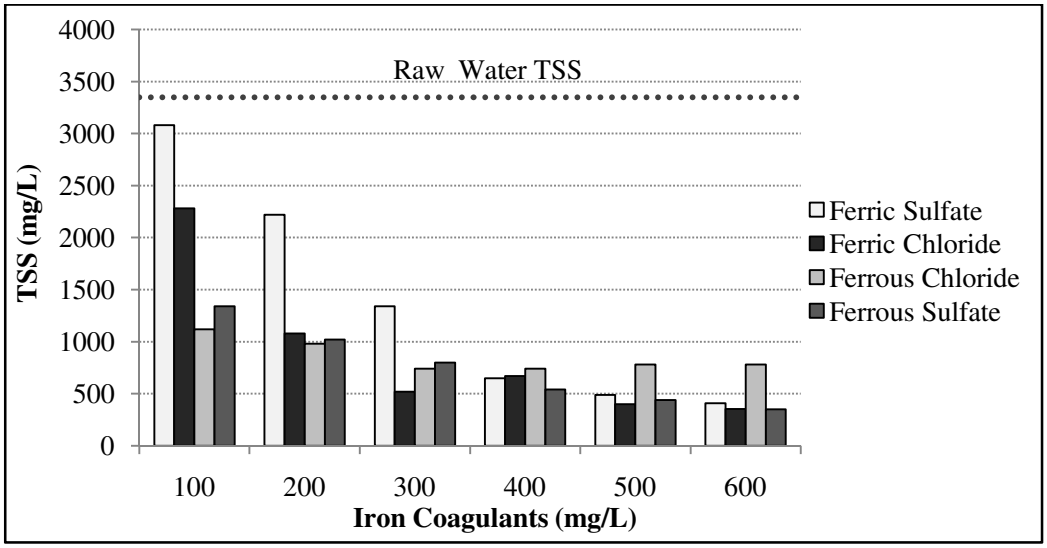

Figure 3.3: The concentration of TSS in the supernatant of poultry processing wastewater after treatment with iron coagulants. Samples were mixed at 120 rpm for 2 minutes, followed by 30 rpm for 20 minutes, and one hour of settling.

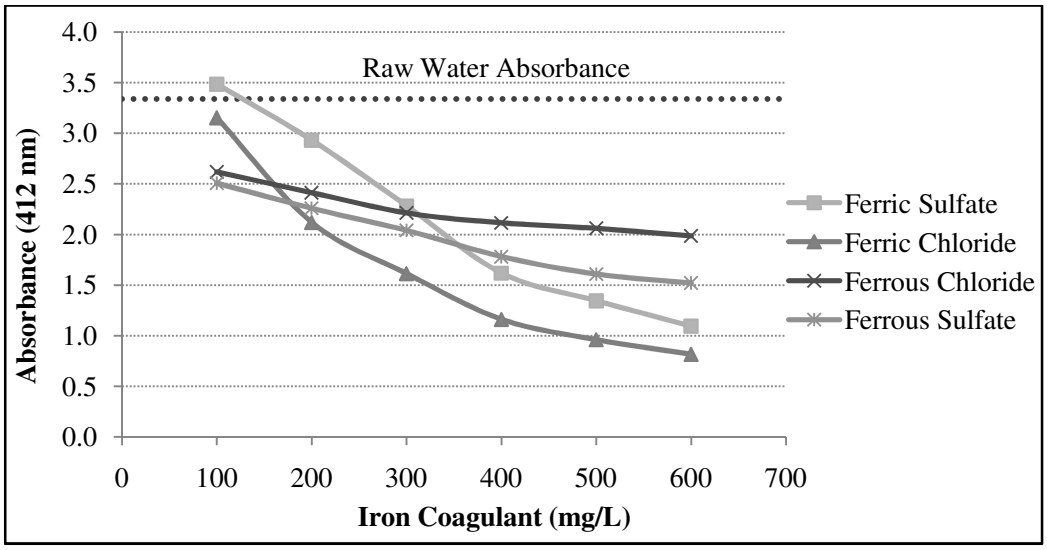

Figure 3.4: The absorbance at 412 nm of the supernatant of poultry processing wastewater after treatment with iron coagulants. Samples were mixed at 120 rpm for 2 minutes, followed by 30 rpm for 20 minutes, and one hour of settling.

3.4.3 Oil Emulsion Breakers

A jar tester was set up to analyze the effect of the oil emulsion breakers (CPF-4265, CPF-4168, and CPF-4275) at concentrations of 100, 200, 300, 400, 500, and 600mg/L. A flash mix of

120 rpm (G: 90 s^{-1}) was used for two minutes (GT: 10,800), followed by a 20 minute slow mix of 30 rpm (G: 13.9 s^{-1}, GT: 16,680) and a one hour settling time. After settling, the height of the settled solids was measured, and pictures were taken to note the compactness of settled solids. The supernatant was collected from the treated samples and tested for TSS, VSS, and optical density.

Once again better clarity and settling were achieved as the concentrations of coagulants increased from 100 mg/L to 600 mg/L. In this group, CPF-4168 was superior in water clarification with TSS and VSS reductions of 93.7% and 91.4% respectively (Figure 3.5) and with a 79.9% increase in clarity (Figure 3.6) when 600 mg/L of coagulant was used.

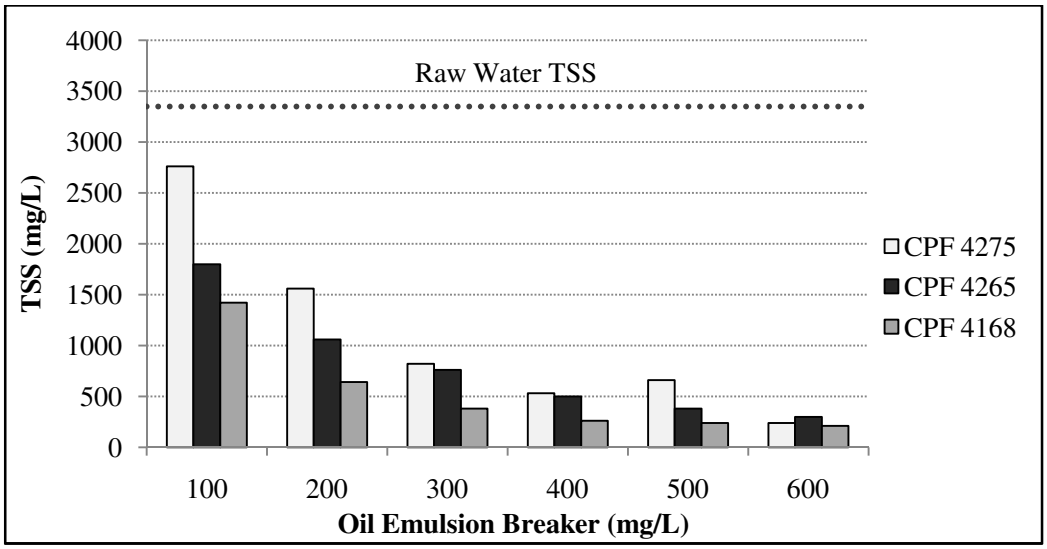

Figure 3.5: The concentration of TSS in the supernatant of poultry processing wastewater after treatment with oil emulsion breakers. Samples were mixed at 120 rpm for 2 minutes, followed by 30 rpm for 20 minutes, and one hour of settling.

Again, the difference between the three oil emulsion breakers was minimal in their ability to reduce the TSS (2.7% difference). At 600 mg/L all three were able to remove at least 91% of the TSS from the supernatant. The main difference was seen in CPF 4168 which was 10% better in the optical density tests. Despite the similarities, CPF 4168 was chosen for continued testing.

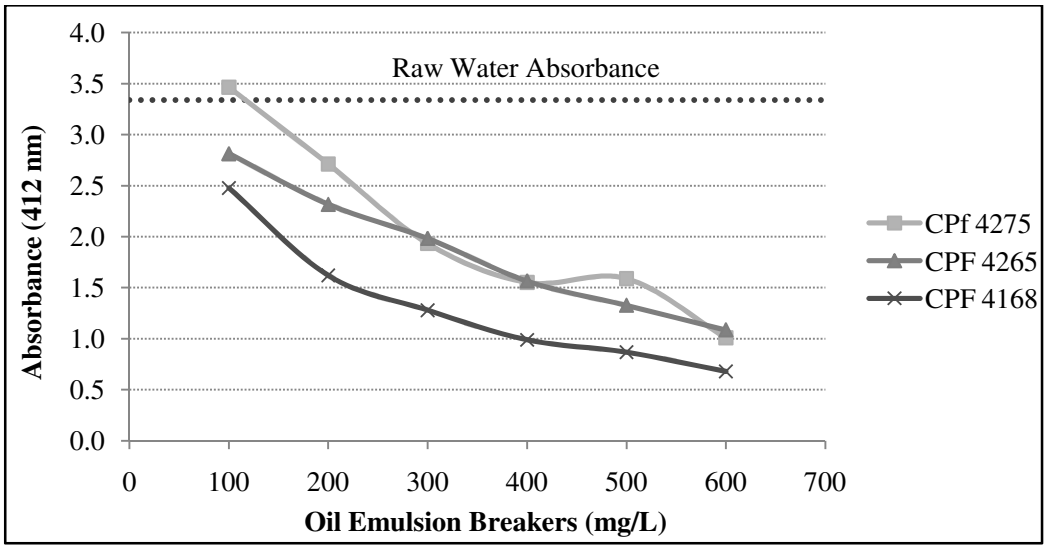

Figure 3.6: The absorbance at 412 nm of the supernatant of poultry processing wastewater after treatment with oil emulsion breakers. Samples were mixed at 120 rpm for 2 minutes, followed by 30 rpm for 20 minutes, and one hour of settling.

3.4.4 Comparative Testing

The best performing coagulant of each group (EC-309, ferric chloride, and CPF 4168) was selected for further testing. A jar test was set up to analyze the effect of the three coagulants at concentrations of 50, 250, 450, 650, 850, and 1050 mg/L. A flash mix of 120 rpm (G: 90 s^{-1}) was used for two minutes (GT: 10,800), followed by a 20 minute slow mix of 30 rpm (G: 13.9 s^{-1} and GT: 16,680) and a one hour settling time. After settling, the height of the settled solids was measured, and pictures were taken to note the compactness of settled solids. The supernatant was collected from the treated samples and tested for TSS, VSS, and optical density. A metal analysis was also performed on the samples to detect excess iron or aluminum in the supernatant, which would indicate the use of excess coagulant.

Typically, during a second round of coagulant testing, a narrower range would be selected to pinpoint the smallest concentration necessary for optimum treatment. The concentrations at which the coagulants were performing the best (400-600 mg/L), however, were not showing a significant difference in their ability to remove solids. Therefore, the goal was to

indicate that a more reasonable concentration of 50 mg/L was not sufficient in treating the wastewater, while clarity continued to increase as chemical concentrations exceeded previous doses.

From a visual standpoint, the volume of supernatant decreased due to poor settling of the flocs as the concentrations of coagulant used increased (Figure 3.7). According to Spicer and coworkers (1998), coagulation increases the average floc size, but decreases its average compactness. With greater coagulation, the flocs increased in size but became fluffy and would not settle. This type of hindered (Type III) settling was caused by the interparticle charges after intense coagulation (Reynolds and Richards, 1996). This was apparent when 850 mg/L and 1050 mg/L of coagulant were used in the jar tests, indicating overdosing of coagulant.

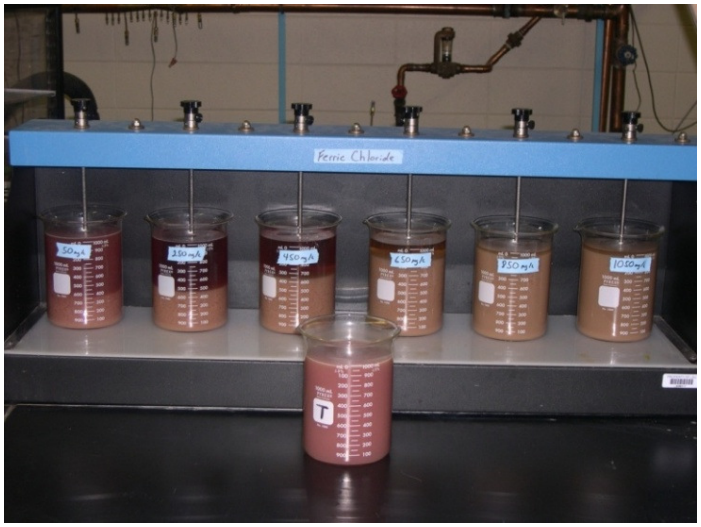

Figure 3.7: The settling of flocs formed by the addition of ferric chloride after 1 hour. Doses increased from left to right, starting at 50 mg/L and finishing at 1050 mg/L. The single beaker in front was raw wastewater.

The clarity of the supernatant, however, continued to increase as the coagulant concentrations increased. Ferric chloride outperformed the other two chemicals with TSS levels reduced to zero at a concentration of 1050 mg/L (Figure 3.8). However, at a 650 mg/L ferric chloride concentration, the TSS and VSS were reduced by 99.6% and 93.8% respectively. Ferric

chloride also had the smallest absorbance at a 650 mg/L which showed a 93.7% increase in clarity (Figure 3.9).

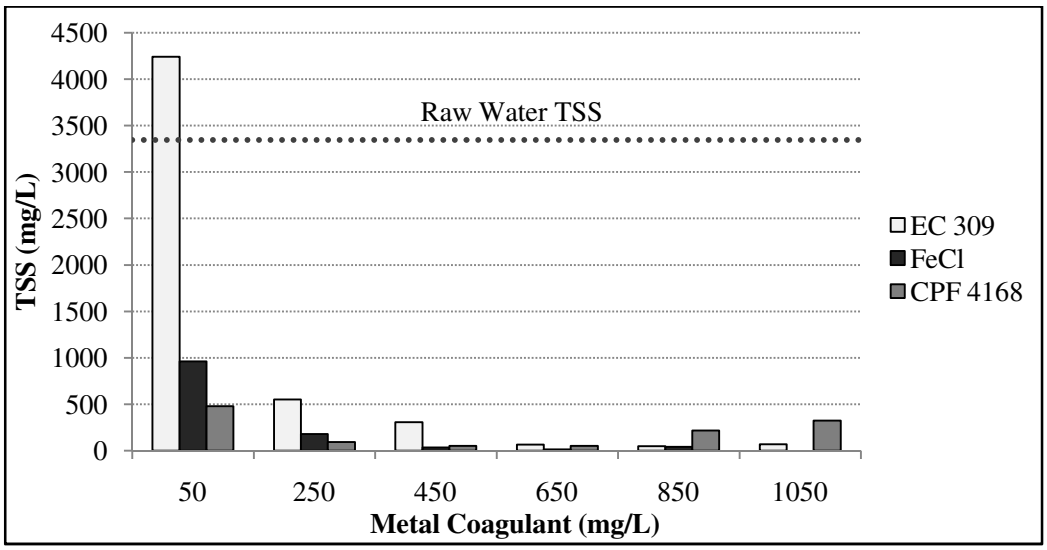

Figure 3.8: The concentration of TSS in the supernatant of poultry processing wastewater after the treatment with EC 309, FeCl, and CPF 4168. Samples were mixed at 120 rpm for 2 minutes, followed by 30 rpm for 20 minutes, and one hour of settling.

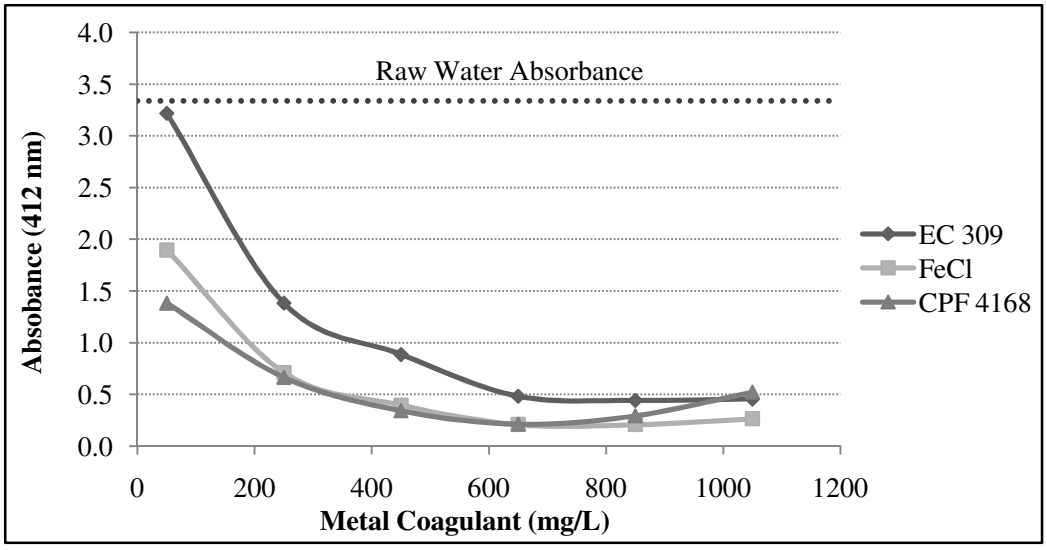

Figure 3.9: The absorbance at 412 nm of the supernatant of poultry processing wastewater after the treatment with EC 309, FeCl, and CPF 4168. Samples were mixed at 120 rpm for 2 minutes, followed by 30 rpm for 20 minutes, and one hour of settling.

The metal analysis did not show any major shifts in the amount of iron or aluminum found in the supernatant after the addition of the coagulants. Before any treatment, the raw water indicated approximately 0.9 mg/L of aluminum and 7 mg/L of iron. As the concentration of

coagulant increased, the metal values in the supernatant remained relatively consistent. The greatest increase seen was a doubling of the values of aluminum and iron to 1.8 mg/L and 16.4 mg/L when 1050 mg/L of their respected coagulants were used. Considering the amount of coagulants used and the residual amount detected, this increase was negligible.

Since the residual metals detected by Callegari Environmental Center were considered negligible, and superior water clarity was achieved when 650 mg/L of ferric chloride was used, overdosing was not suspected at the time. However, alkalinity concentrations were not considered when applying the coagulants. It was later determined that 0.56 mg/L of alkalinity as $CaCO_3$ would be required to react with 1 mg/L of $FeCl_3$. According to the Hammond Water and Sewer Department, their ground water only averaged 141 mg/L of alkalinity and was not adjusted before entering the plant. Sanderson Farms indicated no change in alkalinity before they begin their wastewater treatment process. Therefore, the appropriate dose of ferric chloride would average 250 mg/L.

At 250 mg/L doses of ferric chloride and CPF 4168 were seen to reduce the TSS of the supernatant by 94.6% and 97.2% respectively (Figure 3.8). This seemed to indicate that the selected dose of 650 mg/L of ferric chloride was too much.

The lack of excess iron or aluminum in the supernatant and the previously unnoticed overdosing, therefore, was most likely associated with the precipitation of phosphate. From the metal analysis, it was determined that the poultry processing wastewater averaged 437 mg/L of phosphate. The basic reaction involved in the precipitation of phosphate required one mole of aluminum or iron to precipitate one mole of phosphate (Metcalf and Eddy, 2003). This reaction was competitive with the formation of metal hydroxide bonds forming $FePO_4$ or $AlPO_4$ flocs at the expense of hydroxide flocs with decreasing pH (Fair, Geyer, and Okun, 1968).

Boisvert and coworkers (1997) noted that in the presence of PO_4, the average size flocs derived from the coagulants decreased significantly. Despite the significant water clarity achieved with the coagulants after settling, it was believed that these fragile flocs would not be suitable for DAF application. Further investigation into floc formation was continued with the synthetic polyelectrolyte.

3.4.5 Synthetic Polyelectrolyte

The polyelectrolyte, Floccin 1115, was selected by Integrated Engineers (Oakhurst, California) as their most suitable bridging agent for the wastewater flocculation. Destabilization by bridging occurs when segments of a polymer chain absorb on more than one particle, thereby linking the particles together (Li et al. 2006). Preliminary tests with the substance were outstanding, with the formation of solid flocs that would maintain shape and leave the supernatant clear of any particulates within minutes. One obvious consequence of bridging flocculation is that the flocs produced can be much stronger than those formed when particles are destabilized by simple salts (Yukselen and Gregory 2004). However, a concentration of 1.5 g/L was required to achieve these results.

A series of jar tests were conducted to optimize the amount of Floccin added for appropriate floc production. As recommended by the manufacturer, the wastewater was subjected to steady flash mixing at a consistent speed of 120 rpm (G: 90 s^{-1}) until a noticeable change in water clarity was achieved. The supernatant of all the following samples were tested for TSS, VSS, and optical density.

The first set of tests used 1, 1.5, 2, 2.5 and 3 g/L of Floccin 1115 to compare the variations in treatment clarity to chemical concentration. After 10 minutes of stirring, however, no changes were seen. This contradicted the immediate results which were achieved previously with 1.5 g/L.

To induce results, the pH of the five samples, which started at 6.36, was lowered with concentrated sulfuric acid. The first change was seen in the sample with 3 g/L of Floccin when the pH reached 5.3, and eventually the lower concentration followed suit. When the absorbance and TSS of the supernatant was taken, it was determined that 1.5 g/L of Floccin at a pH of 5.0 would yield suitable results (Appendix D).

The low pH was of concern, since it seemed necessary for the Floccin to become active and form flocs. Dropping the pH to such acidic conditions would not be practical for real application. Integrated Engineers claimed that the flocculent would perform better when the wastewater was near neutral pH, so three samples were prepared at pHs of 5.4, 6.4 and 7.4.

Each sample was tested with 1500 mg/L of Floccin, and once again the sample at a lower pH outperformed the original sample (pH 6.4) and sample brought near to neutral (7.4) (Figure 3.10). The sample with a 5.4 pH had reduced the TSS by 93.8% and the VSS by 94.5%. The absorbance reading followed similar trend which showed an 81.8% increase in clarity when the pH was reduced to 5.4.

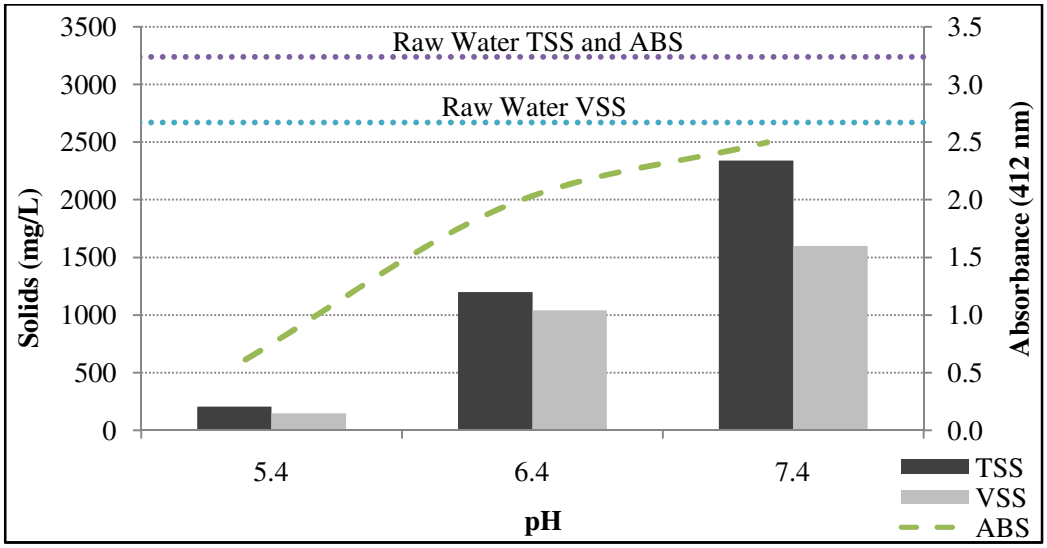

Figure 3.10: The TSS, VSS, and absorbance at 412 nm of the supernatant of poultry processing wastewater after treatment with 1500 mg/L of Floccin. The pH was adjusted to 5.4, 6.4, and 7.4 before the addition of Floccin.

Since the Floccin seemed to perform better at a lower pH, the initial pH of 6.4 was lowered to around 5 for all six samples of the next test. A range from 500 to 2500 mg/L of Floccin was tested after the pH adjustment (Figure 3.11). With a lower pH as compared to the first test, the various concentrations of Floccin were expected to perform better.

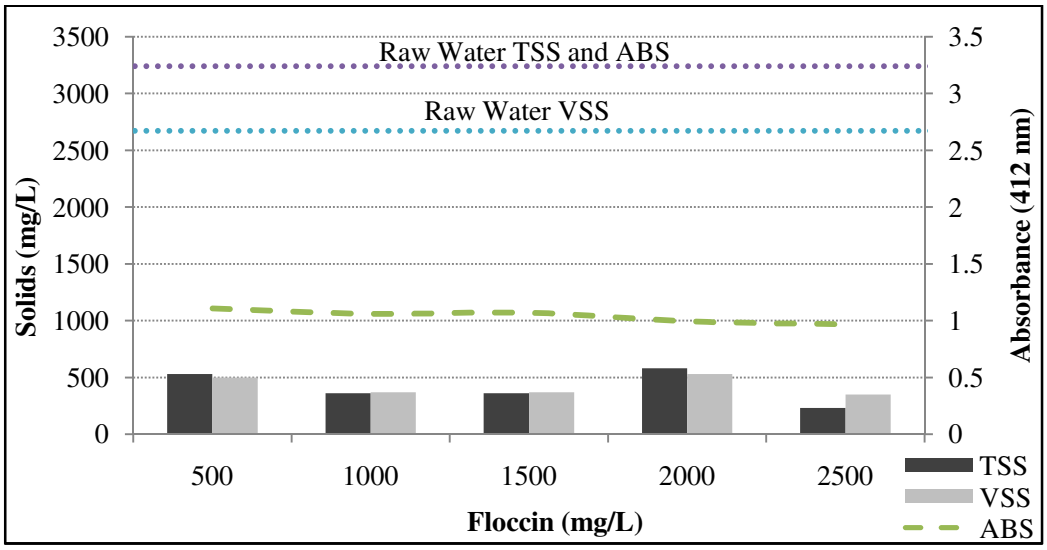

Figure 3.11: The TSS, VSS, and absorbance at 412 nm of the supernatant of the poultry processing wastewater after treatment with 500 to 2500 mg/L of Floccin. The samples were brought to a pH of 5 with sulfuric acid before rapid mixing of Floccin which lasted 10 minutes. Settling occurred almost immediately.

All concentrations formed flocs within 10 minutes, with 1500, 2000, and 2500 mg/L forming flocs in under two minutes. The 2500 mg/L concentration performed the best, but it was noted that too much flocculation was occurring and one large mass of sludge was being formed. Haarhoff and Edzwald (2001) discuss how the bubble size is of negligible importance for large flocs because the bubble/floc ratio is far in excess of what is required. Since large bubbles which could be formed without pressurization could just as easily remove the large flocs formed, concentrations over 1500 mg/L were considered unpractical. Since 500 and 1000 mg/L had cleared 84.2% and 89.2% of TSS respectively from the supernatant with much smaller flocs, more suitable for dissolved air flotation, that range was determined to be the best.

Additional jar tests were conducted to test the performance between 600 and 1000 mg/L, in increments of 100 mg/L when the pH was maintained around 5 (Figure 3.12).

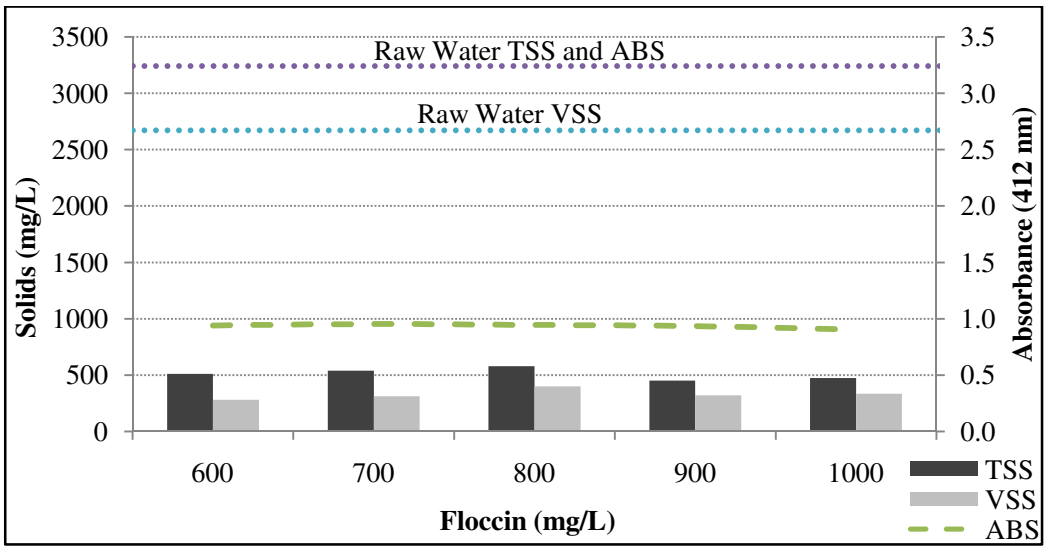

Figure 3.12: The TSS, VSS, and absorbance at 412 nm of the supernatant of the poultry processing wastewater after treatment with 600 to 1000 mg/L of Floccin. The samples were brought to a pH of 5 with sulfuric acid before rapid mixing of Floccin which lasted 10 minutes. Settling occurred almost immediately.

At a concentration of 1000 mg/L, the supernatant had the least absorbance at 0.902, but the worst clarity was only 0.954 which was achieved with 700 mg/L (2% difference in clarity). The best TSS removal was 86.6%, which was achieved with 900 mg/L Floccin. However, 600 mg/L of Floccin was capable of reducing the TSS by 84.7%. Since all concentrations of Floccin provided results that were within 4% TSS reduction and 2% water clarity, 600 mg/L was chosen as the most suitable for water treatment.

Discussion

The floc produced by Floccin was, at times, very inconsistent during the testing, and there was difficulty in determining the cause for all the problems. Maintaining the pH and Floccin concentration would produce strong flocs during one set of tests then provide no results for a different set of tests. The jar testing protocol that accompanied Floccin claimed that it would perform satisfactorily at any pH with best results achieved when near neutral. However,

experimental results indicated that the closer the wastewater was to neutral, the poorer the production of Floccin. The Floccin performed better and was more consistent when the pH was dropped to around 5, but creating such acidic conditions was neither practical nor economical for real world application. To overcome these problems, it was decided to try a combination of inorganic coagulant with the Floccin product.

The use of a metal coagulant with a flocculent was not uncommon since metal salts have a greater ability to destabilize the charge of particles, but lack the ability to form strong bridges between coagulating flocs. The addition of highly charged cations in the form of aluminum or ferric salts effectively induced the destabilization of the emulsions, leading to significant oil separations (Al-Shamrani et al., 2002). With charges stabilized by the metal hydroxides, the Floccin would be used as a coagulant aid and add the strength to form denser flocs. Coagulant aid polyelectrolytes are believed to destabilize suspensions by adsorption of particles as well as the formation of bridges between the particles and the polyelectrolyte (Meyssami and Kasaeian, 2005). Since ferric chloride was previously selected during the comparative testing of metal coagulants, it was chosen for this next set of tests.

3.4.6 Ferric Chloride and Floccin Combination

Previous tests with ferric chloride indicated that a concentration of 650 mg/l provided the best flocculation with good clarity and limited suspended solids in the supernatant (Figures 3.8 and 3.9). Because of this, it was decided to prepare five wastewater samples with a range of ferric chloride that encompassed these values (500, 600, 700, 800, 900 mg/L). The pH started at 6.15 and decreased with increased concentrations of ferric chloride. Steady mixing continued for five minutes to allow charge destabilization.

The last set of tests with just Floccin (Figure 3.12) indicated that 600 mg/L of the flocculating agent was suitable for floc formation, so 600 mg/L of Floccin was added to each of the samples for an additional five minutes (Figure 3.13).

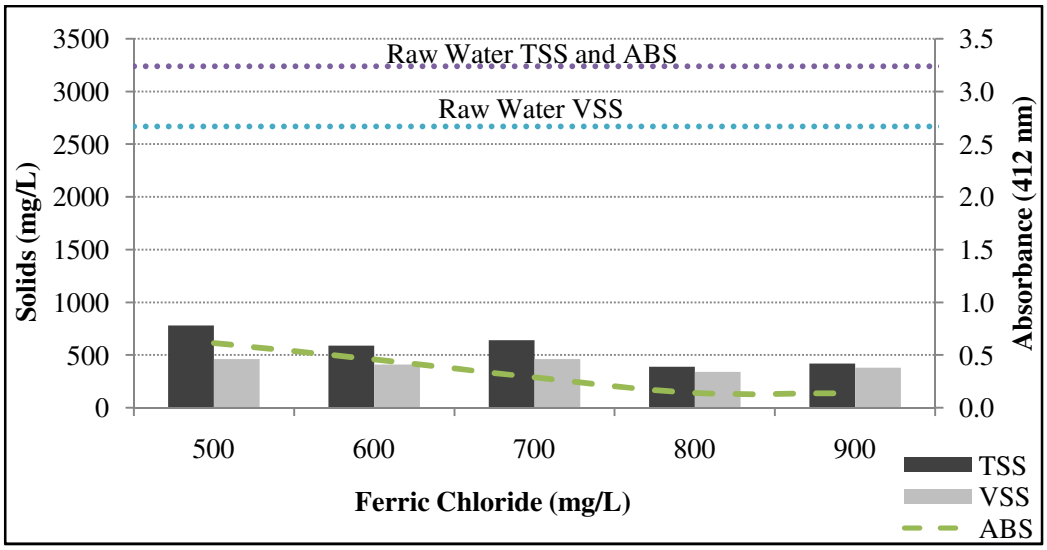

Figure 3.13: The TSS, VSS, and absorbance at 412 nm of the supernatant of poultry processing wastewater after treatment with 500 to 900 mg/L ferric chloride and 600 mg/L Floccin. The samples were treated with ferric chloride and mixed for 5 minutes followed by 5 minutes of mixing with Floccin. Settling occurred almost immediately.

Strong settling flocs formed almost immediately after the addition of Floccin. The combination of 800 mg/L of ferric chloride with 600 mg/L of Floccin performed the best with a 95.7% increase in clarity and an 88.4% reduction in TSS. Because of the addition of ferric chloride, the red color of the supernatant cleared up substantially and the pH dropped from 6.15 to 5.34 without acid addition.

The final set of jar tests used 800 mg/L of ferric chloride for all five samples, and the concentration of Floccin was increased from 600, 700, 800, 900, 1000 mg/L in attempts to achieve better water clarity (Figure 3.14). The absorbance levels did not vary greatly, but 900 mg/L provided the best results with a 96.9% increase in clarity. The TSS values dropped significantly for all concentrations compared to the previous test. The 1000 mg/L and 900 mg/L

concentrations performed the best, removing 98% of TSS, but the worst removal was only 96.4%, achieved with a concentration of 800 mg/L.

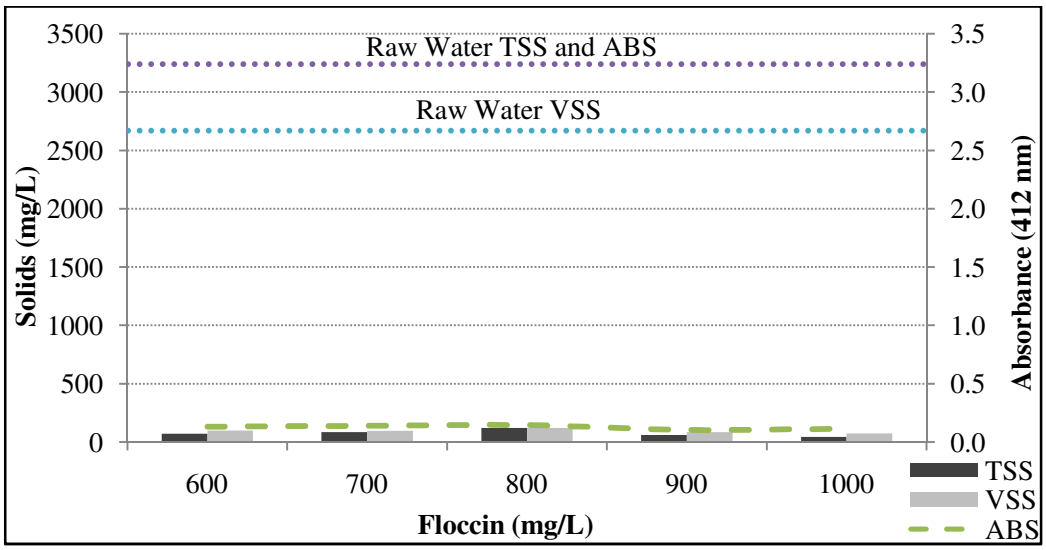

Figure 3.14: The TSS, VSS, and absorbance at 412 nm of the supernatant of poultry processing wastewater after treatment with 800 mg/L ferric chloride and 600 to 1000 mg/L Floccin. The samples were treated with ferric chloride and mixed for 5 minutes followed by 5 minutes of mixing with Floccin. Settling occurred almost immediately.

The removal efficiencies of suspended solids between the Floccin doses were negligible. All doses removed over 96% of the solids and increased the water clarity by at least 95%. Despite the similarities in effectiveness, 900 mg/L of Floccin in combination with 800 mg/L of ferric chloride was chosen because of having the best water clarity.

3.5 Conclusion

Initial testing with the metal coagulants provided superior water clarity after settling, but doses as high as 650 mg/L were determined necessary to achieve substantial water clarity. Al-Shamrani and coworkers (2002) determined that 100 mg/L of aluminum sulphate was need to maximize flocculation and coalesce oil droplets of an emulsion with an initial oil concentration of 1630 ppm and no suspended solid content. This would be equivalent to using nearly 900 mg/L of coagulant on the poultry wastewater to treat the oil parameters alone. Using large chemical doses appeared necessary for the removal of the concentrated oil emulsion at the time.

Later investigation, however, discovered that low alkalinity concentrations and high phosphate concentrations could have led to poor coagulation and subsequent overdosing.

Additional tests with a polyelectrolyte, Floccin 1115, were thought to be able to relieve the problems sustained with the metal coagulants. Floccin created solid flocs that settled almost immediately, but the results were inconsistent. Various combinations of pH and polymer doses were tried, but repeatable results were difficult to achieve. Maintaining the pH around 5 appeared to work best for the Floccin, but this was decided to be impractical for actual application.

Combining the coagulant and flocculent improved the consistency of floc production and floc integrity. The flocs formed were solid and suitable for dissolved air flotation. The addition of ferric chloride caused the pH to fall to around 5.5 which still was not a desirable pH range for final treatment. Baig et al. (2003) indicate, however, that a pH of 5.5 was appropriate to achieve an overall oil removal efficiency over 98% from their vegetable oil emulsion.

High chemical doses were still required to achieve 98% TSS removal and a 97% increase in water clarity, however. With the range of concentrations tested it was determined that a combination of 800 mg/L of ferric chloride and 900 mg/L of Floccin would provide the best clarity in the supernatant.

Chapter 4: Flotation

4.1 Introduction

Dissolved air flotation is a process that supersaturates water with air by pressure saturation. Air and water are introduced in sealed vessel at pressures ranging from 40 to 100 psi, and when this water is released to atmospheric conditions, the excess air comes out of solution to form tiny microbubbles. These bubbles produce a dense cloud that collects the tiny particulates in a water system and carries them to the surface for removal.

This method of treatment could be useful for poultry processing wastewater which consists of an oil emulsion with a concentrated suspended solids content that is resistant to settling due to low densities and strong molecular charges. Because the smaller bubbles are less buoyant than larger bubbles they rise more slowly to the surface, increasing the opportunity for collision with oil drops and particulates for an improved removal process (Mansour and Chalbi, 2006).

The current method for treating Sanderson Farm's wastewater uses two settling lagoons with an average HRT of approximately eight days. These lagoons, due to their need for long HRTs, limit the poultry processing rates. Apart from the processing limitations, most processing plants acquire acres of adjacent land to minimize the community odor concerns, primarily arising from anaerobic digestion. If dissolved air flotation proves to be a viable option for treating the poultry processing wastewater, the lagoon area demands could be reduced significantly.

4.2 Experimental Design

A 1L beaker on a stir plate was used for the flotation tests of the wastewater. The variables of the DAF unit were set to the best performing parameters as determined by the microbubble testing in Chapter 2. The best chemical dose as determined by the jar testing of Chapter 3 was used for all of the experiments. The beaker was filled with 700mL of raw

wastewater for every test. The equivalent of 800 mg/L of ferric chloride was added and mixed for five minutes. Then 900 mg/L of Floccin 1115 was added and mixed for five minutes. Since various recycle flows would result in a different final volume, various quantities of tap water were used to balance the volume of wastewater before flotation began (Table 4-1). This allowed equal floating distance for bubbles and agglomerates at all recycle ratios. The recycle flow was varied from 40, 30, 20, 10, and 0 percent.

Table 4-1: Volume balance and volume of recycle flow for each recycle ratio

Recycle Ratio	0%	10%	20%	30%	40%
Volume Balance	280 ml	210 ml	140 ml	70 ml	0 ml
Recycle Flow	0 ml	70 ml	140 ml	210 ml	280 ml

Pictures were taken after flotation had finished and are presented in Appendix F. The floated solids were collected by a 200 micron nylon mesh screen and labeled in metal pans. The liquid volume was analyzed for metals and fats, oil, and grease residue as well as TSS, VSS and absorbance at 412 nm. The settled solids were also collected with the 200 micron mesh and labeled in separate pans. This was done in triplicate for every recycle ratio.

The screened solids were weighed for their wet mass and dried out at 105 ^{o}C overnight for their dry mass. A portion of the dried samples were scraped off and ashed at 550 ^{o}C for thirty minutes. These masses were recorded as well. These values were used to compare the total solids and volatile solids that were floated to the surface and settled to the bottom of the beaker.

4.3 Presentation of Results and Discussion

As determined by the solubility tests achieved with the dissolved air flotation unit, the pressure was maintained at 90 psi, the water temperature at 21 C, the air flow at 0.3 CFH, and the flow rate at 1.1 L/min. The sample was coagulated with 800 mg/l of FeCl for five minutes and then flocculated with 900 mg/L Floccin for an additional five minutes. The water cleared up

substantially as large flocs began to form after the addition of the polymer. The floc size was larger than what was noticed in previous jar tests, and the wastewater appeared to react more strongly to the addition of ferric chloride since a greater drop in pH was observed.

Previously the pH did not drop below 5.5 after ferric chloride was added, but levels averaged 4.5 in this set of tests. The original pH of the raw wastewater was noted at 6.1, which was lower than usual and could explain the raw final pH. This pH drop was likely due to the various amounts of bleach which are used for cleanup within the plant and are discharged with the process water. Whatever the reason, the wastewater reacted more intensely to the chemical treatment than what previous tests had indicated. Such day to day variations in the wastewater were expected from the processing plant.

The recycle ratios varied from 0% to 40% of the wastewater volume (Figure 4.2). The mass of solids carried to the surface increased as the amount of recycle flow increased. Forty percent recycle flow was required to carry almost all of the solids to the surface (Figure 4.1). At 0% recycle ratio an equivalent amount of solids was found settled at the bottom. As mentioned earlier, the floc size was much larger than anticipated and could have required a greater recycle ratio to carry the heavier particles to the surface. Fukushi and coworkers (1998) mentioned that large flocs are more desirable since the greater number of bubbles attached to them will make the separation more efficient. If smaller flocs were formed, however, perhaps a smaller recycle flow could have been sufficient for carrying the solid matter to the surface.

Figure 4.1: Coagulated solids floated to the surface with a 40% recycle ratio

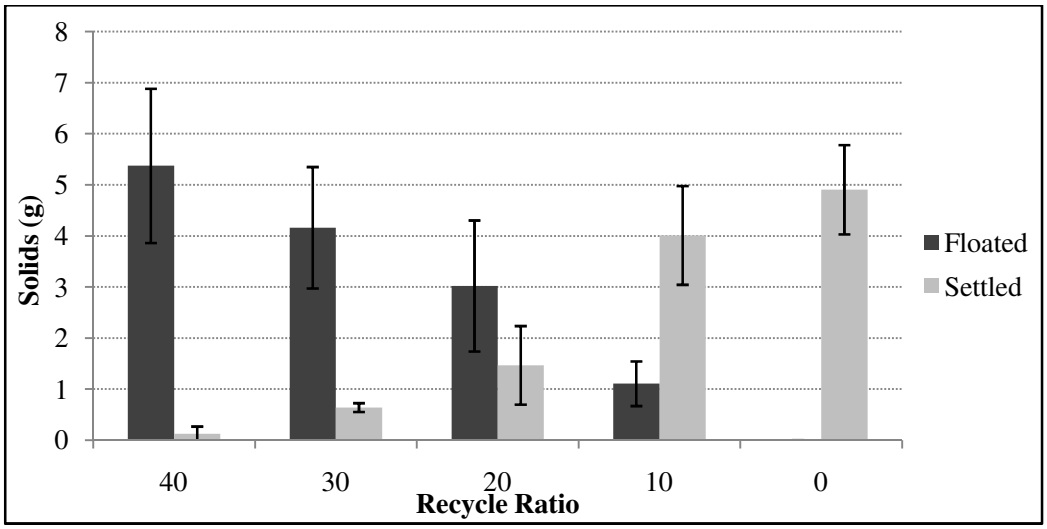

Figure 4.2: The correlation between the amount of solids that were floated to the surface and settled to the bottom compared to the various recycle ratios.

The supernatant of the samples was measured for suspended solids, optical density, COD, and FOG. For all of the recycle ratios these values were fairly consistent, which indicates that flotation was secondary to the chemical treatment. The addition of ferric chloride and Floccin removed most of the particulates from the wastewater. If the flocs were not carried to the surface by flotation, they settled to the bottom. The values of TSS, VSS and absorbance can be seen in Figure 4.3.

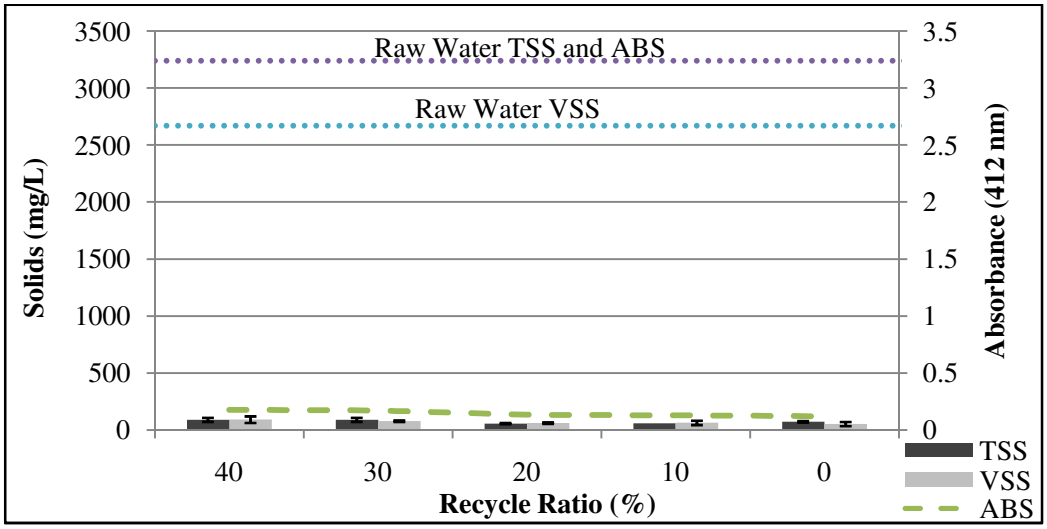

Figure 4.3: The TSS, VSS, and absorbance at 412 nm of the supernatant of the poultry processing wastewater after flotation with various recycle ratios. The wastewater was initially treated with 800 mg/L ferric chloride and 900 mg/L of Floccin.

Since 40% recycle was necessary for complete flotation of the solids, its supernatant values were used to indicate the clarity achieved. The absorbance after flotation measured 0.177 at 412 nm. The original wastewater absorbance of 3.34 indicates that a 94.7% (± 1.4) increase in clarity was achieved. The total suspended solids were reduced from 3347 mg/L to 90 mg/L for a 97.3% (± 0.5) reduction. Volatile solids were reduced 96.6% (± 1.1) as its values dropped from approximately 2667 mg/L to 91.67 mg/L. The COD values were lowered from over 10,000 mg/L to only 900 mg/L for 91% reduction. The fats, oils, and greases which were originally measured to be over 14,000 mg/L were essentially eliminated since no values could be detected.

4.4 Conclusion

The microbubbles produced by a 40% recycle flow were sufficient to carry 98% of the flocculated solids to the surface. The resulting supernatant was extremely clear with significant TSS, COD, and FOG removal. However, the supernatants for the other tests showed similar clarity as compared to the 40% recycle flow. If the flocculated solids did not float to the surface, they immediately settled to the bottom of the beaker. Typically flotation allows for quicker separation of particulates from the solution and forms a denser layer that is easier to remove. Since such large concentrations of chemicals were used, however, the settling occurred just as rapidly.

Chapter 5: Global Conclusion

A combination of ferric chloride and Floccin 1115 proved to be a very effective method for treating the wastewater with over a 97% (± 0.5) removal of TSS, 96% (± 1.1) removal of VSS, 91% removal of COD, and 100% removal of FOG. The concentrations used, however, were much too high to be economical for Sanderson Farms or any other water treatment facility. It was determined that by using 800 mg/L of ferric chloride and 900 mg/L of Floccin 1115 to treat an approximated 1 million gallons of wastewater a day would cost the processing plant $10,829 per day in chemical costs alone (Appendix F). This was nearly twice Sanderson Farms' daily treatment costs, and did not include additional costs such as electricity, pH neutralization, and disposal of excess sludge that would be generated from the chemical use.

However, it was determined that overdosing had occurred during the testing of metal coagulants and the polymer. It was later discovered that the alkalinity levels of the water would not support ferric chloride doses over 250 mg/L. Even though at 250 mg/L of ferric chloride, the greatest TSS removal was not seen, there was still a reduction of 95% suspended solids from the supernatant. Goals of reaching 100% TSS removal had overshadowed the practicality of using significantly less coagulant with a smaller reduction in efficiency.

It was also believed that high levels of phosphate may have interfered with the formation of the metal hydroxide flocs. Boisvert and coworkers (1997) noted that the formation of phosphate-alum bonds increased as the pH decreased to 5 and the hydroxide-alum bonds were decreased. This would have been the cause for higher levels of metal coagulants in the initial testing because of the competition for cationic charges on the metal species.

The high levels of coagulants used during the testing made the incorporation of the DAF unit unnecessary since the flocs that formed quickly sank to the bottom. The rapid settling was largely associated with the high concentration of clay within the Floccin polymer. If the

concentrations of coagulants added were significantly reduced or a polymer without clay additives was used, then the incorporation of a DAF unit would become more practical. However, the efficiency of this dissolved air flotation unit needed improvement as well.

Typically efficiency ranges for an unpacked saturator seemed to run between 60 and 70% (Edzwald, 1995), but it was noted that large air bubbles (2 mm in diameter) were what made the difference between an efficiency of 25% and 70% in this bench scale unit. The goal was to produce a maximum number of bubbles in the 10-100 um diameter range. For this unit it appeared that for immediate startup, 25-30 ml of microbubbles was the best that could be achieved. Increasing the air saturation beyond this volume produced larger bubbles not suited for DAF.

The large bubbles were a result of the turbulence at the release point of the dissolution tank and continued coalescing through the 3/8 inch tubing that delivered the saturated flow to the flotation vessel. Immediate release of the pressurized flow from a larger nozzle directly to the flotation tank without additional tubing for transfer of the flow was believed to be necessary for better microbubble production in future DAF applications.

The coagulation pretreatment and flotation process of the poultry processing wastewater was not practical for actual application due to high coagulant doses increasing operation costs. However, by sacrificing minimum treatment efficiency by significantly reducing the amount of coagulants used, the speedy removal process of a dissolved air flotation unit becomes more appealing for future use.

References

Al-Mutairi, N. et al. (2008) Evaluation study of a slaughterhouse wastewater treatment plant including contact-assisted activated sludge and DAF. Desalination 225, 167-175.

Al-Shamrani, A. et al. (2002) Destabilization of oil-water emulsions and separation by dissolved air flotation. Water Research 36, 1503-1512.

Al-Shamrani, A. et al. (2002) Separation of oil from water by dissolved air flotation. Colloids and Surfaces 209, 15-26.

APHA, AWWA, and WPCF. Standard Methods: for the examination of water and wastewater. 15th Ed., Washington D.C.: American Public Health Association, 1980.

Baig, M. et al. (2003) Removal of oil and grease form industrial effluents. Electron. J. Environ. Agric. Food Chem, ISSN: 1579-4377, 577-585.

Bensadok, K. et al. (2007) Treatment of cutting oil/water emulsion by coupling coagulation and dissolved air flotation. Desalination 206, 440-448.

Bratby J. (1978) Aspects of sludge thickening by dissolved-air flotation. Water Pollution Control 77(3), 421–32.

Boisver, J. et al. (1997) Phosphate adsorption in flocculation processes of aluminum sulfphate and poly-aluminum-silicate-sulfphate. Wat. Res. 31(8), 1939-1946.

Cheremisinoff, N. Handbook of Water and Wastewater Treatment Technologies. Woburn, MA: Butterworth-Heinemann, 2002.

Chung, T. and Kim, D. (1997) Significance of pressure and recirculation in sludge thickening by dissolved air flotation. Wat. Sci. Tech. 36(12), 223-230.

Chung Y. et al. (2000) A demonstration scaling-up of the dissolve air flotation. Wat. Res., Vol. 34(3), 817-824.

Couto, H. et al. Dissolved air flotation technique for oily effluent treatment. Chemical Engineering Program/COPPE, Federal University of Rio de Janeiro.

De Rijk, S. et al. (1994) Bubble size in flotation thickening. Wat. Res. 28, 465-473.

Edzwald, J. (1995) Principles and applications of dissolved air flotation. Wat. Sci. Tech. 31(3-4), 1-23.

Fair, G., Geyer, J. and Okun, D. Water Purification and Wastewater Treatment and Disposal. Vol. 2 New York: John Wiley and Sons, Inc. 1968.

Faust, S. and Aly, O. Chemistry of Water Treatment. 2nd Ed. Chelsea, Michigan: Ann Arbor Press. 1997.

Feris, L. et al. (2001) Optimizing dissolved air flotation design and saturation. Wat. Sci. Tech. 43(8), 145-157.

Filho, A. and Brandao, C. (2001) Evaluation of flocculation and dissolved air flotation as an advanced wastewater treatment. Wat. Sci. Tech. 43(8), 83-90.

Fukushi, K. et al. (1995) A kinetic model for dissolved air flotation in water and wastewater treatment. Wat. Sci. Tech. 31(3-4), 37-47.

Fukushi, K et al. (1998) Dissolved air flotation: experiments and kinetic analysis. Water Supply: Res Tech-Aqua. 47(2), 76-86.

Geraldes, V. et al. (2008) Dissolved air flotation of surface water for spiral-wound module nanofiltration pre-treatment. Desalination 228, 191-199.

Gregor, J et al. (1997) Optimizing natural organic matter removal from low turbidity waters by controlled pH adjustment of aluminum coagulation. Wat. Res. 31, 2949–2958.

Gurnham, C. Principles of Industrial Waste Treatment. New York: John Wiley & Sons. 1955.

Han, M. (2001) Modeling of DAF: the effect of particle and bubble characteristics. J. Water Supply: Res. Technol.-AQUA, 51(1), 27–34.

Han, M. et al. (2001) Collision efficiency factor of bubble and particle in DAF: theory and experimental verification. Wat. Sci. Tech. 43(8), 139-144.

Han, M. et al. (2007) Effects of floc and bubble size on the efficiency of the dissolved air flotation (DAF) process. Wat. Sci. Tech. 56(1), 109-115.

Haarhoff, J. and Edzwald, J. (2001) Modeling of floc-bubble aggregate rise rates in dissolved air flotation. Wat. Sci. Tech. 43(8), 175-184.

Haarhoff, J. and Rykaart, E. (1995) Rational design of packed saturators. Wat. Sci. Tech. 31(3-4), 179-190.

Haarhoff, J. and Steinback, S. (1996) A model for the prediction of the air composition in pressure saturators. Wat. Res. 30(12), 3074-3082.

Haarhoff, J. and van Vuuren, L. (1995) Design parameters for dissolved air flotation in South Africa. Wat. Sci. Tech. 31(3-4), 203-212.

Jarvis, P. et al. (2005) A review of floc strength and breakage. Wat. Res. 39, 3121-3137.

Kiepper, B. et al. (2008) Proximate composition of poultry processing wastewater particulate matter from Broller slaughter plants. Poultry Science 87, 1633-1636.

Kitchener, J. and Gochin, R. (1981) The mechanism of dissolved air flotation for potable water: basic analysis and a proposal. Wat. Res. 15(5), 585–90.

Leppinen, D. et al. (2001) Modelling the global efficiency of dissolved air flotation. Wat. Sci. Tech., Vol. 43, No. 8, 159-166

Li, T. et al. (2006) Characterization of floc size, strength and structure under various coagulation mechanisms. Powder Technology. 168, 104-110.

Lundh, M. et al. (2000) Experimental studies of the fluid dynamics in the separation zone in dissolved air flotation. Wat. Res. 34(1), 21-30.

Lundh, M. et al. (2002) The influence of contact zone configuration on the flow structure in dissolved air flotation pilot plant. Wat. Res. 36, 1585-1595.

Mansour, L. and Chalbi, S. (2006) Removal of oil from oil/water emulsions using electroflotation process. Journal of Applied Electrochemsitry 36, 577-581.

Meyssami, B. and Kasaeian, A. (2005) Use of coagulation in treatment of olive oil wastewater model solutions by induced air flotation. Bioresource Technology 96, 303-307.

Metcalf & Eddy, Inc. Wastewater Engineering: Treatment and Reuse, 4th ed. New York: McGraw Hill, 2003

Nemerow, N. Industrial Water Pollution: Origins, Characteristics, and Treatment. Addison-Wesley, 1978

Ponasse, M. et al. (1998) Bubble formation by water release in nozzle—II. Influence of various parameters on bubble size. Wat. Res. 32(8), 2498-2506.

Reynolds, T. and Richards, P. Unit Operations and Processes in Environmental Engineering. 2nd ed. Boston, Massachusetts: PWS Publishing Co, 1996.

Rhee, C. et al. (1987) Removal of oil and grease in oil processing wastewaters. Los Angeles County Sanitation Districts.

Ross, C. et al. (2000) Rethinking dissolved air flotation (DAF) design for industrial pretreatment. Water Environment Federation.

Rubio, J. et al. (2002) Overview of flotation as a wastewater treatment technique. Minerals Engineering 15, 139-155.

Russel, L. David. Practical Wastewater Treatment. Hoboken, New Jersey: John Wiley & Sons Inc, 2006.

Sarrot, V. et al. (2007) Experimental determination of particles capture efficiency in flotation. Chemical Engineering Science 62, 7359-7369.

Schwoyer, W. Polyelectrolytes for Water and Wastewater Treatment. Boca Raton, Florida: CRC Press, 1981.

Sena, R. et al. (2009) Treatment of meat industry wastewater using dissolved air flotation and advanced oxidation processes monitored by GC-MS and LC-MS. Chemical Engineering Journal 152, 151-157.

Spicer, P. et al. (1998) Effect of shear schedule on particle size, density, and structure during flocculation in stirred tanks. Powder Technology 97, 26-34.

Steinbach S. and Haarhoff J. (1998) A simplified method for assessing the saturation efficiency at full-scale dissolved air flotation plants. Wat. Sci. Tech. 38(6), 303-310.

Telang, A. (1996) Waste water treatment systems. 22nd WEDC Conference.

Timmons, M. et al. Recirculating Aquaculture Systems. 2nd Ed. Ithaca, New York: Cayuga Aqua Ventures, 2002.

Viessman, W. and Hammer, M. Water Supply and Pollution Control. 4th Ed. New York: Harper and Row, 1985.

Vlyssides, A et al. (2004) Size distribution formed by depressurizing air-saturated water. Ind. Eng. Chem. Res 43, 2775-2780.

Wang, L. and Ouyang, F. (1994) Hydrodynamic characteristics of the process of depressurization of saturated water. Chin. J. Chem. Eng. 2, 211-218

Yukselen, M. and Gregory, J. (2004) The reversibility of floc breakage, International Journal of Mineral Processing 73, 251–259.

Zouboulis, A. and Avranas, A. (2000) Treatment of oil-in-water emulsions by coagulation and dissolved air flotation. Colloids and Surfaces A. 172, 153-161

Appendix A: Raw Data, Graphs, and Statistics for Air Solubility and Energy Efficiency Testing

Pressure Testing

Water Volume: 20 L
Flow Rate: 1.8 L/min
Temperature: 21 C
Air Flow: .3 SCFH

Pressure (psi)	mL Air/ L Water			Average	Std. Dev.	95% C.I.
	Test 1	Test 2	Test 3			
50	7	11	9	9	2	2.26
60	13	13	13	13	0	0
70	18	15	14	15.67	2.08	2.36
80	20	16	17	17.67	2.08	2.36
90	20	19	20	19.67	0.58	0.65

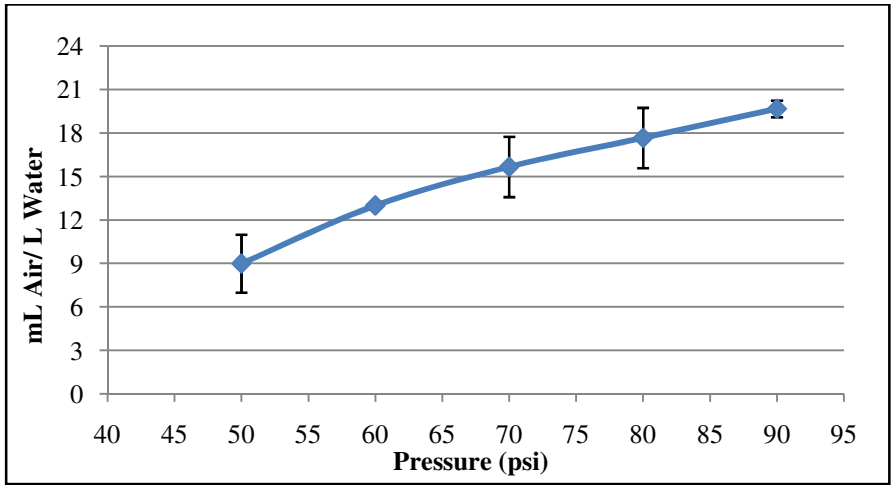

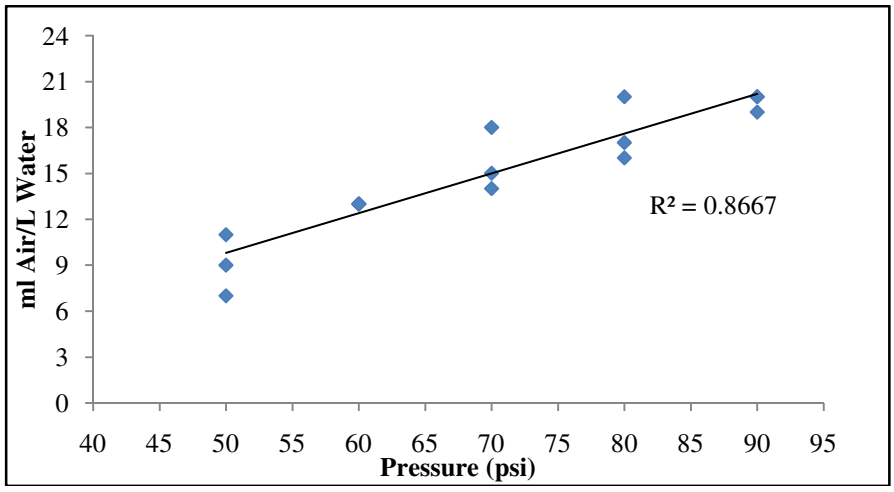

Temperature Testing

Water Volume: 20 L
Flow Rate: 1.8 L/min
Pressure: 80 psi
Air Flow: .3 SCFH

Temperature ©	mL Air/L Water			Average	Std. Dev.	95% C.I.
	Test 1	Test 2	Test 3			
7	34	34	32	33.33	1.15	1.31
14	25	28	28	27	1.73	1.96
21	16	19	20	18.33	2.08	2.36
28	30	30	31	30.33	0.58	0.65
35	29	29	30	29.33	0.58	0.65

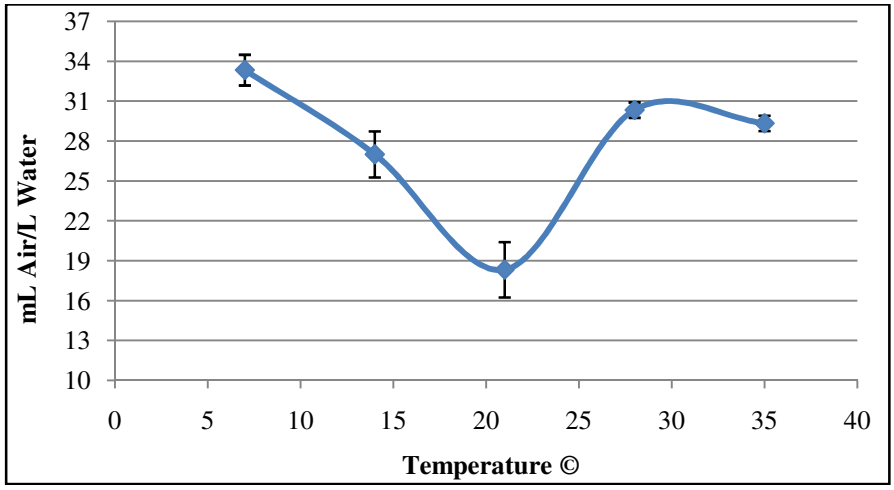

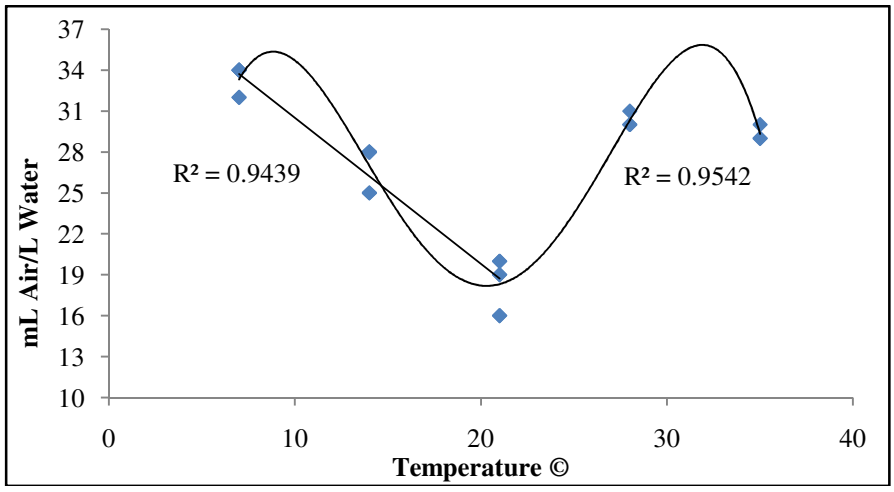

Retention Time Testing

Water Volume: 20 L
Temperature: 21 C
Pressure: 80 psi
Air Flow: .3 SCFH

Flow Rate (L/min)	mL Air/L Water			Average	Std. Dev.	95% C.I.	Air Volume (mL)
	Test 1	Test 2	Test 3				
0.8	26	25	25	25.33	0.58	0.65	20.27
1.3	21	20	20	20.33	0.58	0.65	26.43
1.8	18	17	20	18.33	1.53	1.73	33
2.3	16	15	16	15.67	0.58	0.65	36.03
2.8	13	13	14	13.33	0.58	0.65	37.33

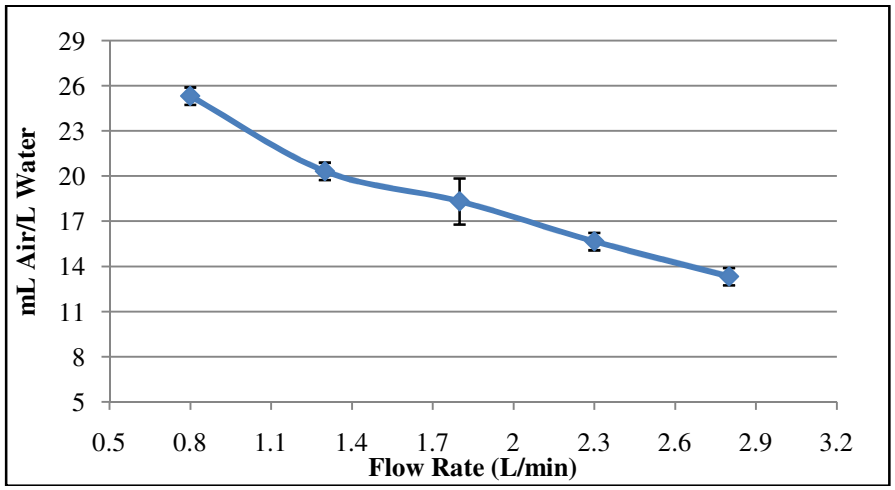

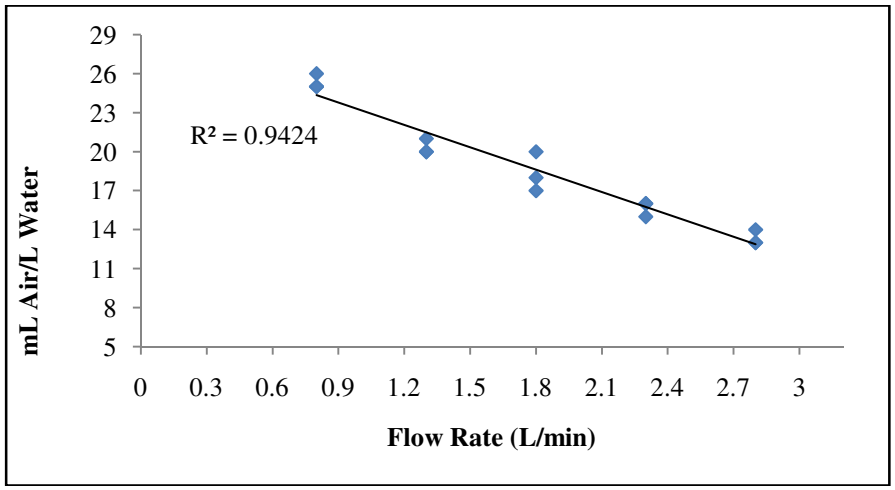

Air Flow Testing

Water Volume: 20 L
Flow Rate: 1.8 L/min
Temperature: 21 C
Pressure: 80 psi

SCFH Air	ml Air/L Water			Average	Std. Dev.	95% C.I.
	Test 1	Test 2	Test 3			
0	0	0	0	0	0	0
0.2	14	17	14	15	1.73	1.96
0.4	17	17	18	17.33	0.58	0.65
0.6	18	21	20	19.67	1.53	1.73
0.8	18	17	19	18	1	1.13

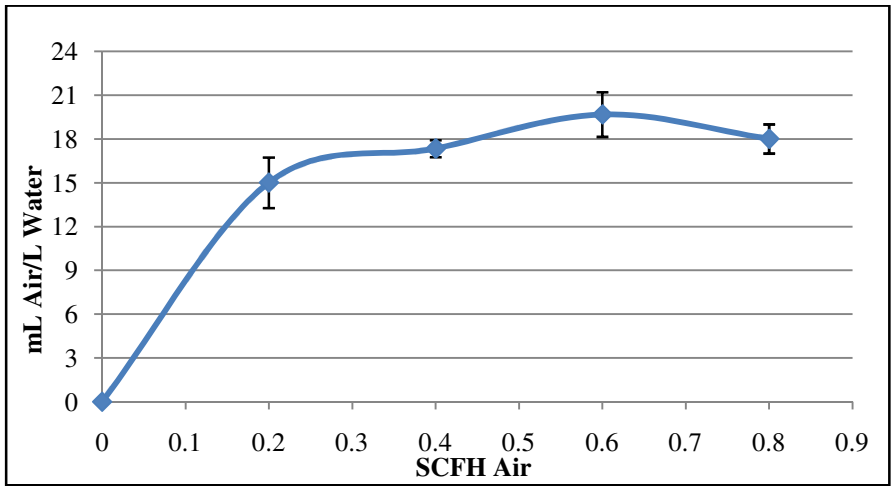

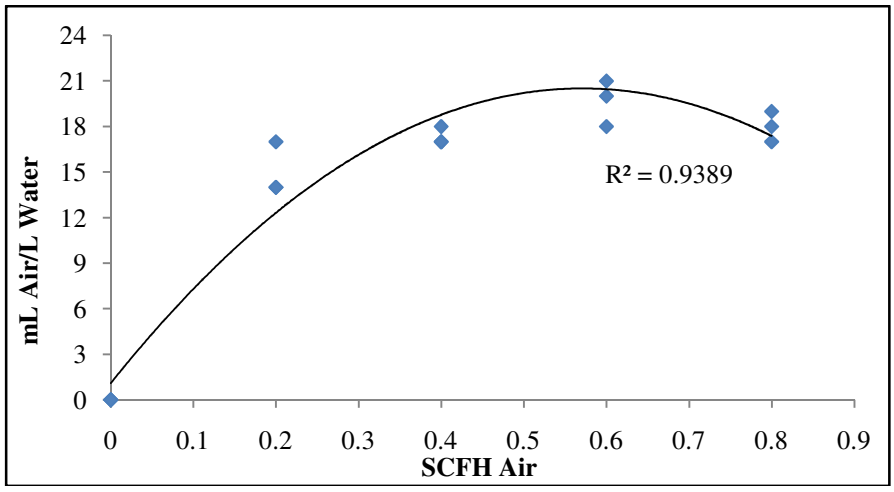

Maximum Production

Water Volume: 20 L
Temperature: 12 C
Pressure: 90 psi
Air Flow: 0.3 SCFH

Minutes Aerated	mL of Air/L of Water			Average	Std. Dev.	95% C.I.
	Test 1	Test 2	Test 3			
0	32	30	33	31.67	1.53	1.73
5	48	52	55	51.67	3.51	3.97
10	66	64	65	65.00	1.00	1.13
15	74	74	78	75.33	2.31	2.61
20	86	83	85	84.67	1.53	1.73
30	84	84	86	84.67	1.15	1.31
60	86	81	84	83.67	2.52	2.85
120	100	112	107	106.33	6.03	6.82
1080	107	110	106	107.67	2.08	2.36

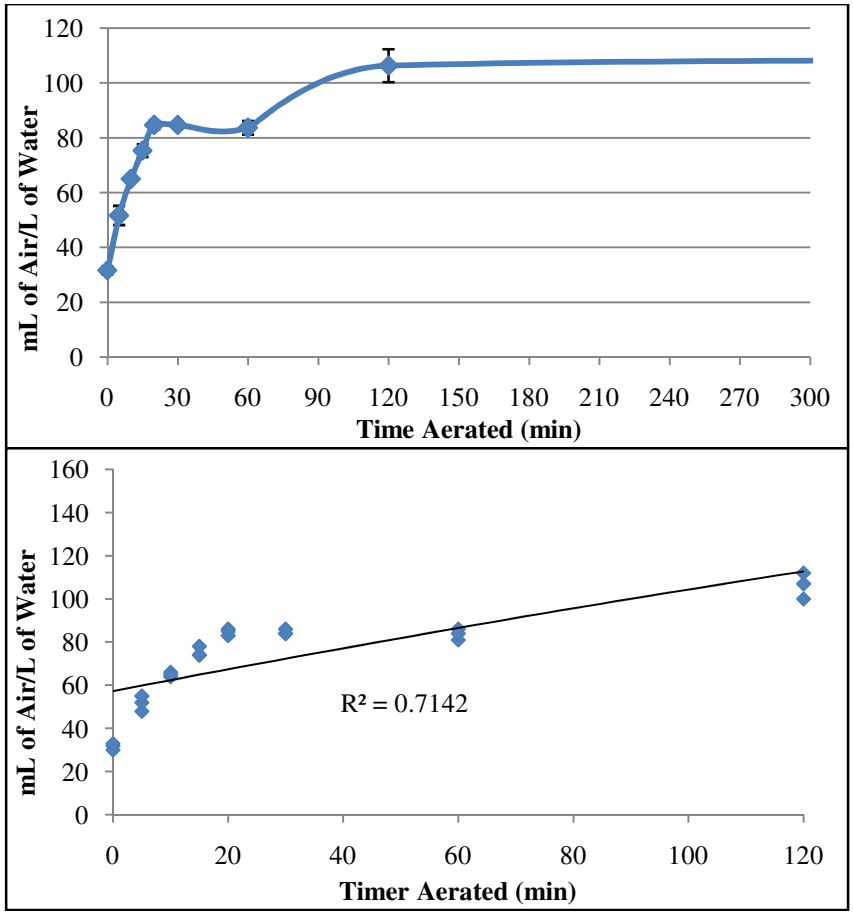

Power Consumption vs. Pressure

Pressure	Watts 1	Watts 2	Watts 3	Average	Std. Dev.	95% C.I.
0	24	24	24	24.0	0.00	0.00
10	26	25	25	25.3	0.58	0.65
20	28	27	26	27.0	1.00	1.13
30	30	30	34	31.3	2.31	2.61
40	34	32	37	34.3	2.52	2.85
50	36	34	38	36.0	2.00	2.26
60	37	36	40	37.7	2.08	2.36
70	40	39	46	41.7	3.79	4.28
80	44	44	49	45.7	2.89	3.27
90	51	48	52	50.3	2.08	2.36

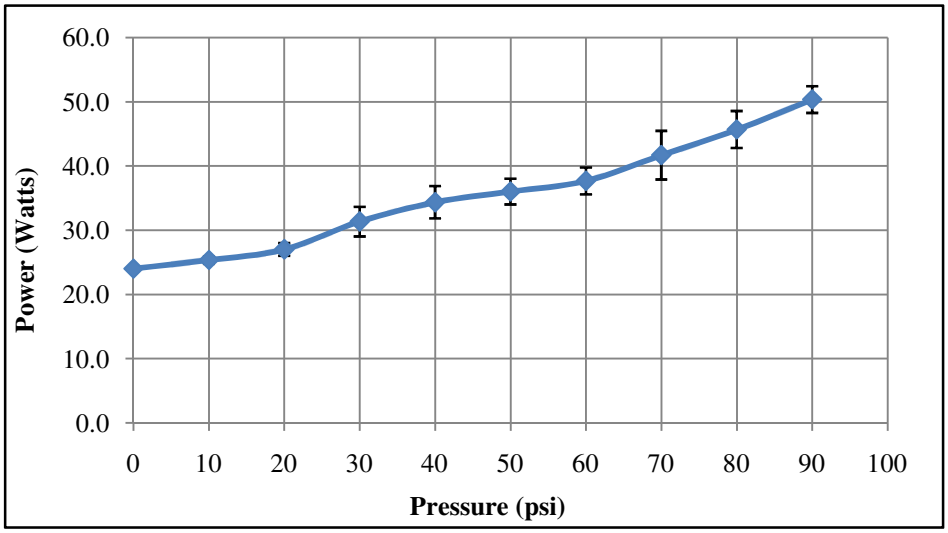

Theoretical Air Solubility vs. Pressure

PSI	Kpa	Cs,o (mg/L)	Cs,n (mg/L)	Total (mg/L)	Minus Ca (mg/L)	Total (mL/L)	92% (mL/L)
10	68.95	9.50	27.22	36.71	13.01	10.84	9.98
20	137.90	13.34	38.24	51.58	27.88	23.23	21.37
30	206.85	17.19	49.26	66.45	42.75	35.62	32.77
40	275.80	21.04	60.28	81.32	57.62	48.01	44.17
50	344.75	24.88	71.30	96.18	72.48	60.40	55.57
60	413.70	28.73	82.33	111.05	87.35	72.79	66.97
70	482.65	32.57	93.35	125.92	102.22	85.18	78.37
80	551.60	36.42	104.37	140.79	117.09	97.57	89.77
90	620.55	40.27	115.39	155.66	131.96	109.96	101.17

Ca = air mass concentration of incoming water = 23.7 mg/L

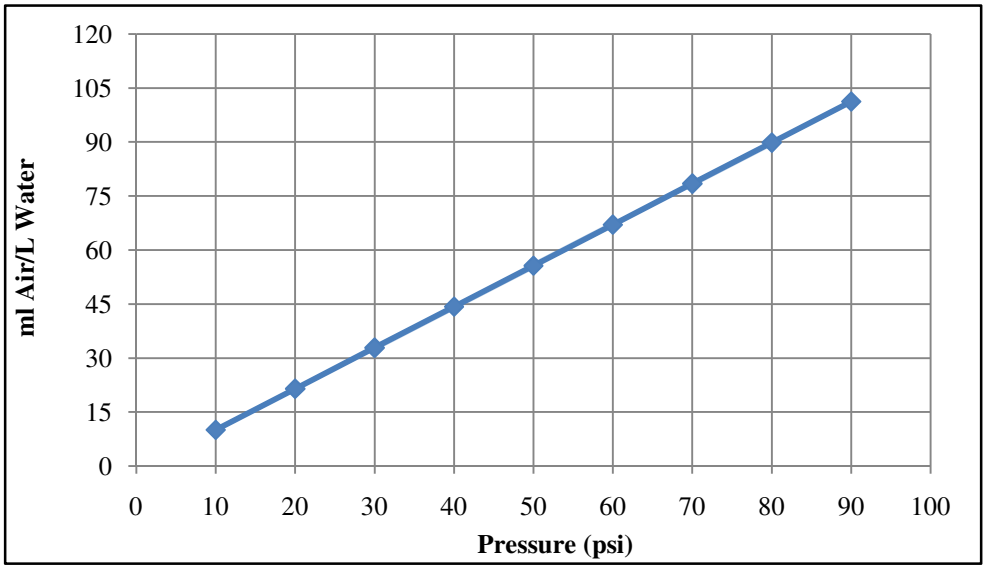

Theoretical Air Solubility at 80 psi vs. Temperature

Temp ©	Kelvin	Ho	Hn	Cs,o	Cs,n	Total (n)	Ca,o	Ca,n
5	278.15	23.9	49.8	50.27	137.61	187.88	12.26	19.48
10	283.15	26.4	54	44.70	124.66	169.37	10.90	17.65
15	288.15	28.8	58.2	40.27	113.66	153.93	9.82	16.09
20	293.15	31.3	62.3	36.42	104.37	140.79	8.88	14.77
25	298.15	33.8	66.5	33.16	96.14	129.30	8.09	13.61
30	303.15	36.3	70.7	30.37	88.94	119.30	7.40	12.59

Temp ©	Kelvin	Total (a)	n-a	mL/L	92%
5	278.15	31.73	156.14	130.12	119.71
10	283.15	28.55	140.82	117.35	107.96
15	288.15	25.91	128.02	106.68	98.15
20	293.15	23.65	117.14	97.61	89.80
25	298.15	21.69	107.60	89.67	82.50
30	303.15	19.99	99.31	82.76	76.14

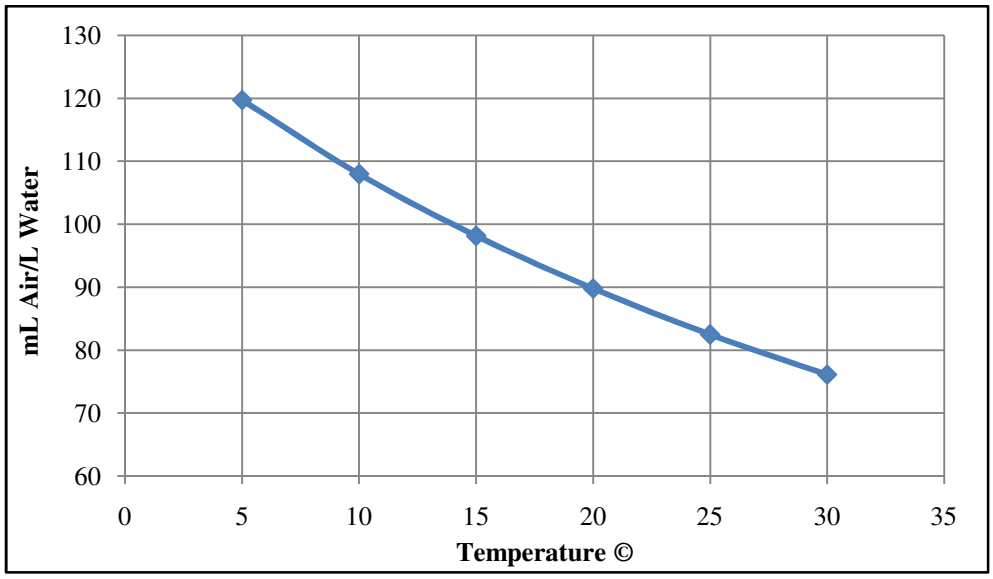

Air Solubility vs. Watts

Pressure	Watt	mL Air/L Water	mL AIr/W
50	36.00	9.00	0.250
60	37.67	13.00	0.345
70	41.67	15.67	0.376
80	45.67	17.67	0.387
90	50.33	19.67	0.391

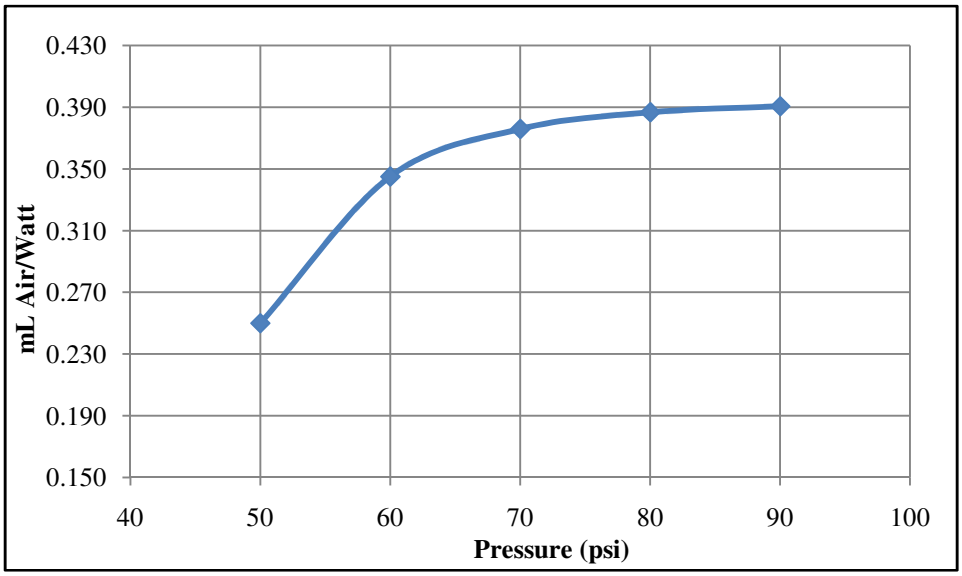

Appendix B: Raw Data and Statistics for Raw Poultry Processing Wastewater

UV-Vis Scanning Spectrophotometer – 25% wastewater

TEST SETUP
GENESYS 6 v1.120 2M6G056001

Scanning	1:47pm 17Dec08
Test Name	200-900nm[Saved]
Measurement Mode	Absorbance
Start Wavelength	200.0nm
Stop Wavelength	900.0nm
Sample Positioner	Manual 6
Scan Speed	Fast
Interval	1.0nm
ID# (0=OFF)	1
Auto Print	On
Auto Save Data	Off

ID#: 4

Wavelength	Abs
200	0.389
201	0.63
202	0.445
203	0.804
204	0.562
205	0.505
206	0.661
207	0.861
208	0.786
209	0.828
210	1.154
211	0.961
212	1.022
213	1.303
214	1.835
215	1.732
216	2.391
217	2.113
218	2.352
219	2.426
220	2.735
221	2.808
222	2.932
223	2.942
224	[****]
225	[****]
226	[****]
227	[****]
228	[****]
229	2.988
230	2.93

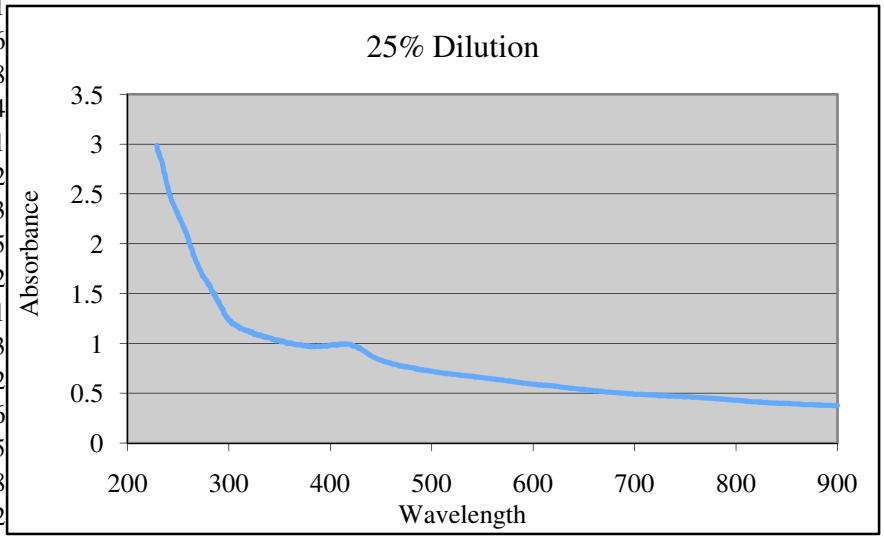

UV-Vis Scanning Spectrophotometer – 50% wastewater

TEST SETUP
GENESYS 6 v1.120 2M6G056001

Scanning	1:49pm 17Dec08
Test Name	200-900nm[Saved]
Measurement Mode	Absorbance
Start Wavelength	200.0nm
Stop Wavelength	900.0nm
Sample Positioner	Manual 6
Scan Speed	Fast
Interval	1.0nm
ID# (0=OFF)	1
Auto Print	On
Auto Save Data	Off

ID#: 5

Wavelength	Abs
200	0.249
201	0.301
202	0.778
203	0.608
204	0.615
205	0.708
206	0.708
207	0.456
208	1.064
209	0.78
210	0.677
211	1.186
212	1.236
213	1.169
214	1.645
215	1.711
216	2.279
217	2.325
218	2.536
219	2.522
220	2.741
221	2.834
222	[****]
223	[****]
224	[****]
225	[****]
226	[****]
227	[****]
228	[****]
229	2.948
230	2.896

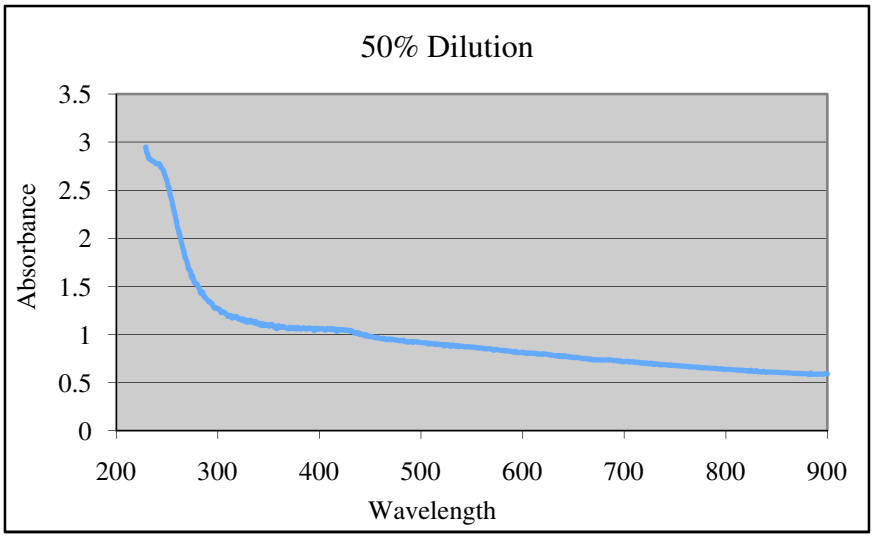

UV-Vis Scanning Spectrophotometer – 75% wastewater

TEST SETUP
GENESYS 6 v1.120 2M6G056001

Scanning	1:42pm 17Dec08
Test Name	200-900nm[Saved]
Measurement Mode	Absorbance
Start Wavelength	200.0nm
Stop Wavelength	900.0nm
Sample Positioner	Manual 6
Scan Speed	Fast
Interval	1.0nm
ID# (0=OFF)	1
Auto Print	On
Auto Save Data	Off

ID#: 2

Wavelength	Abs
200	0.356
201	0.556
202	0.685
203	1.073
204	0.832
205	1.013
206	0.724
207	0.858
208	1.002
209	0.867
210	0.933
211	0.968
212	1.207
213	1.182
214	1.591
215	1.853
216	2.028
217	2.248
218	2.633
219	2.783
220	2.794
221	2.984
222	[****]
223	[****]
224	[****]
225	[****]
226	[****]
227	[****]
228	[****]
229	[****]
230	[****]

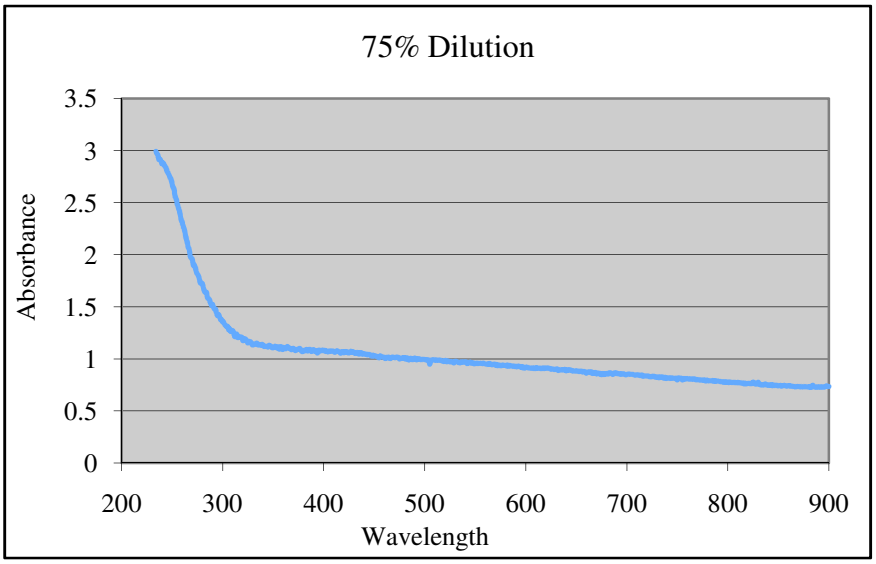

UV-Vis Scanning Spectrophotometer – 100% wastewater

TEST SETUP
GENESYS 6 v1.120 2M6G056001

Scanning	1:39pm 17Dec08
Test Name	200-900nm[Saved]
Measurement Mode	Absorbance
Start Wavelength	200.0nm
Stop Wavelength	900.0nm
Sample Positioner	Manual 6
Scan Speed	Fast
Interval	1.0nm
ID# (0=OFF)	1
Auto Print	On
Auto Save Data	Off

ID#: 1

Wavelength	Abs
200	0.35
201	0.427
202	0.865
203	1.249
204	0.849
205	0.765
206	0.799
207	0.709
208	0.773
209	0.974
210	1.088
211	1.062
212	1.34
213	1.425
214	1.939
215	1.783
216	2.087
217	2.163
218	2.514
219	2.567
220	[****]
221	2.884
222	2.953
223	[****]
224	[****]
225	[****]
226	[****]
227	[****]
228	[****]
229	[****]
230	2.953

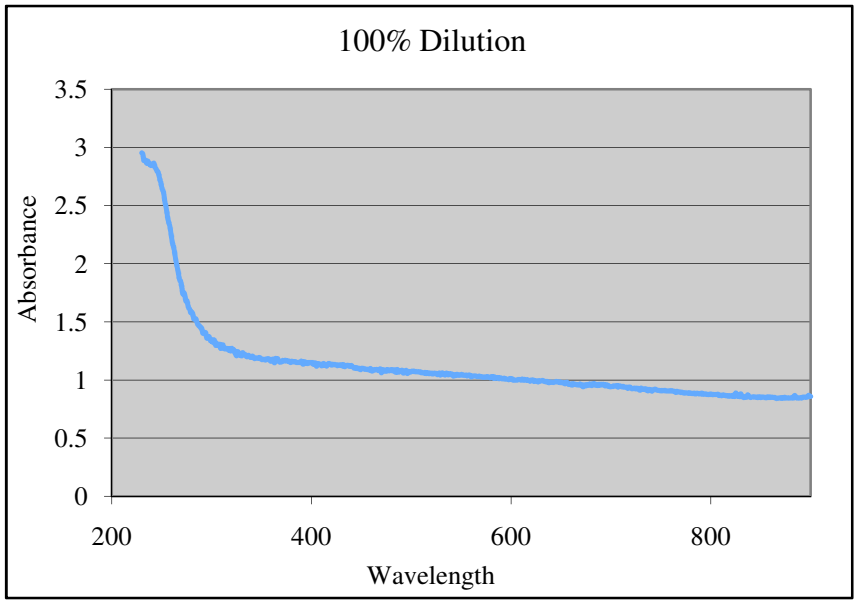

Raw Wastewater Absorbance, TSS, and VSS Values

	Test 1	Test 2	Test 3	Test 4	Test 5	Test 6	AVG	Std. Dev.	95% C.I.
Abs	3.4	3.42	3.573	3.154	3.192	3.292	3.3385	0.1569	0.1255

Vol (mL)	Filter Mass (mg)	Filter+Sample (mg)	Ignited (mg)	TSS (mg/L)	VSS (mg/L)
5	89	104	91.8	3000	2440
5	87.2	105	92.3	3560	2540
5	86.2	103.6	88.5	3480	3020
AVG				3347	2667
Std. Dev.				303	310
95% C.I.				343	351

Fatty Acid Concentrations of Raw Wastewater

W.A Callegari Environmental Center
Water Quality Laboratory
Baton Rouge, LA 70820
Ph: (225) 765-5155
Fax: (225)765-5158

Analytical Results

Chicken Fats as Fatty Acid Methyle Esters (FAME)

Client Name: Adam Dassey
BAE
Date received:
Date Completed: 9/19/2009

Matrix: Waste Water
No. of Samples: 1
Date Sampled:

Target Compounds

Peaks#	RT (min)	Peak Name	Concentration mg/L	%
17	14.759	Hexadec acid, 2-hydroxy-, me	Internal Standard	
1	6.243	Methyl Decanoate (Caprate) C10:0	0.00	0.00
2	7.278	Undecanoic acid, methyl ester C11:0	0.00	0.00
3	8.254	Methyl Laurate C12:0	0.00	0.00
4	9.186	Methyl Tridecanoate C13:0	0.00	0.00
5	10.071	Methyl Myristate C14:0	51.84	0.36
6	10.401	Myristoleic Acid ME C14:0	3.84	0.03
7	10.49	13-Tetradecynoic acid, me C15:1	0.00	0.00
8	10.921	Methyl Pentadecanoate C15:0	0.00	0.00
9	11.735	Methyl Palmitate C16:0	3832.32	26.81
10	11.945	Methyl Palmitoleate C16:1	783.36	5.48
11	12.504	Methyl Heptadecanoate C17:0	7.22	0.05
12	13.251	Methyl Stearate C18:0	1113.60	7.79
13	13.411	Cis-9-Oleic Methyl Ester C18:1	5514.24	38.57
14	13.755	Methyl Linoleate C18:2	2774.40	19.41
15	14.224	Methyl Linolenate C18:3	197.76	1.38
16	14.711	Methyl Arachidate C20:0	0.00	0.00
18	14.76	11-Eicosenoic acid, methyl ester C21:0	18.43	0.13
19	16.602	Methyl Behenate C22:0	0.00	0.00
20	16.882	Methyl Erucate C22:1	0.00	0.00
		Total:	14297.01	100.00

Chromograph of Fatty Acid Peaks

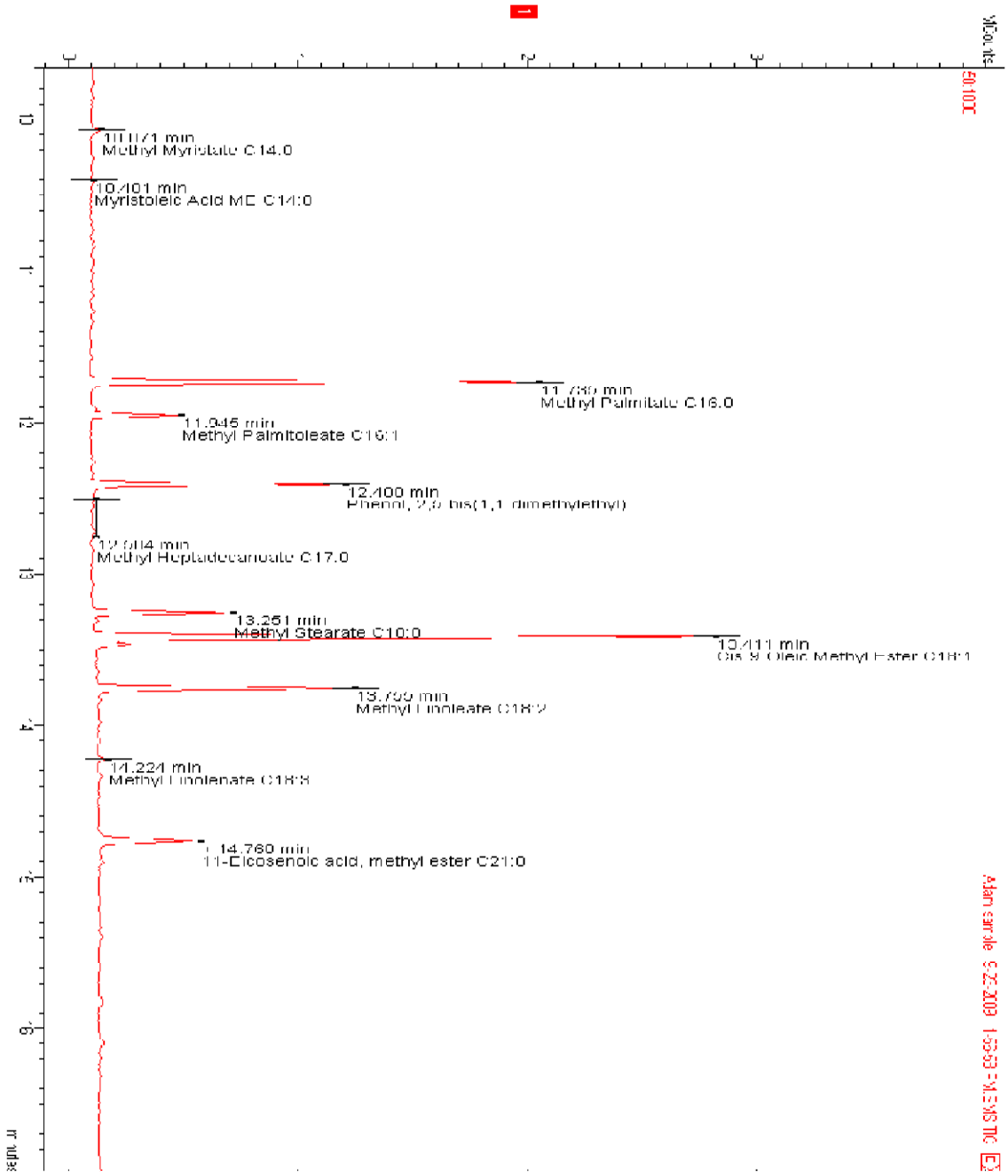

Metal Analysis of Raw Wastewater

Metals (EPA 200.7)	**Result**		
Sample Lab ID:		290712-11	290712-12
Sample Field ID:	*MDL*	**No ID 1**	**No ID 2**
Unit:	*mg/L*	*mg/L*	*mg/L*
Aluminum (Al)	*0.06*	0.910	0.896
Arsenic (As)	*0.01*	0.033	0.051
Boron (B)	*0.02*	1.269	1.214
Barium (Ba)	*0.02*	4.120	4.191
Beryllium (Be)	*0.01*	ND	ND
Calcium (Ca)	*0.02*	5.871	6.181
Cadmium (Cd)	*0.01*	ND	ND
Cobalt (Co)	*0.01*	ND	ND
Chromium (Cr)	*0.01*	0.009	0.009
Copper (Cu)	*0.01*	0.287	0.292
Iron (Fe)	*0.01*	6.419	7.789
Potassium (K)	*0.032*	338.370	342.013
Magnesium (Mg)	*0.01*	25.629	25.940
Manganese (Mn)	*0.01*	0.103	0.107
Molybdenum (Mo)	*0.038*	ND	ND
Sodium (Na)	*0.029*	58.008	58.380
Nickel (Ni)	*0.01*	0.081	0.084
Phosphorus (P)	*0.024*	196.165	198.009
Lead (Pb)	*0.01*	ND	ND
Sulfur (S)	*0.011*	161.212	165.225
Antimony (Sb)	*0.01*	ND	0.010
Selenium (Se)	*0.01*	ND	ND
Silicone (Si)	*0.7*	33.761	33.817
Tin (Sn)	*0.01*	ND	ND
Strontium (Sr)	*0.02*	ND	ND
Thallium (Tl)	*0.01*	ND	ND
Vanadium (V)	*0.01*	ND	ND
Yttrium (Y)	*0.01*	ND	ND
Zinc (Zn)	*0.01*	2.960	2.901
Anios by EPA300.0 method:			
Chloride (mg/L)	*0.1*	414.3964	402.0228
Nitrate (NO_3-N mg/L)	*0.07*	1.2502	1.2007
Nitrite (NO_2-N mg/L)	*0.06*	11.272	11.0546
Phosphate (mg/L)	*0.03*	443.307	430.4696
Sulfate (mg/L)	*0.06*	31.8823	31.3309
Fluoride (mg/L)	*0.04*	155.6571	156.1814

Appendix C: Raw Data, Statistics, and Images for First Round of Metal Coagulant Testing

Aluminum Coagulant TSS and VSS

(mg/L)	Pan #	Volume (ml)	Filter Mass (mg)	Filter + Sample (mg)	Ignited Mass (mg)	TSS (mg/L)	VSS (mg/L)
EC 309							
100	A1	5	88.1	94.0	89.3	1180	940
200	A2	15	89.0	98.1	91.1	606.7	466.7
300	A3	15	89.5	95.0	90.3	366.7	313.3
400	A4	15	91.3	95.5	91.7	280	253.3
500	A5	15	90.9	93.5	90.8	173.3	180
600	A6	15	90.9	92.6	90.4	113.3	146.7
EC 409							
100	B1	10	89.3	99.0	93.0	970	600
200	B2	10	89.2	95.9	91.1	670	480
300	B3	15	90.1	98.5	92.6	560	393.3
400	B4	15	89.5	95.4	91.2	393.3	280
500	B5	15	89.7	93.4	90.4	246.7	200
600	B6	20	89.4	95.4	90.9	300	225
EC 509							
100	C1	5	89.7	96.2	91.4	1300	960
200	C2	6	89.1	93.0	90.0	650	500
300	C3	10	90.5	93.3	90.8	280	250
400	C4	15	90.4	94.2	91.1	253.3	206.7
500	C5	15	90.5	94.1	91.1	240	200
600	C6	20	89.0	92.8	89.8	190	150
EC 609							
100	D1	5	90.4	98.2	92.0	1560	1240
200	D2	5	89.3	96.4	90.6	1420	1160
300	D3	10	90.2	99.0	91.9	880	710
400	D4	15	89.0	93.9	89.4	326.7	300
500	D5	15	89.4	94.9	89.9	366.7	333.3
600	D6	20	88.5	94.8	88.4	315	320

Optical Density - Aluminum Coagulants

EC 309 (mg/L)	Abs. 1	Abs. 2	Abs. 3	AVG	Std. Dev.	95% C.I.
100	2.465	2.426	2.423	2.438	0.023	0.027
200	1.808	1.812	1.742	1.787	0.039	0.044
300	1.341	1.366	1.331	1.346	0.018	0.020
400	1.167	1.155	1.161	1.161	0.006	0.007
500	0.951	0.960	0.966	0.959	0.008	0.009
600	0.798	0.780	0.792	0.790	0.009	0.010
EC 409						
100	2.208	2.307	2.268	2.261	0.050	0.056
200	1.904	1.889	1.879	1.891	0.013	0.014
300	1.582	1.597	1.595	1.591	0.008	0.009
400	1.311	1.321	1.284	1.305	0.019	0.022
500	1.124	1.125	1.147	1.132	0.013	0.015
600	1.062	1.030	1.053	1.048	0.017	0.019
EC 509						
100	2.541	2.527	2.523	2.530	0.009	0.011
200	1.808	1.830	1.829	1.822	0.012	0.014
300	1.264	1.259	1.217	1.247	0.026	0.029
400	1.159	1.140	1.317	1.205	0.097	0.110
500	1.017	0.992	1.002	1.004	0.013	0.014
600	0.848	0.869	0.885	0.867	0.019	0.021
EC 609						
100	2.469	2.463	2.460	2.464	0.005	0.005
200	2.310	2.248	2.174	2.244	0.068	0.077
300	1.974	1.980	1.902	1.952	0.043	0.049
400	1.649	1.637	1.636	1.641	0.007	0.008
500	1.333	1.348	1.359	1.347	0.013	0.015
600	1.309	1.311	1.318	1.313	0.005	0.005

EC 309 After Coagulation

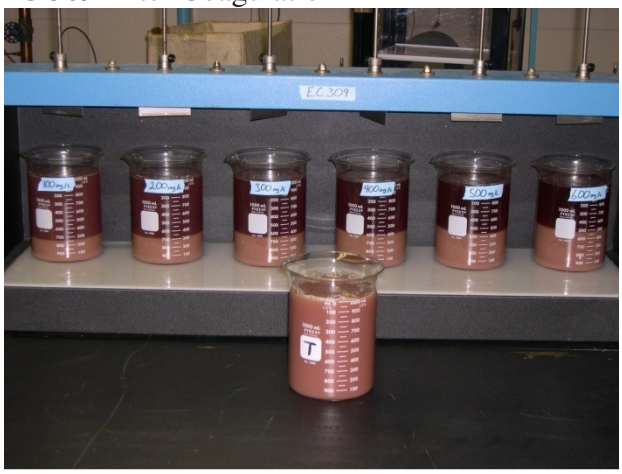

EC 409 After Coagulation

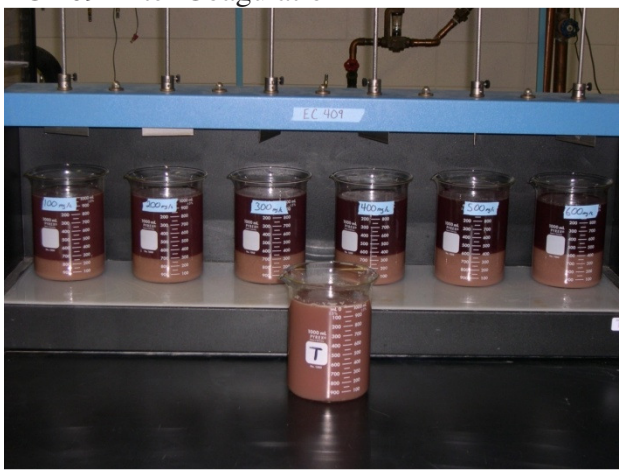

EC 509 After Coagulation

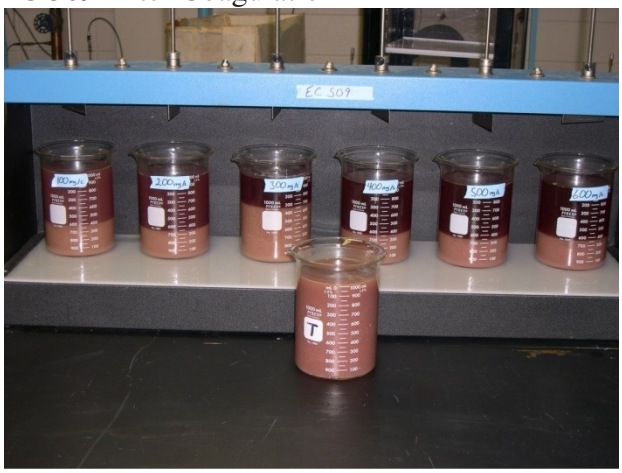

EC 609 After Coagulation

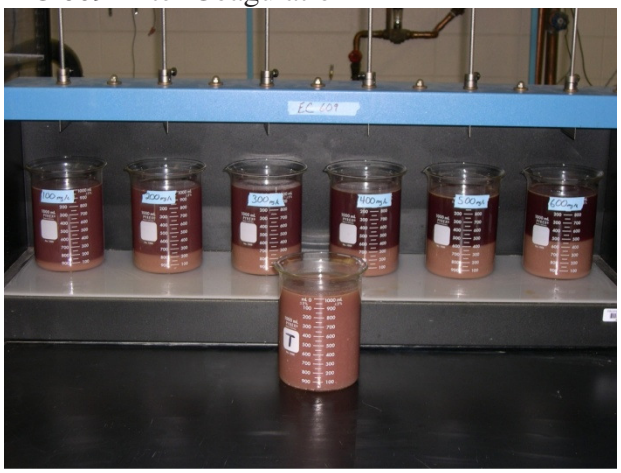

TSS and VSS – Iron Coagulants

(mg/L)	Pan #	Volume (ml)	Filter Mass (mg)	Filter + Sample (mg)	Ignited Mass (mg)	TSS (mg/L)	VSS (mg/L)
Ferrous Chlordide							
100	A1	5	90.6	96.2	91.8	1120	880
200	A2	5	88.8	93.7	89.7	980	800
300	A3	5	90.0	93.7	90.5	740	640
400	A4	10	89.7	97.1	91.6	740	550
500	A5	5	89.0	92.9	89.3	780	720
600	A6	5	90.7	94.6	91.4	780	640
Ferrous Sulfate							
100	B1	5	89.6	96.3	92.4	1340	780
200	B2	5	90.0	95.1	91.4	1020	740
300	B3	5	90.1	94.1	91.1	800	600
400	B4	10	90.8	96.2	92.1	540	410
500	B5	10	90.1	94.5	91.0	440	350
600	B6	10	90.2	93.7	90.7	350	300
Ferric Chloride							
100	C1	5	88.6	100	92.7	2280	1460
200	C2	5	90.0	95.4	91.4	1080	800
300	C3	10	90.0	95.2	90.4	520	480
400	C4	10	88.5	95.2	91.4	670	380
500	C5	15	88.6	94.6	90.4	400	280
600	C6	15	88.9	94.2	90.0	353.3	280
Ferric Sulfate							
100	D1	5	88.7	104.1	96.4	3080	1540
200	D2	5	89.2	100.3	94.8	2220	1100
300	D3	5	89.6	96.3	92.7	1340	720
400	D4	10	89.9	96.4	92.8	650	360
500	D5	10	89.2	94.1	91.0	490	310
600	D6	10	89.0	93.1	90.7	410	240

Optical Density - Iron Coagulants

Ferrous Chloride (mg/L)	Abs. 1	Abs. 2	Abs. 3	AVG	Std. Dev.	95% C.I.
100	2.614	2.612	2.627	2.618	0.008	0.009
200	2.429	2.382	2.425	2.412	0.026	0.029
300	2.230	2.201	2.207	2.213	0.015	0.017
400	2.104	2.106	2.130	2.113	0.014	0.016
500	2.050	2.067	2.065	2.061	0.009	0.011
600	1.974	2.000	1.981	1.985	0.013	0.015
Ferrous Sulfate (mg/L)						
100	2.514	2.521	2.486	2.507	0.019	0.021
200	2.276	2.252	2.246	2.258	0.016	0.018
300	2.044	2.033	2.043	2.040	0.006	0.007
400	1.784	1.773	1.784	1.780	0.006	0.007
500	1.598	1.608	1.617	1.608	0.010	0.011
600	1.514	1.508	1.538	1.520	0.016	0.018
Ferric Chloride (mg/L)						
100	3.150	3.141	3.171	3.154	0.015	0.017
200	2.119	2.161	2.082	2.121	0.040	0.045
300	1.587	1.626	1.630	1.614	0.024	0.027
400	1.203	1.114	1.171	1.163	0.045	0.051
500	0.967	0.945	0.972	0.961	0.014	0.016
600	0.817	0.821	0.813	0.817	0.004	0.005
Ferric Sulfate (mg/L)						
100	3.375	3.534	3.549	3.486	0.096	0.109
200	2.949	2.887	2.960	2.932	0.039	0.045
300	2.304	2.250	2.294	2.283	0.029	0.033
400	1.620	1.624	1.612	1.619	0.006	0.007
500	1.324	1.358	1.354	1.345	0.019	0.021
600	1.096	1.098	1.089	1.094	0.005	0.005

Ferrous Chloride After Coagulation

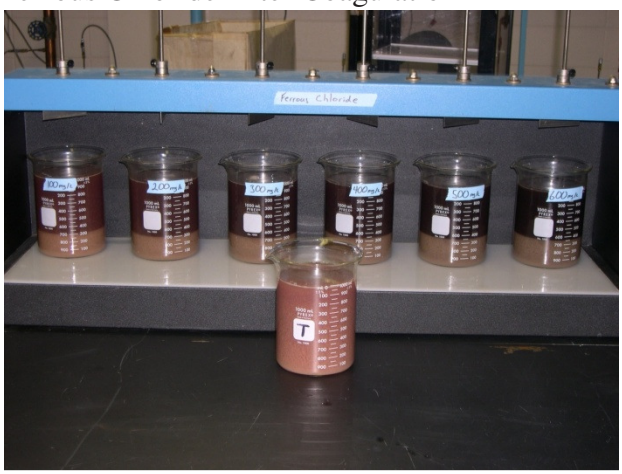

Ferrous Sulfate After Coagulation

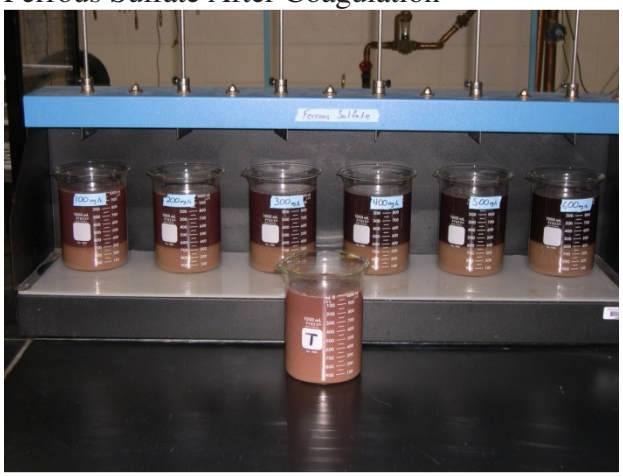

Ferric Chloride After Coagulation

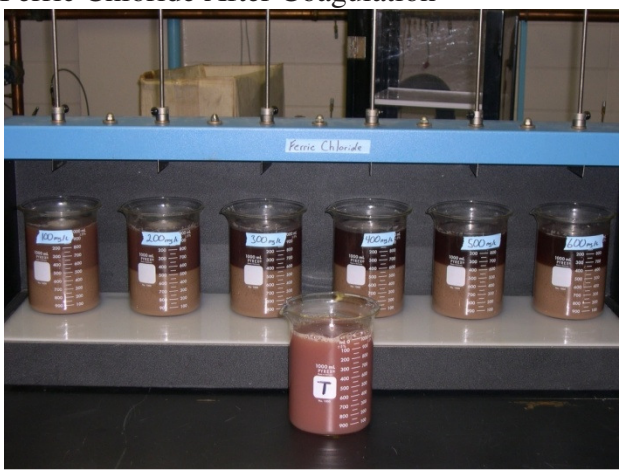

Ferric Sulfate After Coagulation

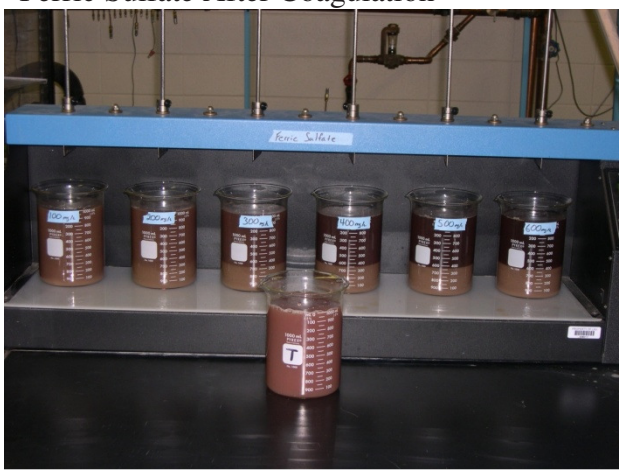

TSS and VSS – Oil Emulsion Breaker

(mg/L)	Pan #	Volume (mL)	Filter Mass (mg)	Filter + Sample (mg)	Ignited Mass (mg)	TSS (mg/L)	VSS (mg/L)
CPF 4265							
100	A1	5	90.4	99.4	92.7	1800	1340
200	A2	5	91.1	96.4	92.0	1060	880
300	A3	10	90.6	98.2	92.2	760	600
400	A4	10	90.4	95.4	91.2	500	420
500	A5	15	89.1	94.8	90.0	380	320
600	A6	15	90.3	94.8	90.5	300	286.7
CPF 4168							
100	B1	5	89.3	96.4	90.4	1420	1200
200	B2	5	89.6	92.8	89.4	640	680
300	B3	10	90.1	93.9	89.8	380	410
400	B4	15	89.8	93.7	89.9	260	253.3
500	B5	20	90.0	94.8	90.1	240	235
600	B6	20	89.7	93.9	89.3	210	230
CPF 4275							
100	C1	5	90.3	104.1	94.9	2760	1840
200	C2	5	89.5	97.3	91.7	1560	1120
300	C3	5	88.5	92.6	89.47	820	626
400	C4	10	88.9	94.2	90.1	530	410
500	C5	10	89.5	96.1	91.0	660	510
600	C6	15	90.3	93.9	90.8	240	206.7

Optical Density - Oil Emulsion Breakers

CPF 4265 (mg/L)	Abs. 1	Abs. 2	Abs.3	AVG	Std. Dev.	95% C.I.
100	2.792	2.820	2.831	2.814	0.020	0.023
200	2.285	2.355	2.311	2.317	0.035	0.040
300	1.952	1.993	2.003	1.983	0.027	0.031
400	1.559	1.544	1.592	1.565	0.025	0.028
500	1.315	1.318	1.350	1.328	0.019	0.022
600	1.094	1.093	1.070	1.086	0.014	0.015
CPF 4168 (mg/L)						
100	2.480	2.440	2.515	2.478	0.038	0.042
200	1.578	1.656	1.627	1.620	0.039	0.045
300	1.284	1.284	1.269	1.279	0.009	0.010
400	0.985	0.971	1.010	0.989	0.020	0.022
500	0.868	0.868	0.865	0.867	0.002	0.002
600	0.679	0.681	0.676	0.679	0.003	0.003
CPF 4275 (mg/L)						
100	3.494	3.479	3.424	3.466	0.037	0.042
200	2.718	2.729	2.689	2.712	0.021	0.023
300	1.948	1.952	1.897	1.932	0.031	0.035
400	1.555	1.541	1.555	1.550	0.008	0.009
500	1.573	1.595	1.597	1.588	0.013	0.015
600	0.999	1.025	1.000	1.008	0.015	0.017

CPF 4265 After Coagulation

CPF 4168 After Coagulation

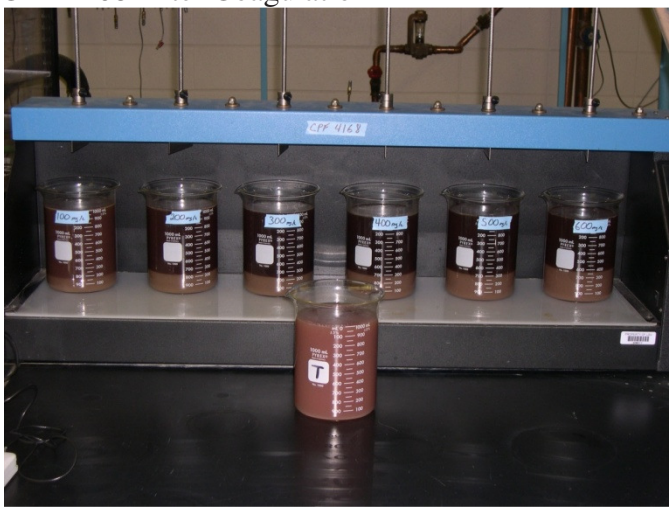

CPF 4275 After Coagulation

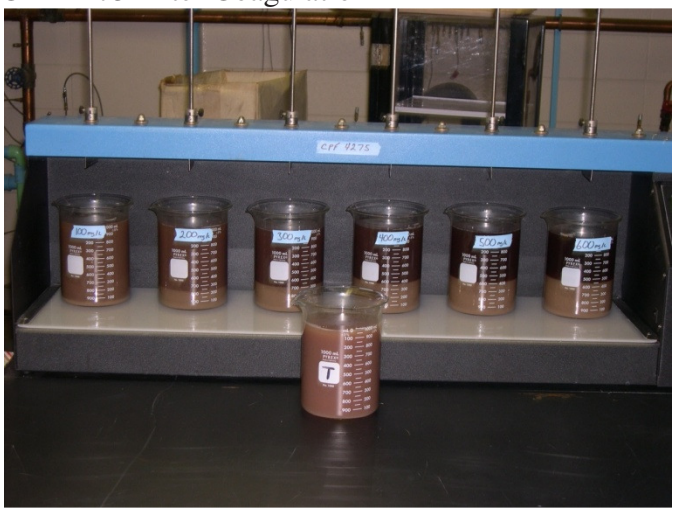

Velocity Gradient

Rapid Mixing – 120 rpm for 2 minutes

$N_{Re} = D_i^2 n\rho/\mu$

$= (0.0762\ m)^2(2\ rps)(1000\ kg/m^3)/4.3*10^{-3}\ N*s/m^2$

$= \underline{2700}$

$P = K_T n^3 D_i^5 \rho$

$= (2.25)(2\ rps)^3(0.0762\ m)^5(1000\ kg/m^3)$

$= \underline{0.0462\ N*m/s}$

Since beakers are round with no baffles: P*0.75 = 0.0347 N*m/s

$G = (P/uV)-2$

$= [(0.0347\ N*m/s)/(7.3*10^{-3}\ N*s/m^2)(.001\ m^3)]^{-2}$

$= \underline{90\ s^{-1}}$

Rapid mixing occurred for 2 minutes, therefore: <u>GT = 10,800</u>

Flocculation – 30 rpm for 20 minutes

30 rpm = 0.5 rps

$V = (rps)(\pi D/rev)0.75$

$= (0.5\ rps)(\pi(0.0762\ m)/rev)0.75$

$V = \underline{0.09\ m/s}$

$P = C_D A\rho(v3/2)$

$= (1.2)(0.0019\ m^2)(1000\ kg/m^3)((0.09\ m/s)^3/2)$

$= \underline{8.31*10^{-4}\ N*m/s}$

$G = (P/uV)^{-2}$

$= [(8.31*10^{-4}\ M*m/s)/94.3*10^{-3}\ N*s/m^2)(.001\ m^3)]^{-2}$

$G = \underline{13.9\ s^{-1}}$

Flocculation occurred for 20 minutes, therefore: GT = <u>16,680</u>

Appendix D: Raw Data, Statistics, and Images for Comparative Testing

TSS and VSS – EC 309, FeCl, CPF 4168

The best from every coagulant group was selected and tested over a larger range

EC 309 (mg/L)	Abs 1	Abs 2	Abs 3	Average	Std. Dev.	95% C.I.
50	3.151	3.223	3.281	3.218	0.065	0.074
250	1.362	1.381	1.405	1.383	0.022	0.024
450	0.863	0.905	0.893	0.887	0.022	0.024
650	0.481	0.495	0.471	0.482	0.012	0.014
850	0.446	0.445	0.438	0.443	0.004	0.005
1050	0.463	0.458	0.450	0.457	0.007	0.007
Ferric Chloride						
50	1.883	1.906	1.904	1.898	0.013	0.014
250	0.686	0.734	0.718	0.713	0.024	0.028
450	0.393	0.394	0.405	0.397	0.007	0.008
650	0.217	0.205	0.206	0.209	0.007	0.008
850	0.220	0.208	0.199	0.209	0.011	0.012
1050	0.265	0.259	0.272	0.265	0.007	0.007
CPF 4168						
50	1.366	1.431	1.357	1.385	0.040	0.046
250	0.673	0.666	0.660	0.666	0.007	0.007
450	0.331	0.351	0.349	0.344	0.011	0.012
650	0.215	0.210	0.217	0.214	0.004	0.004
850	0.305	0.289	0.288	0.294	0.010	0.011
1050	0.551	0.482	0.536	0.523	0.036	0.041

Optical Density - EC 309, FeCl, CPF 4168

EC 309 (mg/L)	Pan #	Volume (ml)	Filter Mass (mg)	Filter + Sample (mg)	Ignited Mass (mg)	TSS (mg/L)	VSS (mg/L)
50	A1	5	90.5	111.7	98.3	4240	2680
250	A2	10	91.0	96.5	92.5	550	400
450	A3	20	88.9	95.0	90.4	305	230
650	A4	20	88.4	89.7	88.8	65	45
850	A5	15	89.6	90.3	89.6	46.7	46.7
1050	A6	10	89.6	90.3	89.5	70	80
Ferric Chloride							
50	B1	5	91.6	96.4	92.7	960	740
250	B2	15	89.9	92.6	91.3	180	86.7
450	B3	20	89.5	90.2	89.1	35	55
650	B4	20	89.8	90.1	89.2	15	45
850	B5	10	89.7	90.1	89.0	40	110
1050	B6	11	91.3	90.4	89.2	0	109.1
CPF 4168							
50	C1	5	89.9	92.3	90.0	480	460
250	C2	15	89.0	90.4	88.9	93.3	100
450	C3	20	89.7	90.7	90.1	50	30
650	C4	20	90.6	91.6	90.7	50	45
850	C5	6	89.1	90.4	88.8	216.7	266.7
1050	C6	12	89.5	93.4	89.5	325	325

Correlation Between TSS and Optical Density

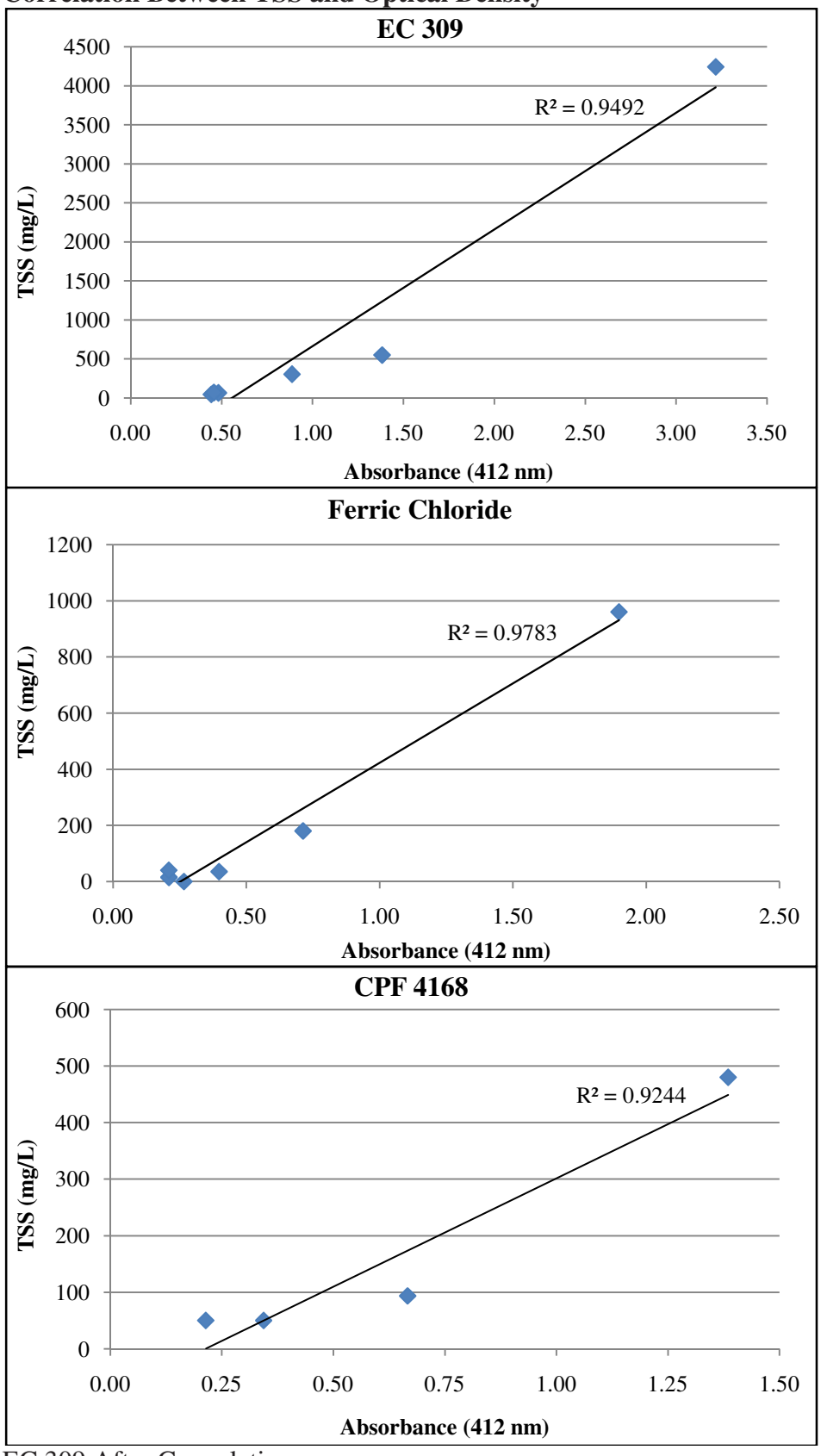

EC 309 After Coagulation

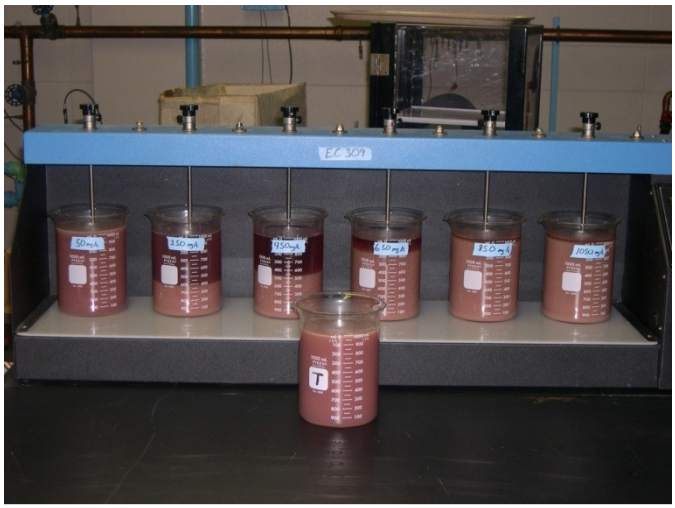

FeCl After Coagulation

CPF 4168 After Coagulation

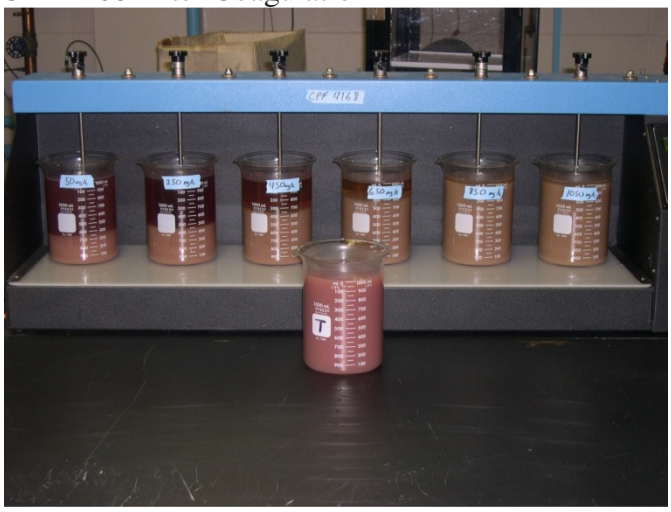

Metal Analysis of Supernatant after Coagulation (50 mg/L)

Metals (EPA 200.7)	**Result**			
Sample Lab ID:		**w290805-01**	**w290805-02**	**w290805-03**
Sample Field ID:		**1 EC 309 50mg/l**	**2 FeCl3 50mg/l**	**3 CPF 50mg/l**
	MDL			
Unit:	*mg/L*	*mg/L*	*mg/L*	*mg/L*
Aluminum (Al)	*0.06*	6.418	1.325	1.339
Arsenic (As)	*0.01*	0.020	0.017	0.022
Boron (B)	*0.02*	0.317	0.323	0.301
Barium (Ba)	*0.02*	0.015	0.004	0.004
Beryllium (Be)	*0.01*	ND	ND	ND
Calcium (Ca)	*0.02*	4.261	3.291	3.336
Cadmium (Cd)	*0.01*	0.008	0.003	0.003
Cobalt (Co)	*0.01*	0.005	ND	ND
Chromium (Cr)	*0.01*	0.011	0.005	0.004
Copper (Cu)	*0.01*	0.203	0.155	0.139
Iron (Fe)	*0.01*	4.915	7.155	6.369
Potassium (K)	*0.032*	187.051	187.941	191.735
Magnesium (Mg)	*0.01*	16.652	15.977	16.057
Manganese (Mn)	*0.01*	0.092	0.087	0.085
Molybdenum (Mo)	*0.038*	ND	ND	ND
Sodium (Na)	*0.029*	35.728	35.677	36.797
Nickel (Ni)	*0.01*	0.119	0.065	0.053
Phosphorus (P)	*0.024*	110.913	99.629	97.009
Lead (Pb)	*0.01*	0.021	0.012	0.014
Sulfur (S)	*0.011*	64.266	60.341	59.284
Antimony (Sb)	*0.01*	ND	ND	ND
Selenium (Se)	*0.01*	0.005	ND	ND
Silicone (Si)	*0.7*	26.769	26.939	27.035
Tin (Sn)	*0.01*	0.023	0.011	0.016
Strontium (Sr)	*0.02*	ND	ND	ND
Thallium (Tl)	*0.01*	ND	ND	ND
Vanadium (V)	*0.01*	0.001	ND	0.002
Yttrium (Y)	*0.01*	0.002	ND	ND
Zinc (Zn)	*0.01*	0.577	0.374	0.318

Anios by EPA300.0 method:

Sample Field ID:	***MDL***	**1 EC 50mg/L**	**2 FeCl 50mg/L**	**3 CPF 50mg/L**
Chloride (mg/L)	*0.1*	291.368	299.857	299.289
Nitrate (NO_3-N mg/L)	*0.07*	1.055	1.142	1.705
Nitrite (NO_2-N mg/L)	*0.06*	9.294	9.135	10.364
Phosphate (mg/L)	*0.03*	247.197	242.799	239.752
Sulfate (mg/L)	*0.06*	12.342	12.077	13.350
Fluoride (mg/L)	*0.04*	102.926	101.773	100.757

Metal Analysis of Supernatant after Coagulation (250 mg/L)

Metals (EPA 200.7)	**Result**			
Sample Lab ID:		**w290805-04**	**w290805-05**	**w290805-06**
Sample Field ID:		**4 EC 309**	**5 FeCl3**	**6 CPF 4168**
	MDL	**250mg/l**	**250mg/l**	**250mg/l**
Unit:	*mg/L*	*mg/L*	*mg/L*	*mg/L*
Aluminum (Al)	*0.06*	2.890	1.324	1.291
Arsenic (As)	*0.01*	0.016	0.012	ND
Boron (B)	*0.02*	0.305	0.285	0.293
Barium (Ba)	*0.02*	0.003	0.002	0.002
Beryllium (Be)	*0.01*	ND	ND	ND
Calcium (Ca)	*0.02*	3.236	3.421	3.613
Cadmium (Cd)	*0.01*	0.003	0.002	0.003
Cobalt (Co)	*0.01*	0.003	0.002	ND
Chromium (Cr)	*0.01*	0.003	0.004	0.004
Copper (Cu)	*0.01*	0.135	0.125	0.122
Iron (Fe)	*0.01*	2.629	5.889	7.257
Potassium (K)	*0.032*	193.874	192.692	197.186
Magnesium (Mg)	*0.01*	15.901	15.983	16.377
Manganese (Mn)	*0.01*	0.060	0.144	0.157
Molybdenum (Mo)	*0.038*	ND	ND	ND
Sodium (Na)	*0.029*	36.762	37.363	37.927
Nickel (Ni)	*0.01*	0.122	0.097	0.068
Phosphorus (P)	*0.024*	85.095	80.347	81.008
Lead (Pb)	*0.01*	0.016	0.013	0.024
Sulfur (S)	*0.011*	59.488	58.439	59.090
Antimony (Sb)	*0.01*	0.020	0.018	ND
Selenium (Se)	*0.01*	ND	ND	ND
Silicone (Si)	*0.7*	26.976	27.164	27.576
Tin (Sn)	*0.01*	ND	0.006	ND
Strontium (Sr)	*0.02*	ND	ND	ND
Thallium (Tl)	*0.01*	ND	ND	ND
Vanadium (V)	*0.01*	ND	ND	ND
Yttrium (Y)	*0.01*	ND	0.000	ND
Zinc (Zn)	*0.01*	0.303	0.234	0.242

Anios by EPA300.0 method:

Sample Field ID:	***MDL***	**4 EC 250mg/L**	**5 FC 250mg/L**	**6 CPF 250mg/L**
Chloride (mg/L)	*0.1*	324.660	342.079	350.425
Nitrate (NO_3-N mg/L)	*0.07*	0.889	1.454	0.896
Nitrite (NO_2-N mg/L)	*0.06*	8.519	9.306	8.914
Phosphate (mg/L)	*0.03*	204.509	192.625	190.982
Sulfate (mg/L)	*0.06*	12.130	13.670	12.672
Fluoride (mg/L)	*0.04*	96.841	93.784	96.192

Metal Analysis of Supernatant after Coagulation (450 mg/L)

Metals (EPA 200.7)	**Result**			
Sample Lab ID:		**w290805-07**	**w290805-08**	**w290805-09**
Sample Field ID:		**7 EC 309 450mg/l**	**8 FeCl3 450mg/l**	**9 CPF 4168 450mg/l**
	MDL			
Unit:	*mg/L*	*mg/L*	*mg/L*	*mg/L*
Aluminum (Al)	*0.06*	3.600	1.484	1.267
Arsenic (As)	*0.01*	0.012	ND	ND
Boron (B)	*0.02*	0.292	0.368	0.303
Barium (Ba)	*0.02*	0.003	0.003	0.002
Beryllium (Be)	*0.01*	ND	ND	ND
Calcium (Ca)	*0.02*	3.394	4.114	3.848
Cadmium (Cd)	*0.01*	0.002	0.002	0.003
Cobalt (Co)	*0.01*	ND	0.003	0.003
Chromium (Cr)	*0.01*	0.002	0.013	0.005
Copper (Cu)	*0.01*	0.125	0.116	0.112
Iron (Fe)	*0.01*	2.132	7.698	9.922
Potassium (K)	*0.032*	197.030	195.861	197.777
Magnesium (Mg)	*0.01*	16.461	16.806	16.972
Manganese (Mn)	*0.01*	0.057	0.235	0.267
Molybdenum (Mo)	*0.038*	ND	ND	ND
Sodium (Na)	*0.029*	37.549	37.970	38.487
Nickel (Ni)	*0.01*	0.069	0.069	0.064
Phosphorus (P)	*0.024*	71.631	68.227	65.318
Lead (Pb)	*0.01*	0.012	0.015	0.019
Sulfur (S)	*0.011*	60.200	65.711	57.581
Antimony (Sb)	*0.01*	0.007	0.017	0.014
Selenium (Se)	*0.01*	ND	ND	#VALUE!
Silicone (Si)	*0.7*	27.715	27.903	28.088
Tin (Sn)	*0.01*	0.015	0.023	#VALUE!
Strontium (Sr)	*0.02*	ND	ND	#VALUE!
Thallium (Tl)	*0.01*	ND	ND	#VALUE!
Vanadium (V)	*0.01*	ND	ND	#VALUE!
Yttrium (Y)	*0.01*	ND	0.001	#VALUE!
Zinc (Zn)	*0.01*	0.257	0.227	0.238

Anios by EPA300.0 method:

Sample Field ID:	***MDL***	**7 EC 450mg/L**	**8 FC 450mg/L**	**9 CPF 450mg/L**
Chloride (mg/L)	*0.1*	376.314	416.470	403.951
Nitrate (NO_3-N mg/L)	*0.07*	0.967	0.817	0.880
Nitrite (NO_2-N mg/L)	*0.06*	9.363	8.833	5.303
Phosphate (mg/L)	*0.03*	169.530	149.660	140.338
Sulfate (mg/L)	*0.06*	13.885	16.992	21.156
Fluoride (mg/L)	*0.04*	99.257	97.747	97.505

Metal Analysis of Supernatant after Coagulation (650 mg/L)

Metals (EPA 200.7)	**Result**			
Sample Lab ID:		**w290805-10**	**w290805-11**	**w290805-12**
Sample Field ID:		**10 EC 309 650mg/l**	**11 FeCl3 650mg/l**	**12 CPF 4168 650mg/l**
	MDL			
Unit:	*mg/L*	*mg/L*	*mg/L*	*mg/L*
Aluminum (Al)	*0.06*	1.630	1.283	1.348
Arsenic (As)	*0.01*	0.007	0.003	ND
Boron (B)	*0.02*	0.317	0.284	0.304
Barium (Ba)	*0.02*	0.003	0.002	0.003
Beryllium (Be)	*0.01*	ND	ND	ND
Calcium (Ca)	*0.02*	3.894	4.177	3.961
Cadmium (Cd)	*0.01*	0.002	0.003	0.003
Cobalt (Co)	*0.01*	0.002	0.005	0.003
Chromium (Cr)	*0.01*	0.003	0.006	0.008
Copper (Cu)	*0.01*	0.123	0.100	0.100
Iron (Fe)	*0.01*	1.696	9.700	11.978
Potassium (K)	*0.032*	207.254	196.005	197.933
Magnesium (Mg)	*0.01*	17.661	16.907	17.024
Manganese (Mn)	*0.01*	0.060	0.354	0.394
Molybdenum (Mo)	*0.038*	ND	ND	ND
Sodium (Na)	*0.029*	39.978	37.691	38.707
Nickel (Ni)	*0.01*	0.082	0.068	0.074
Phosphorus (P)	*0.024*	57.662	51.114	48.879
Lead (Pb)	*0.01*	0.020	0.007	0.008
Sulfur (S)	*0.011*	62.026	55.585	56.294
Antimony (Sb)	*0.01*	ND	0.030	0.014
Selenium (Se)	*0.01*	ND	ND	ND
Silicone (Si)	*0.7*	29.038	27.093	27.688
Tin (Sn)	*0.01*	0.014	#VALUE!	#VALUE!
Strontium (Sr)	*0.02*	ND	ND	ND
Thallium (Tl)	*0.01*	ND	ND	ND
Vanadium (V)	*0.01*	0.001	ND	ND
Yttrium (Y)	*0.01*	0.001	0.001	ND
Zinc (Zn)	*0.01*	0.229	0.274	0.323

Anios by EPA300.0 method:

Sample Field ID:	***MDL***	**10 EC 650mg/L**	**11 FC 650mg/L**	**12 CPF 650mg/L**
Chloride (mg/L)	*0.1*	395.207	465.218	461.953
Nitrate (NO_3-N mg/L)	*0.07*	0.527	0.470	0.384
Nitrite (NO_2-N mg/L)	*0.06*	8.805	5.694	5.067
Phosphate (mg/L)	*0.03*	125.366	104.813	94.205
Sulfate (mg/L)	*0.06*	17.503	17.944	18.475
Fluoride (mg/L)	*0.04*	99.527	95.338	93.170

Metal Analysis of Supernatant after Coagulation (850 mg/L)

Metals (EPA 200.7)	**Result**		
Sample Lab ID:		**w290805-14**	**w290805-15**
Sample Field ID:		**14 EC 309 850mg/l**	**15 FeCl3 850mg/l**
	MDL		
Unit:	*mg/L*	*mg/L*	*mg/L*
Aluminum (Al)	*0.06*	1.818	1.213
Arsenic (As)	*0.01*	ND	0.010
Boron (B)	*0.02*	0.294	0.279
Barium (Ba)	*0.02*	0.005	0.002
Beryllium (Be)	*0.01*	ND	ND
Calcium (Ca)	*0.02*	4.068	4.339
Cadmium (Cd)	*0.01*	0.003	0.002
Cobalt (Co)	*0.01*	0.002	0.005
Chromium (Cr)	*0.01*	0.008	0.009
Copper (Cu)	*0.01*	0.113	0.089
Iron (Fe)	*0.01*	1.949	11.267
Potassium (K)	*0.032*	198.315	199.312
Magnesium (Mg)	*0.01*	17.206	17.266
Manganese (Mn)	*0.01*	0.061	0.510
Molybdenum (Mo)	*0.038*	ND	ND
Sodium (Na)	*0.029*	38.534	38.768
Nickel (Ni)	*0.01*	0.103	0.121
Phosphorus (P)	*0.024*	44.502	34.521
Lead (Pb)	*0.01*	0.029	0.020
Sulfur (S)	*0.011*	60.045	55.664
Antimony (Sb)	*0.01*	0.015	0.015
Selenium (Se)	*0.01*	ND	ND
Silicone (Si)	*0.7*	27.719	27.503
Tin (Sn)	*0.01*	0.019	0.021
Strontium (Sr)	*0.02*	ND	ND
Thallium (Tl)	*0.01*	ND	ND
Vanadium (V)	*0.01*	0.002	ND
Yttrium (Y)	*0.01*	ND	ND
Zinc (Zn)	*0.01*	0.225	0.379

Anios by EPA300.0 method:

Sample Field ID:	***MDL***	**14 EC 850mg/L**	**15 FC 850mg/L**
Chloride (mg/L)	*0.1*	427.613	555.268
Nitrate (NO_3-N mg/L)	*0.07*	0.535	0.636
Nitrite (NO_2-N mg/L)	*0.06*	5.747	5.445
Phosphate (mg/L)	*0.03*	95.837	66.791
Sulfate (mg/L)	*0.06*	18.911	20.345
Fluoride (mg/L)	*0.04*	99.044	87.577

Metal Analysis of Supernatant after Coagulation (1050 mg/L)

Metals (EPA 200.7)	**Result**		
Sample Lab ID:		**w290805-13**	**w290805-16**
Sample Field ID:		**13 EC 309 1050mg/l**	**16 FeCl3 1050mg/l**
	MDL		
Unit:	*mg/L*	*mg/L*	*mg/L*
Aluminum (Al)	*0.06*	1.631	1.887
Arsenic (As)	*0.01*	ND	0.002
Boron (B)	*0.02*	0.286	0.362
Barium (Ba)	*0.02*	0.003	0.006
Beryllium (Be)	*0.01*	ND	ND
Calcium (Ca)	*0.02*	4.209	5.189
Cadmium (Cd)	*0.01*	0.003	0.003
Cobalt (Co)	*0.01*	0.003	0.006
Chromium (Cr)	*0.01*	0.002	0.016
Copper (Cu)	*0.01*	0.105	0.092
Iron (Fe)	*0.01*	1.484	16.411
Potassium (K)	*0.032*	196.387	192.603
Magnesium (Mg)	*0.01*	17.186	18.200
Manganese (Mn)	*0.01*	0.065	0.634
Molybdenum (Mo)	*0.038*	ND	ND
Sodium (Na)	*0.029*	38.634	38.043
Nickel (Ni)	*0.01*	0.191	0.126
Phosphorus (P)	*0.024*	31.789	23.249
Lead (Pb)	*0.01*	0.025	0.015
Sulfur (S)	*0.011*	57.825	54.918
Antimony (Sb)	*0.01*	0.019	0.020
Selenium (Se)	*0.01*	ND	ND
Silicone (Si)	*0.7*	27.196	27.628
Tin (Sn)	*0.01*	0.009	0.021
Strontium (Sr)	*0.02*	ND	ND
Thallium (Tl)	*0.01*	ND	ND
Vanadium (V)	*0.01*	ND	ND
Yttrium (Y)	*0.01*	0.001	0.001
Zinc (Zn)	*0.01*	0.212	0.495

Anios by EPA300.0 method:

Sample Field ID:	***MDL***	**13 EC 1050mg/L**	**16 FC 1050mg/L**
Chloride (mg/L)	*0.1*	463.467	599.330
Nitrate (NO_3-N mg/L)	*0.07*	0.020	0.025
Nitrite (NO_2-N mg/L)	*0.06*	5.550	5.271
Phosphate (mg/L)	*0.03*	66.634	36.199
Sulfate (mg/L)	*0.06*	21.175	20.019
Fluoride (mg/L)	*0.04*	95.149	85.295

Ferric Chloride and Alkalinity Reaction

$2FeCl_3*6H_20 + 3Ca(HCO_3)_2 = 2Fe(OH)_3 + 3CaCl_2 + 6CO_2 + 12H_20$

Molecular weight of $FeCl_3*6H_20 = 270$

Molecular weight of $Ca(HCO_3)_2 = 162$

2 moles $FeCl_3*6H_2O$ react with 3 moles of $Ca(HCO_3)_2$

1 mg/L $FeCl_3*6H_2O$ [(1 mole $FeCl_3*6H_2O$)/ (270 mg/L $FeCl_3*6H_2O$)]*

[(3 mole $Ca(HCO_3)_2$)/ (2 mole $FeCl_3*6H_2O$)]*

[(162 mg/L $Ca(HCO_3)_2$/ (1 mole $Ca(HCO_3)_2$)]

= 0.9 mg/L $Ca(HCO_3)_2$

0.9 mg/L $Ca(HCO_3)_2$ [(100 mg/l $CaCO_3$)/(162 $Ca(HCO_3)_2$)]

= 0.56 mg/L $CaCO_3$

Ferric Chloride and Phosphate Reaction

$FeCl_3*6H_2O + PO_4^{3-} = FePO_4 + 3Cl^- + 6H_20$

Molecular weight of $FeCl_3*6H_20 = 270$

Molecular weight of $PO_4 = 95$

1 mg/L PO_4 [(1 mole PO_4)/ (95 mg/L) PO_4]*

[(1 mole $FeCl_3*6H_20$)/ (1 mole PO_4)]*

[(270 mg/L $FeCl_3*6H_20$)/ (1 mole $FeCl_3*6H_20$)]

= 2.84 mg/L $FeCl_3*6H_20$

Appendix E: Raw Data, Graphs, Statistics, and Images for Polyelectrolyte Testing

First Experimental Test with Floccin – Optical Density

Temperature 23 C, pH
6.36

The Floccin agent was added to the samples, but no change was noted after a few minutes. Previously flocs would form almost immediately. The pH was adjust to create results.

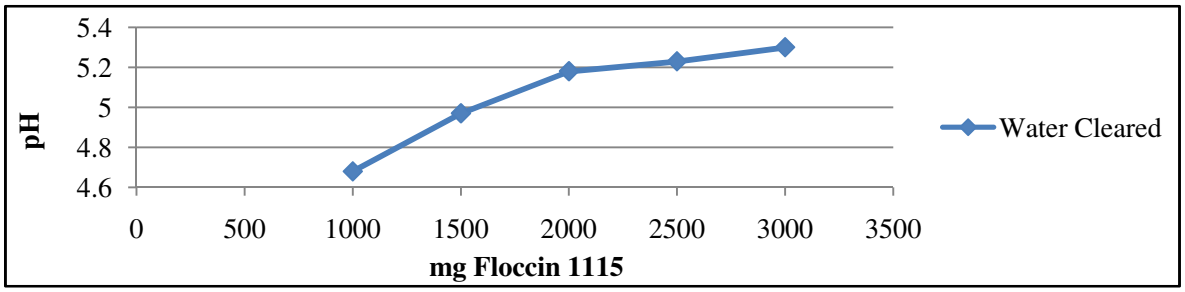

Floccin (mg)	Abs 1	Abs 2	Abs 3	Average	Std. Dev.	95 % C.I.
1000	1.245	1.232	1.111	1.196	0.074	0.029
1500	1.198	1.203	1.222	1.208	0.013	0.005
2000	1.098	1.101	1.110	1.103	0.006	0.002
2500	1.205	1.194	1.189	1.196	0.008	0.003
3000	1.060	1.064	1.095	1.073	0.019	0.007

Floccin	Pan #	Volume (mL)	Filter Mass (mg)	Filter + Sample Mass (mg)	Ignited Mass (mg)	TSS (mg/L)	VSS (mg/L)
1000	B1	20	85.4	88.4	85.5	150	145
1500	B2	20	86.9	89.4	86.8	125	130
2000	B3	20	86.2	87.0	85.8	40	60
2500	B4	20	88.3	92.1	87.9	190	210
3000	B5	15	86.2	89.6	86.5	227	206.7

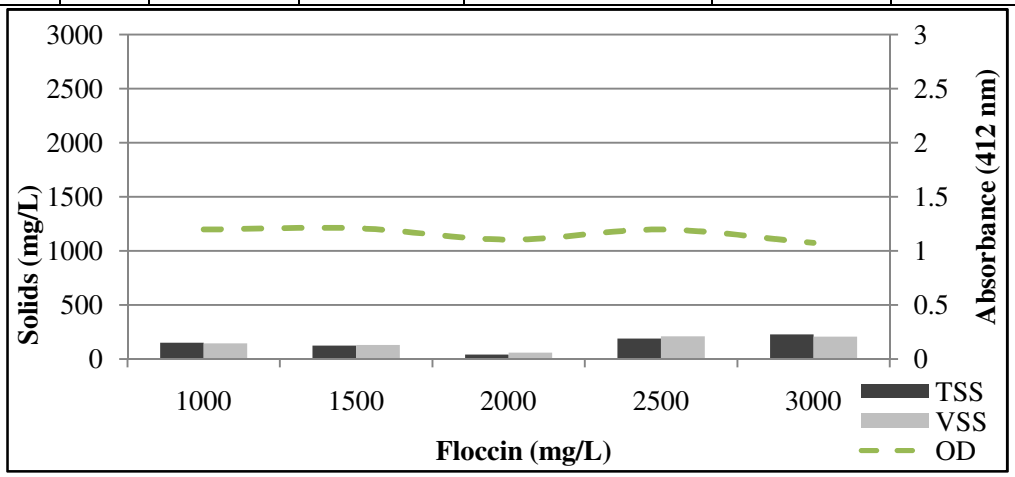

pH Testing

pH	Abs 1	Abs 2	Abs 3	Average	Std. Dev.	95% C.I.
5.4	0.623	0.605	0.605	0.611	0.0104	0.0118
6.4	1.957	1.936	1.943	1.945	0.0107	0.0121
7.4	2.485	2.47	2.536	2.497	0.0346	0.0392

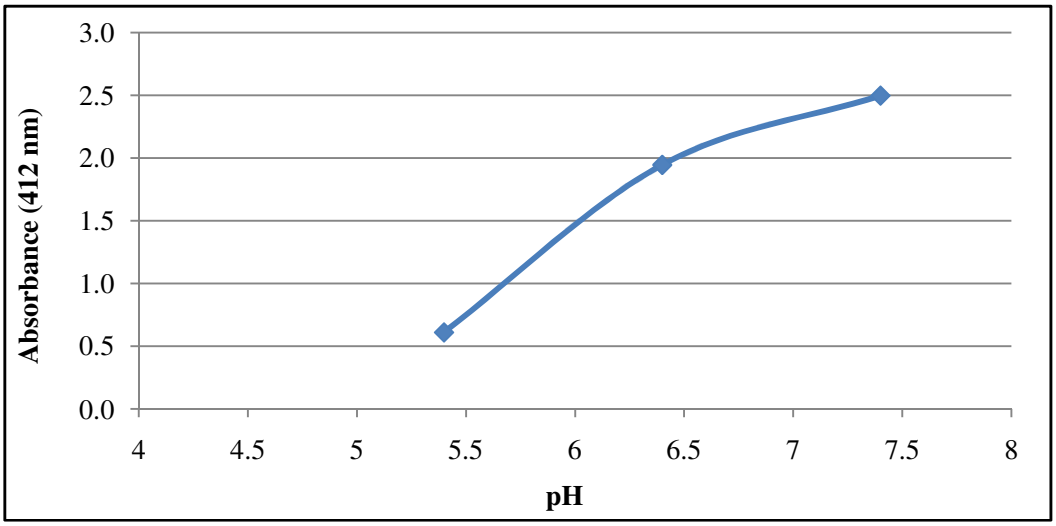

pH	Pan #	Volume (mL)	Filter Mass (mg)	Filter + Sample Mass (mg)	Ignited Mass (mg)	TSS (mg/L)	VSS (mg/L)
5.4	A1	15	85.7	88.8	86.6	207	147
6.4	A2	5	85.8	91.8	86.6	1200	1040
7.4	A3	5	85.6	97.3	89.3	2340	1600

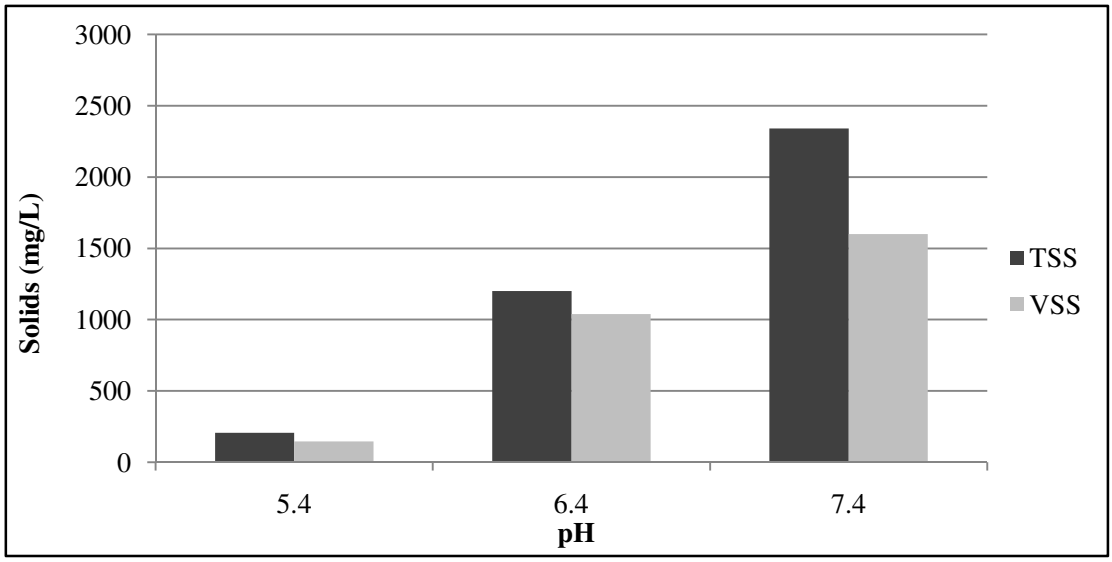

Temperature 25 C, pH 6.35
2000 mg of Floccin would be used with various pH

pH	Abs 1	Abs 2	Abs 3	Average	Std. Dev.	95% C.I.
6.3	2.07	2.104	2.084	2.086	0.017	0.007
6.01	1.157	1.169	1.175	1.167	0.009	0.004
5.71	1.021	1.036	0.998	1.018	0.019	0.007
5.34	0.986	1.039	1.051	1.025	0.035	0.013
4.98	1.396	1.462	1.491	1.450	0.049	0.019

pH	Pan #	Volume (mL)	Filter Mass (mg)	Filter + Sample Mass (mg)	Ignited Mass (mg)	TSS (mg/L)	VSS (mg/L)
6.3	C1	5	86.6	94.1	88.7	1500	1080
6.01	C2	10	89.0	92.2	89.8	320	240
5.71	C3	20	89.1	89.9	88.9	40	50
5.34	C4	20	88.9	89.7	88.6	40	55
4.98	C5	20	90.9	94.6	90.8	185	190

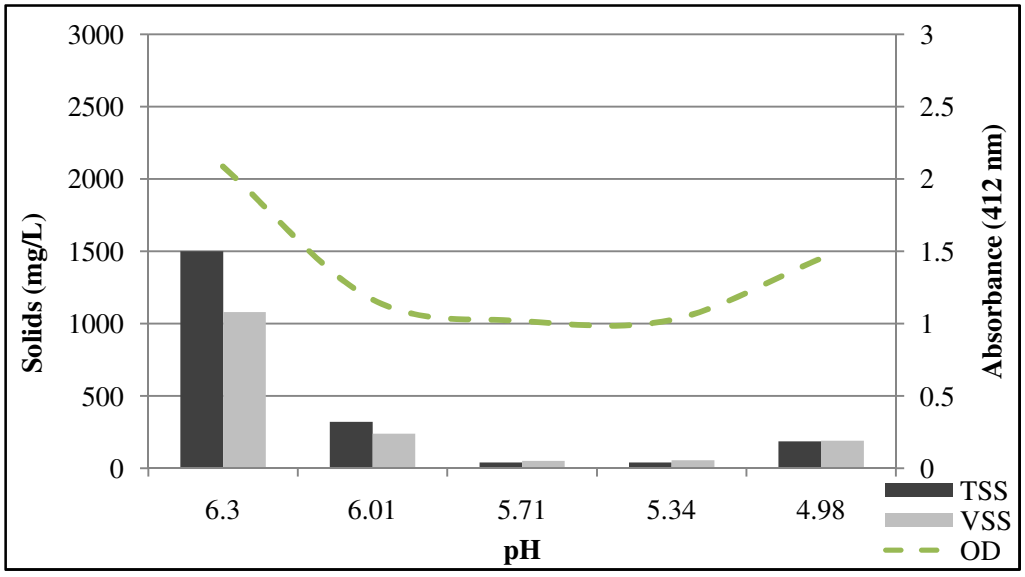

Temperature 24 C, pH 6.10
Adjusted the pH initially and then added the Floccin.

pH	5.03	5.08	5.07	5.03	5.08
Floccin (mg)	500	1000	1500	2000	2500

Floc	Abs 1	Abs 2	Abs 3	Average	Std. Dev	95% C.I.
500	1.123	1.094	1.107	1.108	0.015	0.006
1000	1.072	1.046	1.064	1.061	0.013	0.005
1500	1.073	1.07	1.068	1.070	0.003	0.001
2000	1.002	0.978	1.005	0.995	0.015	0.006
2500	0.98	0.965	0.957	0.967	0.012	0.005

Floccin (mg)	Pan #	Volume (mL)	Filter Mass (mg)	Filter + Sample Mass (mg)	Ignited Mass (mg)	TSS (mg/L)	VSS (mg/L)
500	D1	10	86.4	91.7	86.7	530	500
1000	D2	10	86.3	89.9	86.2	360	370
1500	D3	10	86.5	90.1	86.4	360	370
2000	D4	10	85.4	91.2	85.9	580	530
2500	D5	10	86.6	88.9	85.4	230	350

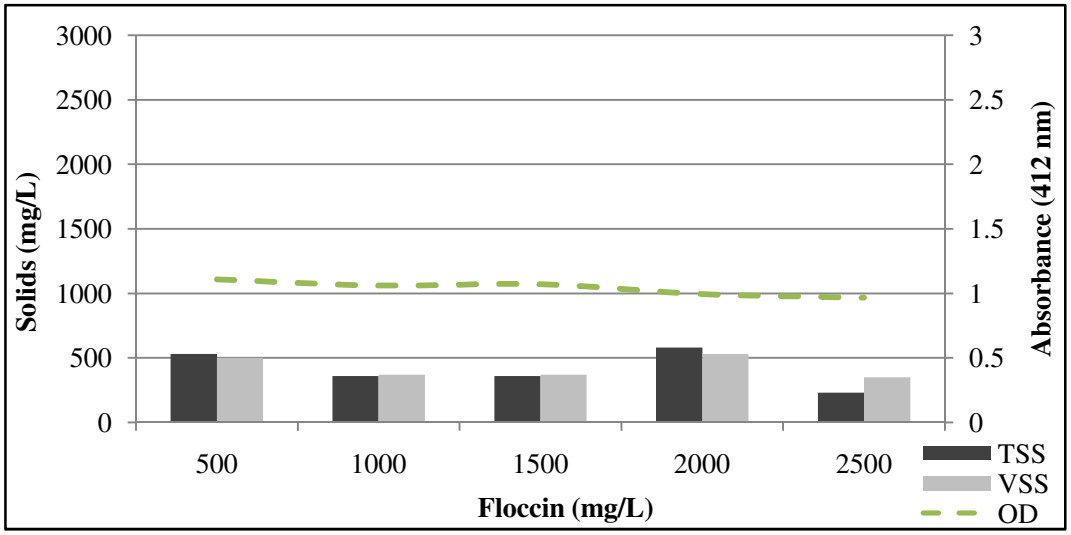

Temperature 24 C, pH 6.08
Adjusted the pH initially and then added Floccin

pH	5.07	5.08	5.07	5.09	5.06
Floccin (mg)	600	700	800	900	1000

Floc	Abs 1	Abs 2	Abs 3	Average	Std. Dev.	95% C.I.
600	0.935	0.941	0.947	0.941	0.006	0.002
700	0.954	0.958	0.949	0.954	0.005	0.002
800	0.961	0.927	0.947	0.945	0.017	0.007
900	0.948	0.928	0.93	0.935	0.011	0.004
1000	0.908	0.897	0.9	0.902	0.006	0.002

Floccin (mg)	Pan #	Volume (mL)	Filter Mass (mg)	Filter + Sample Mass (mg)	Ignited Mass (mg)	TSS (mg/L)	VSS (mg/L)
600	B1	10	86.5	91.6	88.8	510	280
700	B2	15	83.8	91.9	87.2	540	313.3
800	B3	10	85.0	90.8	86.8	580	400
900	B4	10	86.6	91.1	87.9	450	320
1000	B5	11	86.2	91.4	87.7	473	336.4

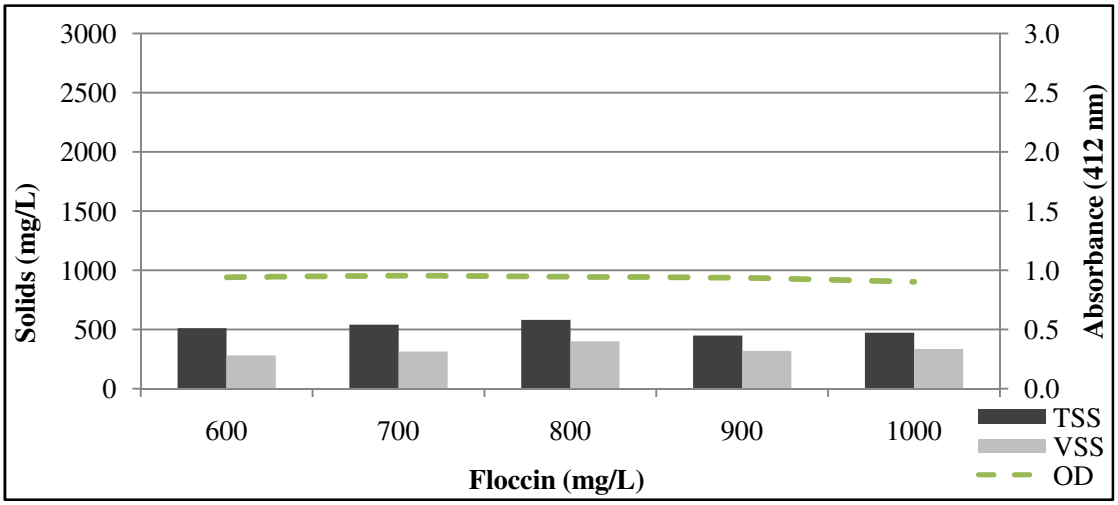

Temperature 24 C, pH 6.15
Ferric Chloride was added initially followed by 600 mg Floccin

FeCl (mg/L)	500	600	700	800	900
pH	5.68	5.56	5.46	5.34	5.3

FeCl	Abs 1	Abs 2	Abs 3	Average	Std. Dev.	95% C.I.
500	0.636	0.627	0.582	0.615	0.029	0.011
600	0.463	0.457	0.46	0.460	0.003	0.001
700	0.285	0.296	0.288	0.290	0.006	0.002
800	0.146	0.139	0.143	0.143	0.004	0.001
900	0.14	0.136	0.145	0.140	0.005	0.002

FeCl (mg/L)	Pan #	Volume (mL)	Filter Mass (mg)	Filter + Sample Mass (mg)	Ignited Mass (mg)	TSS (mg/L)	VSS (mg/L)
500	C1	10	84.7	92.5	87.9	780	460
600	C2	10	86.2	92.1	88.0	590	410
700	C3	10	85.8	92.2	87.6	640	460
800	C4	10	85.9	89.8	86.4	390	340
900	C5	10	85.2	89.4	85.6	420	380

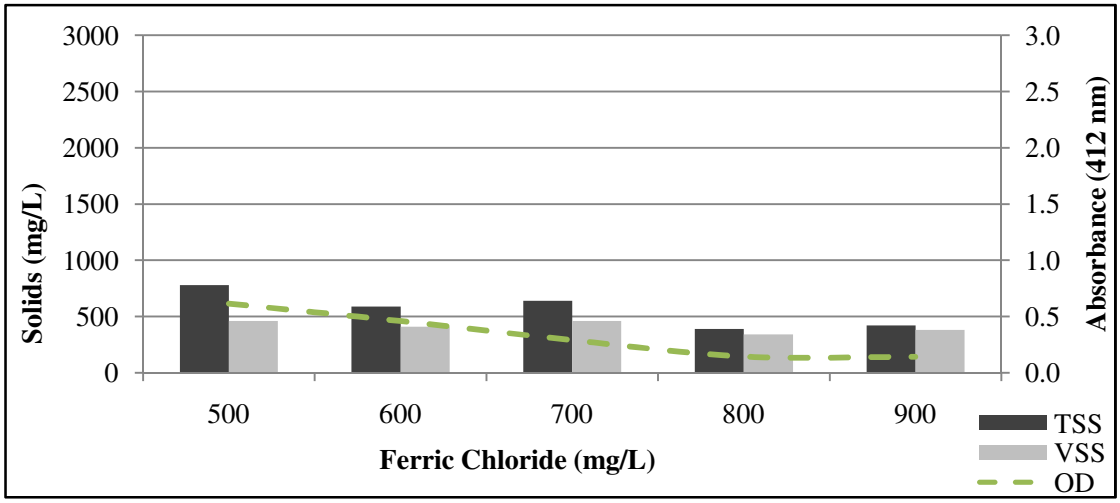

Temperature 23.5 C, pH 6.48
Ferric Chloride was added initially, followed by 1600mg Floccin

FeCl (mg/L)	100	200	300	400	500
pH	6.28	6.04	5.81	5.62	5.37

FeCl	Abs 1	Abs 2	Abs 3	Average	Std. Dev.	95% C.I.
100	0.872	0.834	0.844	0.850	0.020	0.008
200	0.725	0.727	0.723	0.725	0.002	0.001
300	0.579	0.578	0.576	0.578	0.002	0.001
400	0.520	0.526	0.519	0.522	0.004	0.001
500	0.405	0.405	0.403	0.404	0.001	0.000

FeCl (mg/L)	Pan #	Volume (mL)	Filter Mass (mg)	Filter + Sample Mass (mg)	Ignited Mass (mg)	TSS (mg/L)	VSS (mg/L)
100	A1	20	86.5	88.8	86.9	115	95
200	A2	20	86.1	88.0	85.7	95	115
300	A3	20	87.6	89.2	86.9	80	115
400	A4	20	86.7	87.9	86.2	60	85
500	A5	20	86.0	87.4	85.2	70	110

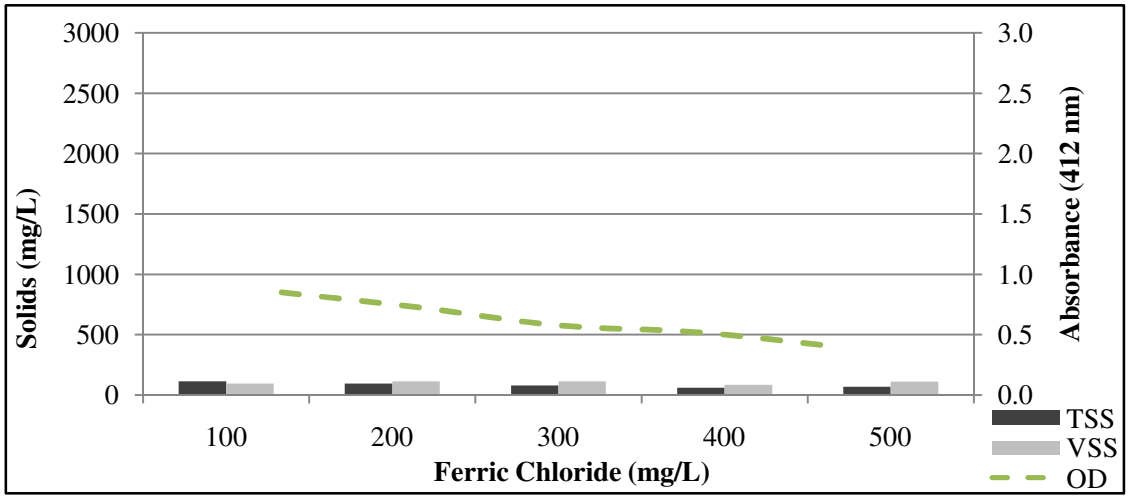

Temperature 25 C, pH 6.25
Added 800 mg/L FeCl and let spin for 5 min, pH 5.51

Floccin (mg)	Abs 1	Abs 2	Abs 3	Average	Std. Dev.	95% C.I.
500	0.289	0.3	0.308	0.299	0.010	0.004
1000	0.123	0.131	0.119	0.124	0.006	0.002
1500	0.187	0.199	0.191	0.192	0.006	0.002
2000	0.237	0.238	0.229	0.235	0.005	0.002
2500	0.235	0.262	0.262	0.253	0.016	0.006

Floccin (mg)	Pan #	Volume (mL)	Filter Mass (mg)	Filter + Sample Mass (mg)	Ignited Mass (mg)	TSS (mg/L)	VSS (mg/L)
500	A1	20	85.2	89.2	85.8	200	170
1000	A2	20	84.7	85.9	84.5	60	70
1500	A3	20	85.9	87.4	86.1	75	65
2000	A4	10	85.9	87.3	85.6	140	170
2500	A5	10	86.0	88.6	86.3	260	230

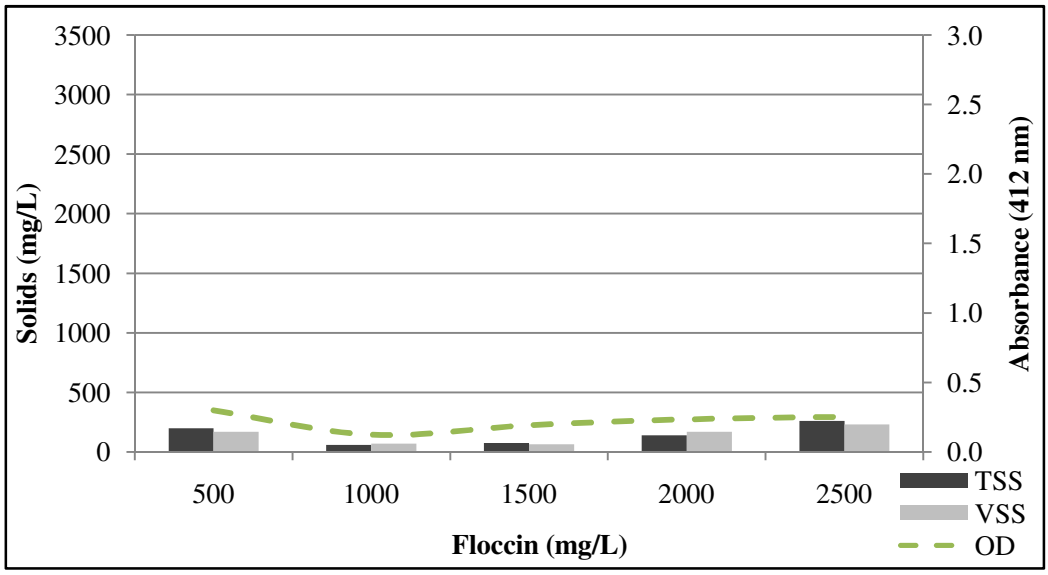

Temperature 25, pH 6.10
Added 800 mg/L FeCl and let spin for 5 min, pH 5.47

Floccin (mg)	Abs 1	Abs 2	Abs 3	Average	Std. Dev.	95% C.I.
600	0.143	0.123	0.134	0.133	0.010	0.004
700	0.135	0.139	0.149	0.141	0.007	0.003
800	0.141	0.148	0.151	0.147	0.005	0.002
900	0.114	0.096	0.103	0.104	0.009	0.004
1000	0.118	0.110	0.116	0.115	0.004	0.002

Floccin (mg)	Pan #	Volume (mL)	Filter Mass (mg)	Filter + Sample Mass (mg)	Ignited Mass (mg)	TSS (mg/ L)	VSS (mg/ L)
600	B1	20	86.2	87.6	85.6	70	100
700	B2	20	86.7	88.4	86.5	85	95
800	B3	20	86.0	88.4	86.0	120	120
900	B4	20	87.6	88.8	87.1	60	85
1000	B5	20	87.1	88.0	86.5	45	75

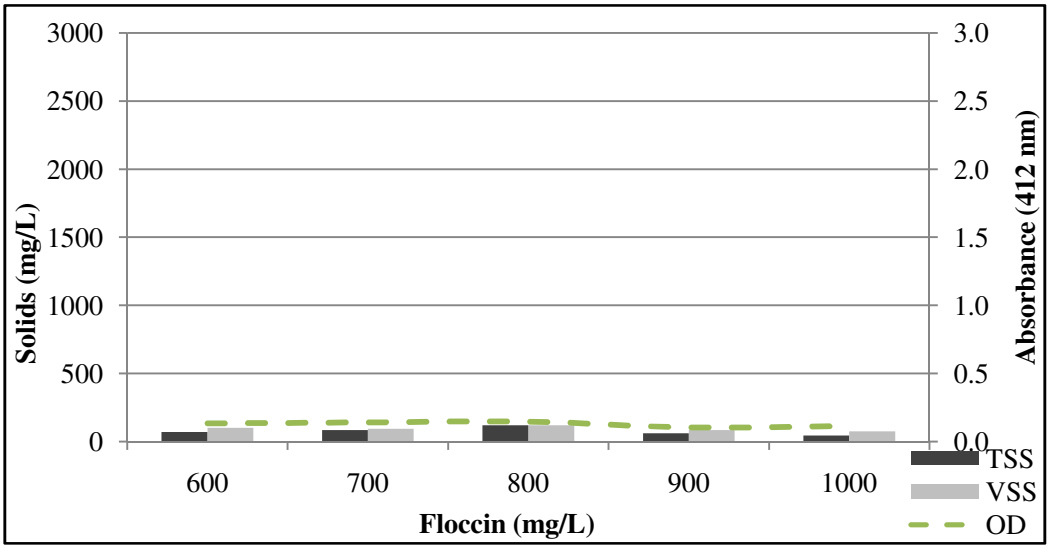

Appendix F: Raw Data, Graphs, Statistics, and Images of Flotation Testing

%	Pan #	Pan Mass	Screen Mass 1	Wet Mass 1	Dry Mass 1	Solids	Vol. 1	Pan #	Pan Mass	Screen Mass 2	Wet Mass 2	Dry Mass 2	Solids	Vol.2	Total Solids	Total Vol.
40	A1	4.006	1.5224	43.87	9.6435	4.1151	140	D1	4.0379	1.4927	7.33	5.8197	0.2891	360	4.4042	940
30	A2	4.0214	1.4933	37.21	9.0228	3.5081	140	D2	4.0521	1.4959	11.88	6.2851	0.7371	380	4.2452	960
20	A3	4.0239	1.5211	38.03	9.0662	3.5212	140	D3	4.0006	1.4936	12.27	6.2935	0.7993	370	4.3205	950
10	A4	4.0395	1.5078	12.2	6.2953	0.748	140	D4	4.0627	1.5059	38.08	9.1954	3.6268	380	4.3748	960
0	A5	4.0456	1.4914	5.59	5.5371	1E-04	360	D5	4.0461	1.506	48.82	10.088	4.536	100	4.5361	900
40	B1	4.0968	1.5067	50.29	10.556	4.9529	150	E1	4.0529	1.5206	5.67	5.5964	0.0229	360	4.9758	950
30	B2	4.0545	1.4796		11.067	5.5333	260	E2	4.0599	1.5089	10.91	6.1753	0.6065	210	6.1398	910
20	B3	4.0417	1.4912	41.87	9.5109	3.978	180	E3	4.0573	1.5071	17.68	6.8606	1.2962	320	5.2742	940
10	B4	4.0667	1.4818	15.45	6.5266	0.9781		E4	4.0454	1.5095		10.664	5.1094	470	6.0875	910
0	B5	4.0153	1.4811	5.52	5.4749	-0.022	220	E5	4.0501	1.4858		11.441	5.9051	220	5.8836	880
40	C1	4.0442	1.4889	44.92	12.58	7.0467		F1	4.0223	1.4792	6.22	5.5684	0.0669	530	7.1136	970
30	C2	4.026	1.4997	39.92	8.9701	3.4444		F2	4.0564	1.471	12.07	6.1049	0.5775	510	4.0219	950
20	C3	4.0375	1.4884	22.28	7.0878	1.5619	240	F3	4.0566	1.4636	29.68	7.8282	2.308	290	3.8699	970
10	C4	4.0664	1.488	22.32	7.1463	1.5919	180	F4	4.0366	1.4965	44.04	8.8297	3.2966	320	4.8885	940
0	C5	4.027	1.5004	5.67	5.5068	-0.021		F5	4.0618	1.4745		9.8157	4.2794		4.2588	440

Floated and Settled Solids

RR	Floated Solids			AVG	Std Dev	95% CI
40	4.1151	4.9529	7.0467	5.3716	1.5100	1.7087
30	3.5081	5.5333	3.4444	4.1619	1.1881	1.3444
20	3.5212	3.9780	1.5619	3.0204	1.2836	1.4525
10	0.7480	0.9781	1.5919	1.1060	0.4362	0.4936
0	0.0001	-0.0215	-0.0206	-0.0140	0.0122	0.0138
RR	Settled Solids			AVG	Std Dev	95 % CI
40	0.2891	0.0229	0.0669	0.1263	0.1427	0.1615
30	0.7371	0.6065	0.5775	0.6404	0.0850	0.0962
20	0.7993	1.2962	2.3080	1.4678	0.7689	0.8700
10	3.6268	5.1094	3.2966	4.0109	0.9655	1.0926
0	4.5360	5.9051	4.2794	4.9068	0.8740	0.9890

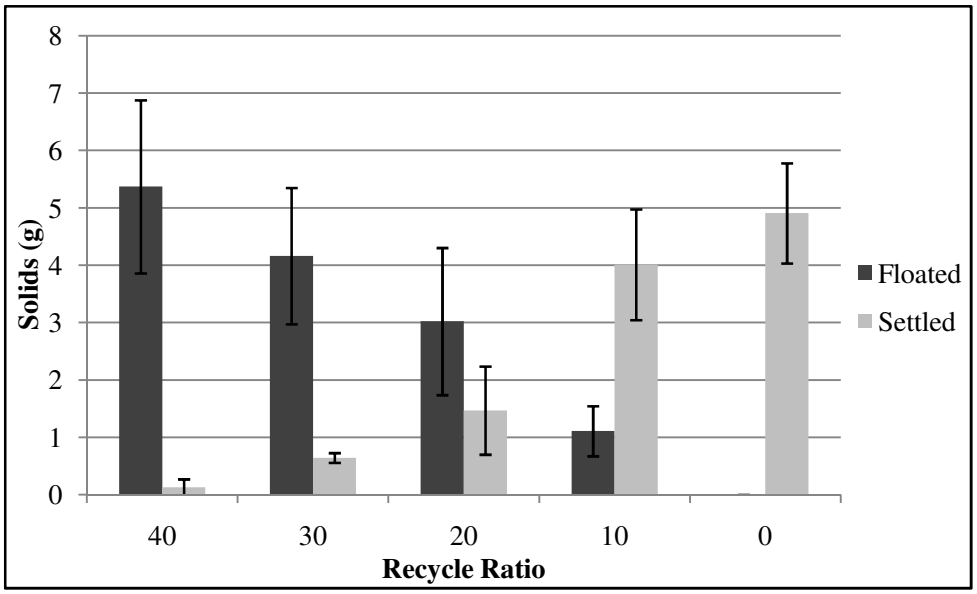

VSS as determined from the floated and settled solids

Pan #	Pan Mass	Solid + Pan Mass	Ignited + Pan Mass	Solids	Ignited
A1	1.1817	4.8673	2.9724	3.6856	1.7907
A2	1.1846	3.4749	2.2242	2.2903	1.0396
A3	1.1644	3.577	2.1749	2.4126	1.0105
A4	1.1804	1.6992	1.4287	0.5188	0.2483
A5	1.1848	1.1903	1.1888	0.0055	0.004
B1	1.1794	4.0371	2.375	2.8577	1.1956
B2	1.1769	4.1073	2.233	2.9304	1.0561
B3	1.1772	3.4624	2.0095	2.2852	0.8323
B4	1.171	1.6951	1.3697	0.5241	0.1987
B5	1.1832	1.1838	1.193	0.0006	0.0098
C1	1.1723	2.6553	1.6573	1.483	0.485
C2	1.1715	3.0148	1.8048	1.8433	0.6333
C3	1.1777	2.1764	1.521	0.9987	0.3433
C4	1.1794	2.2155	1.5204	1.0361	0.341
C5	1.1912	1.1919	1.1925	0.0007	0.0013
D1	1.1712	1.3077	1.2263	0.1365	0.0551
D2	1.1705	1.7189	1.4002	0.5484	0.2297
D3	1.1785	1.816	1.4492	0.6375	0.2707
D4	1.1662	1.9883	1.4965	0.8221	0.3303
D5	1.1834	2.7202	1.8237	1.5368	0.6403
E1	1.1695	1.1747	1.1714	0.0052	0.0019
E2	1.1724	1.3054	1.2195	0.133	0.0471
E3	1.1825	1.6665	1.3522	0.484	0.1697
E4	1.163	1.976	1.4219	0.813	0.2589
E5	1.1749	2.3121	1.5778	1.1372	0.4029
F1	1.1674	1.2066	1.186	0.0392	0.0186
F2	1.1731	1.5839	1.3263	0.4108	0.1532
F3	1.167	2.3988	1.6439	1.2318	0.4769
F4	1.1799	1.6691	1.3608	0.4892	0.1809
F5	1.1725	2.6244	1.7529	1.4519	0.5804

VSS of floated and settled solids continued

RR	Floated Solids			Average	Std. Dev.	95% C.I.
40	1.791	1.196	0.485	1.157	0.654	0.740
30	1.040	1.056	0.633	0.910	0.239	0.271
20	1.011	0.832	0.343	0.729	0.345	0.391
10	0.248	0.199	0.341	0.263	0.072	0.082
0	0.004	0.010	0.001	0.005	0.004	0.005
RR	Settled Solids			Average	Srd. Dev.	95% C.I.
40	0.055	0.002	0.019	0.025	0.027	0.031
30	0.230	0.047	0.153	0.143	0.092	0.104
20	0.271	0.170	0.477	0.306	0.157	0.177
10	0.330	0.259	0.181	0.257	0.075	0.085
0	0.640	0.403	0.580	0.541	0.123	0.140

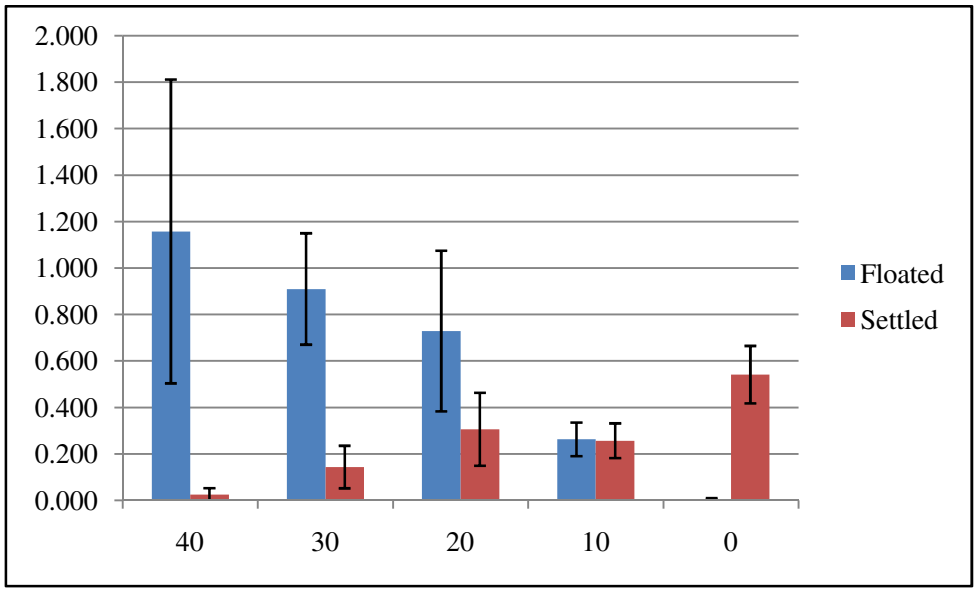

Optical Density Supernatant

A1	0.221	A2	0.188	A3	0.152	A4	0.14	A5	0.129
	0.223		0.186		0.137		0.147		0.132
	0.226		0.176		0.145		0.139		0.128
B1	0.186	B2	0.202	B3	0.157	B4	0.139	B5	0.134
	0.188		0.21		0.156		0.136		0.133
	0.197		0.223		0.148		0.152		0.131
C1	0.119	C2	0.115	C3	0.102	C4	0.094	C5	0.092
	0.116		0.118		0.108		0.103		0.094
	0.117		0.113		0.104		0.098		0.097
Average	0.177		0.170		0.134		0.128		0.119
Std. Dev.	0.0471		0.0433		0.0231		0.0225		0.0186
95% CI	0.0308		0.0283		0.0151		0.0147		0.0121

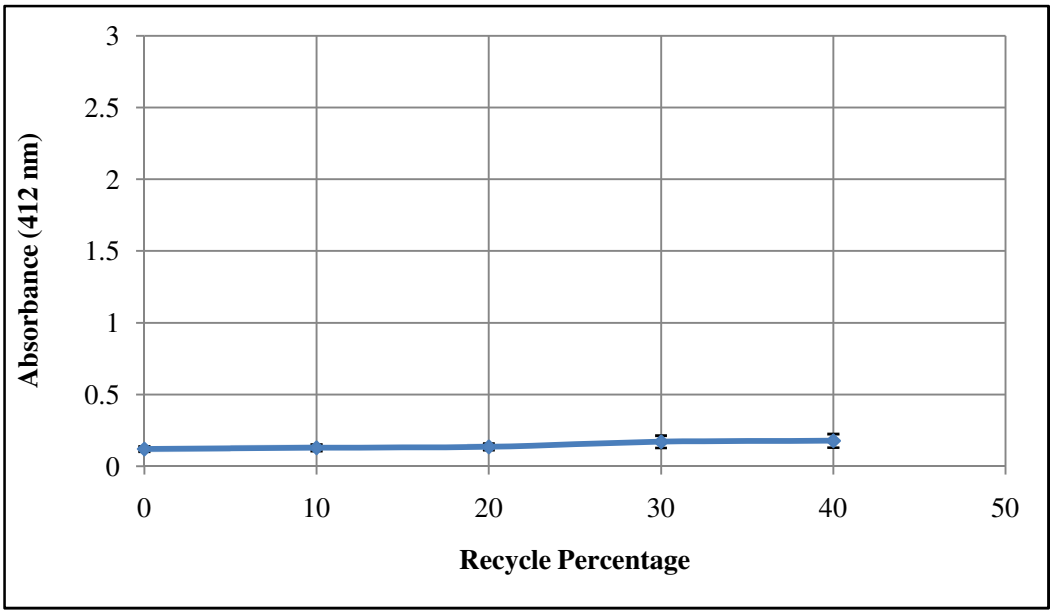

TSS and VSS of Supernatant

Pan #	Filter Mass (mg)	Volume (mL)	Sample Mass (mg)	Ignited Mass (mg)	TSS (mg/L)	VSS (mg/L)
A1	86.6	20	88.8	86.3	110	125
A2	86.9	20	88.3	86.6	70	85
A3	86.5	20	87.5	86.1	50	70
A4	87	20	88.2	86.5	60	85
A5	86.1	20	87.7	86.2	80	75
B1	87.3	20	88.9	87.4	80	75
B2	86.4	20	88.4	86.8	100	80
B3	86.7	20	87.9	86.8	60	55
B4	86.8	20	88	87	60	50
B5	85.6	20	87	86.2	70	40
C1	86	20	87.4	85.9	70	75
C2	87	20	89	87.6	100	70
C3	87	20	88.1	86.9	55	60
C4	87.3	20	88.4	87.3	55	55
C5	87.5	20	88.5	87.6	50	45

%	TSS 1	TSS 2	TSS 3	Average	Std. Dev.	95% C.I.
40	110	80	80	90.00	17.32	19.60
30	70	100	100	90.00	17.32	19.60
20	50	60	60	56.67	5.77	6.53
10	60	60	60	60.00	0.00	0.00
0	80	70	70	73.33	5.77	6.53

%	VSS 1	VSS 2	VSS 3	Average	Std. Dev.	95% C.I.
40	125	75	75	91.67	28.87	32.67
30	85	80	70	78.33	7.64	8.64
20	70	55	60	61.67	7.64	8.64
10	85	50	55	63.33	18.93	21.42
0	75	40	45	53.33	18.93	21.42

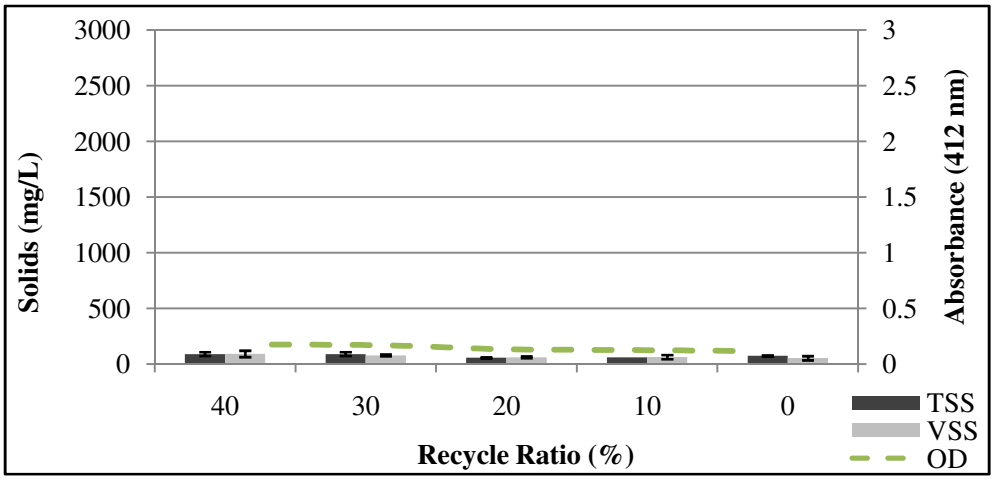

COD analysis

				Average
A1	0.275	0.282	0.283	0.280
A2	0.281	0.614	0.291	0.395
A3	0.281	0.286	0.283	0.283
A4	0.26	0.279	0.281	0.273
A5	0.271	0.279	0.283	0.278
B1	0.268	0.284	0.282	0.278
B2	0.3	0.279	0.285	0.288
B3	0.275	0.277	0.273	0.275
B4	0.275	0.284	0.29	0.283
B5	0.27	0.275	0.293	0.279
C1	0.294	0.276	0.279	0.283
C2	0.273	0.274	0.261	0.269
C3	0.268	0.273	0.302	0.281
C4	0.305	0.28	0.272	0.286
C5	0.266	0.268	0.273	0.269

RR				Avg	Std. Dev.	95% C.I.
40	0.280	0.278	0.283	0.280	0.003	0.003
30	0.395	0.288	0.269	0.318	0.068	0.077
20	0.283	0.275	0.281	0.280	0.004	0.005
10	0.273	0.283	0.286	0.281	0.006	0.007
0	0.278	0.279	0.269	0.275	0.006	0.006

Metal Analysis of Supernatant after Flotation

W.A Callegari Environmental Center
Water Quality Laboratory
Baton Rouge, LA 70820
Ph: (225) 765-5155
Fax: (225)765-5158

Client Name: **Adam Dassey** **Project name:**
Date received:
Date Completed: 1/12/2010

Sample ID	**40%**	**30%**	**20%**	**10%**	**0%**
	mg/L	*mg/L*	*mg/L*	*mg/L*	*mg/L*
Aluminum (Al)	0.503	0.460	0.753	0.812	0.510
Arsenic (As)	ND	ND	ND	ND	ND
Boron (B)	0.162	0.169	0.183	0.183	0.171
Barium (Ba)	0.002	0.001	0.002	0.002	0.001
Beryllium (Be)	ND	ND	ND	ND	ND
Calcium (Ca)	5.507	5.524	6.264	5.840	6.068
Cadmium (Cd)	ND	ND	ND	ND	ND
Cobalt (Co)	ND	ND	ND	ND	ND
Chromium (Cr)	ND	ND	ND	ND	ND
Copper (Cu)	0.177	0.166	0.165	0.178	0.202
Iron (Fe)	8.823	9.422	11.844	13.330	10.444
Potassium (K)	254.284	255.200	277.306	264.874	265.560
Magnesium (Mg)	17.126	16.936	18.747	17.348	17.450
Manganese (Mn)	0.549	0.549	0.628	0.566	0.545
Molybdenum (Mo)	0.064	ND	ND	ND	ND
Sodium (Na)	24.957	24.776	26.502	25.851	25.821
Nickel (Ni)	0.104	0.095	0.093	0.080	0.059
Phosphorus (P)	46.791	49.491	51.041	47.915	47.170
Lead (Pb)	ND	ND	ND	ND	ND
Sulfur (S)	54.077	58.967	63.317	63.706	67.790
Antimony (Sb)	ND	ND	0.010	ND	ND
Selenium (Se)	ND	ND	ND	ND	ND
Silicone (Si)	29.791	29.982	32.916	32.044	31.425
Tin (Sn)	0.010	0.004	0.012	0.020	0.010
Strontium (Sr)	ND	ND	ND	ND	ND
Thallium (Tl)	ND	ND	ND	ND	ND
Vanadium (V)	0.001	0.001	0.002	0.001	ND
Yttrium (Y)	0.000	ND	ND	ND	ND
Zinc (Zn)	0.378	0.338	0.355	0.269	0.463

Recycle Ratio Images

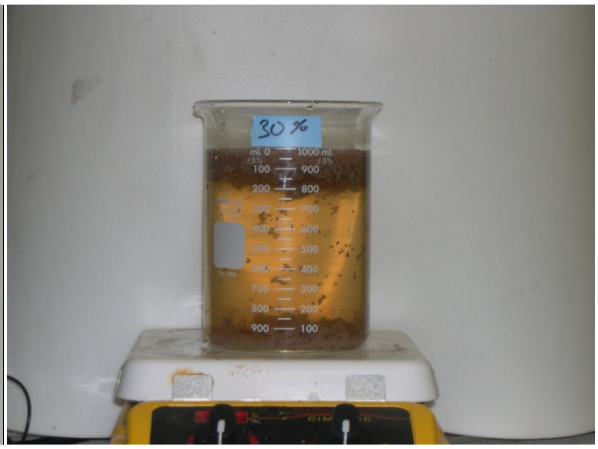

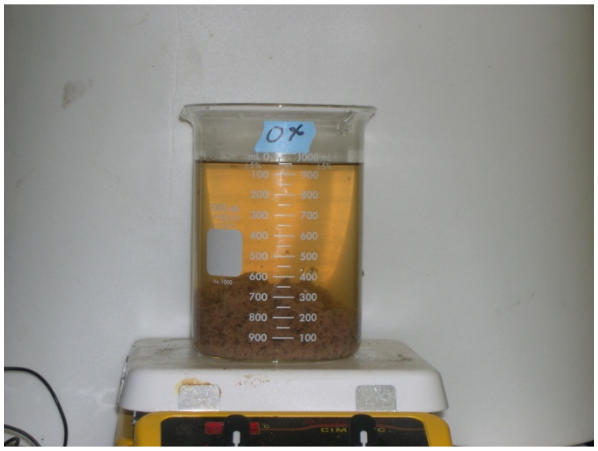

Cost Analysis

Ferric Chloride – 800 mg/L

[$0.15/lb][1 lb/453.6 g][1.3966 g/mL][10% solution][8 mL/L][3.8 L/gal][1 million gal/day]

= $1,404 per day

Floccin 1115 – 900 mg/L

[$1.25/lb][1 lb/453.6 g][1 g/1000 mg][900 mg/L][3.8 L/gal][1million gal/day]

= $9,425 per day

Total: $10,829 per day

Vita

Adam James Dassey was born in New Orleans, Louisiana. There he attended Brother Martin High School before entering the Biological and Agricultural Engineering program at Louisiana State University, Baton Rouge. After completing his bachelor's degree in the fall of 2007, he entered the Master's program in Biological and Agricultural Engineering at Louisiana State University.